

The Impact of Inflammation on the Determinants of Skeletal Muscle Glucose Uptake

By

Kimberly X. Mulligan

Dissertation

Submitted to the Faculty of the
Graduate School of Vanderbilt University
in partial fulfillment of the requirements

for the degree of

DOCTOR OF PHILOSOPHY

In

Molecular Physiology and Biophysics

May, 2012

Nashville, Tennessee

Approved:

David H. Wasserman

Masakazu Shiota

Luc Van Kaer

Alyssa H. Hasty

Mom, Shirley, Grandma, Sonny, and Reggie, thank you for the support you have shown me during the course of my education. You always believed in me, even when I sometimes doubted myself. Your prayers have covered me throughout this journey; this degree is as much yours as it is mine.

TABLE OF CONTENTS

	Page
ACKNOWLEDGMENTS	vi
LIST OF TABLES	viii
LIST OF FIGURES	ix
CHAPTER	
I. INTRODUCTION AND RESEARCH OBJECTIVES.....	1
Impact of Stress on Glucose Homeostasis.....	1
Glucose Homeostasis Maintenance	4
The Liver's Role in Maintaining Glucose Homeostasis	6
Hepatic Glucose Production and Stress	9
Adipose Tissue's Role in Maintaining Glucose Homeostasis	13
Adipose Tissue and Stress	17
Distributed Control of Muscle Glucose Uptake.....	18
Glucose Delivery	20
Glucose Transport.....	23
Glucose Phosphorylation	26
Current Treatments and Controversies	28
Clinical Significance.....	30
Research Objectives.....	31
II. MATERIALS AND METHODS	32
Animal Care and Husbandry.....	32
Mouse Models.....	33
Genetic Manipulations	33
Surgical Procedures	33
<i>In Vivo</i> Metabolic Experiments	35
Hyperinsulinemic-Euglycemic Clamp and Saline Control Experiments.....	35

Indirect Calorimetry	37
Echocardiography	38
Blood Flow Analysis	39
Processing Plasma Samples	40
Blood Glucose Concentrations	40
Plasma Immunoreactive Insulin.....	40
Plasma Cytokines.....	41
Plasma Non-Esterified Fatty Acids.....	42
Plasma Lactate	42
Plasma Radioactivity	43
Processing Muscle Samples.....	44
Muscle Radioactivity	44
Immunoblots	45
Real Time PCR.....	46
Microsphere Isolation	47
Mitochondrial Extraction.....	47
Immunofluorescence Microscopy.....	48
Statistical Analysis.....	49

III. DISASSOCIATION OF MUSCLE INSULIN SIGNALING AND INSULIN-STIMULATED GLUCOSE UPTAKE FOLLOWING LPS INDUCED INFLAMMATION50

Aims.....	50
Experimental Approach	51
Results.....	52
Discussion.....	56
Figures.....	63
Tables.....	70

IV. ENHANCED GLUCOSE TRANSPORT CAPACITY AMELIORATES INFLAMMATION INDUCED IMPAIRMENTS IN INSULIN-STIMULATED MUSCLE GLUCOSE UPTAKE73

Aims.....	73
Experimental Approach	75
Results.....	75
Discussion.....	78
Figures.....	84
Tables.....	88

V. INCREASED GLUCOSE PHOSPHORYLATION CAPACITY IN SKELETAL MUSCLE DOES NOT REDUCE THE INFLAMMATION-INDUCED IMPAIRMENTS IN INSULIN-STIMULATED MUSCLE GLUCOSE UPTAKE	93
Aims	93
Experimental Approach	94
Results	94
Discussion	96
Figures	100
Tables	104
VI. CONCLUSIONS AND FUTURE DIRECTIONS.....	107
Aims	107
Experimental Approach	112
REFERENCES	115

ACKNOWLEDGEMENTS

My time at Vanderbilt has been an amazing journey made possible by a host of individuals. First I would first like to thank my mentor Dr. Owen McGuinness. When I began graduate school, the Department of Molecular Physiology and Biophysics was not where I intended to do my research. However, a chance meeting at the poster session allowed me to train in the laboratory of a brilliant scientist. I appreciate all the conversations we've had throughout the years, not just about science, but about life. He has always been so generous with his time, offering me great advice, and encouraging me to find my own scientific path. Dr. McGuinness exemplifies the true meaning of a mentor and I feel blessed to have had the opportunity to work in his laboratory.

Next, I would like to thank my committee members, Drs. David Wasserman, Masa Shiota, Alyssa Hasty, and Luc Van Kaer. I am grateful for the insightful information they have given me regarding my project as well as their support of my career goals. I appreciate your time and the knowledge you have contributed to this work.

I could not have been successful in my graduate career without an amazing support system. I have had the pleasure of working with some wonderful people in my lab, past and present. I want to thank Andrea Tweedel, who was instrumental in my doing a rotation in the McGuinness lab. Fu-Yu Chuh who is such a wonderful person and great scientist. She has always provided me assistance and encouragement, even after she moved to Chicago. Song Chen, thank you for always making me laugh. Tammy Lundblad, Yolanda Otero, Tyler Morris, and Tammy Santamango thank you for making

it enjoyable to come to work every day; I am so glad that you have not only been my lab mates, but I consider you my friends.

There are some additional people in the Department of Molecular Physiology and Biophysics that I would like to thank. In the Wasserman lab Drs. Robert Young and Li Kang, Bingle Bracey, and Frayja James, I am grateful for all the help you have provided me throughout the years. I would like to thank the MMPC, especially Tasneem Ansari and Carlo Malabanaan who made sure that all my surgeries were completed. Without all of their assistance it would not have been possible for me to finish my dissertation. Thank you Angie Pernell for always making sure I had everything I needed and things I didn't even know I needed.

To my family, you have always supported me in all of my endeavors. Thank you for instilling in me the importance of a good education early. They have lifted me up and given me strength and words of encouragement when I didn't know if I could make it through. Your prayers have covered me and your belief in my ability has sustained me. I could not have completed this journey without you. I love you all very much.

Reggie, you are an incredible source of strength for me. You have been one of my biggest cheerleaders. You listened to presentations (even when you had no idea what I was talking about), made sure I was safe all those late nights in the lab, allowed me to vent my frustrations, as well as shared in my triumphs. I am so grateful to have you in my life and I would not have wanted to experience this journey with anyone else by my side.

Finally, I am grateful to all of my wonderful friends. Your love and support have meant so much to me, more than any words I write on these pages could ever express.

LIST OF TABLES

TABLE	PAGE
3.1. Arterial plasma insulin levels after a hyperinsulinemic-euglycemic clamp following VEH or LPS treatment.	80
3.2. Renal and tissue blood flow following VEH or LPS treatment.	81
3.3. Cardiovascular parameters following VEH or LPS treatment.	82
4.1. Basal arterial plasma insulin following VEH or LPS treatment in WT and GLUT4 ^{Tg} mice.	88
4.2. Arterial plasma insulin following VEH or LPS treatment in WT and GLUT4 ^{Tg} mice.	89
4.3. Plasma NEFA levels following VEH or LPS treatment in WT or GLUT4 ^{Tg} mice.	90
4.4. Plasma lactate levels following VEH or LPS treatment in WT and GLUT4 ^{Tg} mice.	91
4.5. Cardiovascular parameters following VEH or LPS treatment in WT and GLUT4 ^{Tg} mice.	92
5.1. Basal arterial plasma insulin following VEH or LPS treatment in WT and HKII ^{Tg} mice.	104
5.2. Arterial plasma insulin following VEH or LPS treatment in WT and HKII ^{Tg} mice.	105
5.3. Plasma lactate levels following VEH or LPS treatment in WT and HKII ^{Tg} mice.	106

LIST OF FIGURES

FIGURE	PAGE
1.1. Distributed control of muscle glucose uptake. Outlines the three steps involved in the process of MGU are coupled to one another and illustrates the factors that influence each step.....	4
1.2. Major organs involved in maintaining glucose homeostasis	6
1.3. Insulin stimulates AKT activation though the phosphorylation of upstream mediators IRS-1 and PI3-K. Activated AKT phosphorylates AS160 on threonine residues. Phosphorylation of AS160 inhibits Rab-GTPase-activating protein (GAP) which promotes the conversion of GDP Rab to the more active GTP Rab. This allows GLUT4 storage vesicles to move to and fuse with the plasma membrane.	24
1.4 Proposed mechanism by which LPS inhibits glucose uptake by the muscle. LPS binds to its receptor on TLR4 and activates the JNK/IKK pathway. This leads to inhibitory phosphorylation of key enzymes in the insulin signaling pathway. This in turn inhibits GLUT4 tranlocation to the plasma membrane as well as HKII binding to the mitochondria.. ...	28
2.1. Protocol for the <i>in vivo</i> metabolic experiments. Experimental protocol for the hyperinsulinemic-euglycemic clamp and saline control experiments. Mice were fasted for 5 h (t= -300 min) prior to the beginning of the experiment. A 13 μ Ci bolus of ¹⁴ C-2DG was injected after 100 min of the insulin of saline infusion.....	37
3.1. Plasma cytokine levels following VEH orLPS treatment. (A) Plasma concentration of tumor necrosis factor-alpha (TNF- α), (B) interleukin-1 β (IL-1 β), (C) interleukin-6 (IL-6), and (D) interleukin-10 (IL-10) 4- and 6-hours following VEH, low- (1 μ g/g BW) and high- (10 μ g/g BW) dose LPS treatment in chronically catheterized conscious C57Bl/6J mice. Data are expressed as mean \pm SEM. * p<0.05 vs. VEH, # p<0.05 vs. low-dose LPS.....	63
3.2. Basal glucose concentrations and tissue glucose uptake following VEH orLPS treatment. (A) Basal arterial glucose and (B) basal tissue glucose uptake in chronically catheterized 5-hour fasted C57BL/6J mice that received VEH, low- (1 μ g/g BW), or high- (10 μ g/g BW) dose LPS. Data are expressed as mean \pm SEM. * p<0.05 vs. VEH, # p<0.05 vs. low-dose LPS.	64
3.3. Glucose concentrations and glucose infusion rate (GIR) following VEH orLPS treatment. (A) Arterial glucose concentrations and (B) glucose infusion rate (GIR) during a hyperinsulinemic-euglycemic clamp in chronically catheterized 5-hour fasted C57BL/6J mice that received VEH, low- (1 μ g/g BW) LPS, or high- (10 μ g/g BW) dose LPS.....	65

- 3.4. **Insulin-stimulated tissue glucose uptake following VEH orLPS treatment.** (A) Tissue (soleus, gastrocnemius, superficial vastus lateralis (SVL), heart, and brain) glucose uptake and (B) fold-change from basal of insulin-stimulated glucose uptake during a hyperinsulinemic-euglycemic clamp in chronically catheterized 5-hour fasted C57BL/6J mice that received vehicle, low- (1µg/g BW), or high- (10µg/g BW) dose LPS. Data are expressed as mean ±SEM. * p<0.05 vs. VEH, # p<0.05 vs. low-dose LPS..... 66
- 3.5. **Effect of VEH orLPS treatment on insulin signaling in skeletal muscle.** (A) Akt phosphorylation (Ser473) and (B) GSK phosphorylation in the gastrocnemius muscle of C57BL/6J mice that received vehicle or high-dose LPS (10µg/g BW) after a hyperinsulinemic-euglycemic clamp. Data are expressed as mean ±SEM. *p<0.05.. 67
- 3.6. **Effect of VEH orLPS treatment on acute insulin signaling in skeletal muscle.** (A) Akt phosphorylation (Ser473) and (B) phosphorylation of IRS-1 (Tyr895 and Ser307) in the gastrocnemius muscle of C57BL/6J mice after an acute bolus of saline or insulin. Data are expressed as mean ±SEM. *p<0.05..... 68
- 3.7. **Effect of VEH orLPS treatment on the expression of iNOS in skeletal muscle.** Expression of inducible nitric oxide synthase (iNOS) mRNA in the gastrocnemius muscle of C57BL/6J mice that received vehicle, low- (1µg/g BW), or high- (10µg/g BW) dose LPS after a hyperinsulinemic-euglycemic clamp. Data are expressed as mean ±SEM. *p<0.05..... 69
- 4.1. **Basal glucose concentrations and tissue glucose uptake following VEH orLPS treatment in WT and GLUT4^{Tg} mice.** (A) Basal arterial glucose and (B) Basal tissue glucose uptake in chronically catheterized 5-hour fasted C57BL/6J mice that received VEH or high-dose LPS (10µg/g BW). Data are expressed as mean ±SEM. * p<0.05 VEH vs. LPS, # p<0.05 WT vs. GLUT4^{Tg}..... 84
- 4.2. **Glucose concentrations and glucose infusion rate (GIR) following VEH orLPS treatment in WT and GLUT4^{Tg} mice.** (A) Arterial glucose concentrations and (B) Glucose infusion rate (GIR) during a hyperinsulinemic-euglycemic clamp in chronically catheterized 5-hour fasted C57BL/6J mice that received VEH or high-dose LPS (10µg/g BW)..... 85
- 4.3. **Insulin-stimulated tissue glucose uptake following VEH orLPS treatment in WT and GLUT4^{Tg} mice.** Tissue (soleus, gastrocnemius, superficial vastus lateralis (SVL), heart, adipose tissue, and brain) glucose uptake during a hyperinsulinemic-euglycemic clamp in chronically catheterized 5-hour fasted C57BL/6J mice that received VEH or high-dose LPS. Data are expressed as mean ±SEM. * p<0.05 VEH vs. LPS, # p<0.05 WT vs. GLUT4^{Tg}..... 86

4.4. Figure 4.4: Translocation of GLUT4 to the cell surface in the gastrocnemius of WT and GLUT4Tg mice following VEH orLPS treatment. (A) Representative images and (B) quantification of the relative extent of cell surface distribution of GLUT4. Data are expressed as mean \pm SEM.. ..	87
5.1. Basal glucose concentrations and tissue glucose uptake following VEH orLPS treatment. (A) Basal arterial glucose and (B) Basal tissue glucose uptake in chronically catheterized 5-hour fasted C57BL/6J mice that received VEH, low-dose (1 μ g/g BW) LPS, or high-dose LPS (10 μ g/g BW). Data are expressed as mean \pm SEM. * p<0.05 VEH vs. LPS....	100
5.2. Glucose concentrations and glucose infusion rate (GIR) following VEH orLPS treatment in WT and HKII^{Tg} mice. (A) Arterial glucose concentrations and (B) Glucose infusion rate (GIR) during a hyperinsulinemic-euglycemic clamp in chronically catheterized 5-hour fasted C57BL/6J mice that received VEH or high-dose LPS (10 μ g/g BW).....	101
5.3. Insulin-stimulated tissue glucose uptake following VEH orLPS treatment in WT and HKII^{Tg} mice. Tissue (soleus, gastrocnemius, superficial vastus lateralis (SVL), heart, adipose tissue, and brain) glucose uptake during a hyperinsulinemic-euglycemic clamp in chronically catheterized 5-hour fasted C57BL/6J mice that received vehicle or high-dose LPS. Data are expressed as mean \pm SEM. * p<0.05 VEH vs. LPS.....	102
5.4. HKII content in the cytosol and mitochondria in gastrocnemius muscle following VEH orLPS treatment. Data are expressed as mean \pm SEM. * p<0.05 VEH vs. LPS.. ..	103

CHAPTER I

INTRODUCTION

Impact of Stress on Glucose Homeostasis

Stress has a major impact on whole-body metabolism which can be characterized by changes in the body's ability to control glucose, fat, and protein metabolism. This stress response consists of hypermetabolism, a hyperdynamic cardiovascular state, and inflammation (19). Cytokines released during inflammation can affect glucose metabolism directly or indirectly by augmenting glucoregulatory hormone secretion and curtailing insulin release (107). Hyperglycemia persists as a result of amplified gluconeogenesis, which is activated due to a marked elevation in the circulating levels of glucagon, catecholamines, cortisol, and growth hormone in combination with increased insulin resistance despite hyperinsulinemia (99). Glucose is shunted away from its normal sites of utilization to sites that assist in overcoming infection.

In the clinical setting, sepsis is a condition that is characterized by a whole-body inflammatory state and the presence of known or suspected infection (19). Severe sepsis results in ~750,000 affected persons annually in the United States and 67% of those infected require intensive care unit services. In addition to the cardiovascular and pulmonary complications a hallmark of critical illness is dysregulation of glucose homeostasis even without a previous diagnosis of diabetes. Current treatment of the accompanying hyperglycemia in the ICU involves aggressive management of glucose levels through administration of exogenous insulin (166). Initial studies suggested that

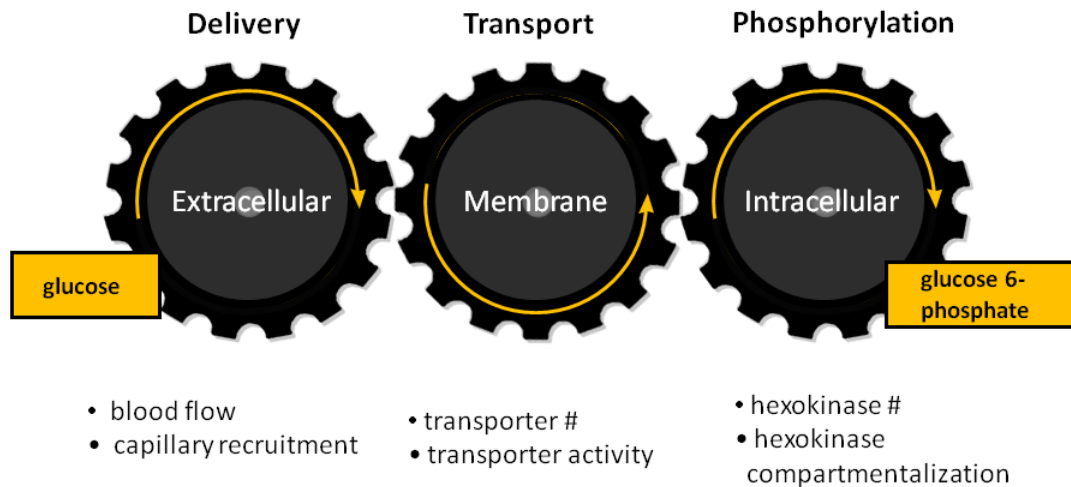
the aggressive management of hyperglycemia improved outcomes. However, with this treatment there runs a risk of inducing hypoglycemia which can be just as detrimental. The increase in the incidence of hypoglycemia may explain the conflicting outcome reports in subsequent studies (72, 106). Therefore understanding the principal mechanism for the underlying insulin resistance may allow the development of new tools to control the hyperglycemia without the confounding effects of insulin which can lead to an increased incidence of hypoglycemia.

Previous work in the McGuinness lab utilizing the conscious dog model has examined the impact of inflammation on glucose homeostasis. Hepatic blood flow was found to be decreased by ~20% in the presence of moderate endotoxin (108). The presence of endotoxin was found to increase the release of counterregulatory hormones such as glucagon, cortisol and epinephrine, which in turn lead to an increase in hepatic gluconeogenic precursors. This led to a significant increase in gluconeogenesis and was accompanied by increased hyperglycemia and hyperinsulinemia (105).

While the previous work in the lab focused on how infection impacted hepatic carbohydrate metabolism, the major focus of my dissertation examines glucose disposal by the periphery. Specifically, I look to define the underlying mechanisms that lead to decreased insulin-stimulated muscle glucose uptake (MGU) during acute inflammatory stress. To help understand this problem, I will first look at how glucose homeostasis is maintained and discuss the major tissues that are involved in this process. I will examine how physiologic regulators (insulin and exercise) augment and inflammatory stressors inhibit MGU.

MGU is a three-step process: the delivery of glucose to the muscle cell, transport of glucose into the muscle cell, and phosphorylation and subsequent metabolism of glucose within the muscle cell (Figure 1.1). Each step can be modulated by both physiologic and pathophysiologic processes. I will primarily focus on which step or combination of steps are affected by acute inflammatory stress induced by lipopolysaccharide (LPS) and how LPS limits the ability of insulin to augment MGU. The following chapters will discuss how the manipulation of key proteins involved in this process affect insulin's ability to increase the amount of glucose taken up by the muscle cell in this setting. I have concluded that acute inflammatory stress decreases insulin-stimulated MGU in a manner that is independent of defects in insulin signaling, which *in vitro* data suggest might also explain a decrease in insulin action. My data suggest that defects in glucose delivery secondary to the cardiovascular response to LPS is a major contributor to a decrease in insulin stimulated MGU. In addition we found that increasing muscle glucose transporter (GLUT4) capacity could partially overcome the impairment in MGU while increased muscle glucose phosphorylation capacity (hexokinase II) expression had no effect. Interestingly, the benefits of GLUT4 may be mediated by an indirect benefit on cardiovascular function.

Determinants of MGU



Wasserman *et al.*, 2009

Figure 1.1: Distributed control of muscle glucose uptake. Outlines how the three steps involved in the process of MGU are coupled to one another and illustrates the factors that influence each step.

Adapted from: Wasserman, DH (2009) Four Grams of Glucose. *Am J Physiol Endocrinol Metab.*, Jan;296:E11-21.

Glucose Homeostasis Maintenance

Glucose is a major source of energy in the body and its levels are tightly regulated. Plasma glucose concentrations are maintained despite fluctuations in the body's supply and demand of glucose. During a 24-h period, glucose concentrations average approximately 90 mg/dl with excursions to about 160 mg/dl after a meal. Mild

hypoglycemia (~60 mg/dl) can develop during prolonged exercise or fasting (63). Maintenance of euglycemia is very important because prolonged hypo- or hyperglycemia can have detrimental consequences on the body. There is a network of organs including the pancreas, liver, muscle, and brain that help to sustain normal blood glucose levels.

Glucose comes from two sources, ingested or produced by the body. The endogenous source is primarily the liver which can produce glucose through the processes of glycogenolysis, the breakdown of glycogen, or gluconeogenesis, the formation of new glucose from other substrates. Most ingested glucose that is not oxidized is stored as glycogen in the liver and muscle, but it can also be stored as fat in the setting of caloric excess. Glycogen stores can be broken down in the liver to offer a supply of glucose to the brain and other neural tissues that require glucose as the major oxidizable fuel. On the other hand, muscle glycogen serves as a local source of glucose due to the fact that muscle lacks glucose-6-phosphatase and therefore is unable to release free glucose into the circulation. Several sources supply precursors to support gluconeogenesis primarily in the liver, but it can also take place in the kidneys after a prolonged fast (121). The muscle provides lactate from incompletely oxidized glucose or from muscle glycogen breakdown and amino acids from muscle proteolysis. Adipose tissue releases glycerol. Several hormones are involved in these processes including glucagon, which stimulates glucose production, catecholamines, which mobilizes gluconeogenic precursors from muscle and adipose tissue as well as stimulates glucose production, and insulin, which opposes their actions (27).

Maintenance of plasma glucose levels require that changes in the rates of glucose delivery into the circulation are balanced by parallel changes in glucose removal by

peripheral tissues and vice versa. The major tissues responsible for the removal of glucose from the systemic circulation are brain, skeletal muscle and liver (80). The liver, adipose tissue, and muscle are all influenced by plasma glucose and insulin levels. While the liver and adipose tissue both play a central role in metabolic homeostasis, skeletal muscle comprises the bulk of insulin-sensitive tissue in the body and therefore plays an integral role in the maintenance of plasma glucose levels (Figure 1.2).

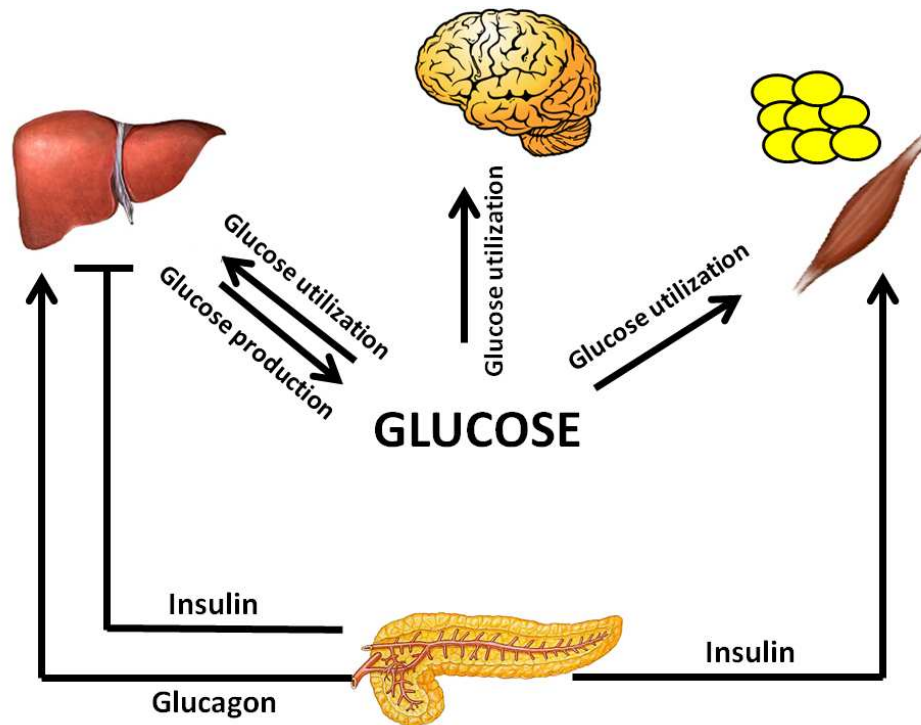


Figure 1.2: Major organs involved in maintaining glucose homeostasis.

The Liver's Role in Maintaining Glucose Homeostasis

The liver is unique in the fact that it is the only organ that is capable of both producing and consuming substantial amounts of glucose. During the fasted state a

continuous supply of glucose is essential for certain tissues, such as the brain, to function properly. The production of glucose by the liver is highly responsive to hormone secretions from the pancreas. Falling blood glucose levels leads to a decrease in insulin and an increase in glucagon release from the pancreas. Glucagon leads to an increase in cAMP levels, which is critical to the production of glucose. Hepatic glucose production on a minute to minute basis is primarily controlled by the stimulatory effects of glucagon and inhibitory effects of insulin (16, 97). Glucagon stimulates the mobilization of glycogen stores in a process known as glycogenolysis. This occurs through the stimulation of the enzyme glycogen phosphorylase which initiates the breakdown of glycogen to become free glucose. This process can lead to increases in glucose output within minutes.

However, during an extended fast, glycogen stores are depleted and gluconeogenesis becomes the primary source of glucose for the body. Gluconeogenesis, which is the metabolic pathway that results in the generation of glucose from non-carbohydrate carbon sources, is also stimulated by glucagon. Gluconeogenesis occurs if there is adequate delivery of precursor substrates such as lactate, glycerol, and alanine, which are by-products of carbohydrate, fat, and protein metabolism, respectively to the liver. Through a series of reactions these substrates are converted to glucose. A portion of this glucose will be delivered to the bloodstream to provide energy to peripheral tissues.

During the fed state glucose enters the body and has access to the liver via the portal vein. This leads to an increase in both glucose and insulin levels which act to suppress glucose output and stimulate glucose uptake by the liver. Insulin can act directly and indirectly on the liver to modulate the hepatic output of glucose. Indirectly insulin

has the ability to decrease hepatic glucose production by inhibiting glucagon secretion by the pancreas, reducing free fatty acid levels and gluconeogenic precursors, and causing changes in neural signaling relayed to the liver. Insulin acts directly on the liver by binding to hepatic insulin receptors and activating insulin-signaling pathways (52). Chronically, insulin modulates the gene expression of key enzymes of gluconeogenesis (118). Once in the liver glucose can be incorporated into glycogen or be utilized for glycolysis. Through a sequence of enzymatic events, glycolysis leads to the production of lactate and pyruvate. On a minute to minute basis it is the direct rather than the indirect effects of insulin that play a dominant role in the regulation of hepatic glucose production. In the case of endogenous insulin secretion the direct actions of insulin are responsible for 60-85% of the hormones inhibitory effect on the liver with the remainder being due to its indirect actions on muscle, fat, and the alpha cell (28).

Glucose has the ability to autoregulate its production and uptake by the liver, independent of changes in insulin and glucagon (38). While insulin has the ability to stimulate glucose uptake by the liver, physiological hyperinsulinemia by itself is relatively ineffective in promoting net hepatic glucose uptake. At basal levels of insulin and glucagon, hyperglycemia results in a modest suppression of glucose release from the liver and supraphysiological hyperglycemia is required to achieve substantial hepatic glucose uptake (17, 122). However when hyperglycemia is combined with an elevated insulin concentration the liver can be a significant consumer of glucose. Liver glucose uptake can be further augmented if glucose is delivered into the portal vein to create a negative arterial portal vein ($[P]>[A]$) glucose gradient as would occur following glucose ingestion (4).

An example of how rapidly the liver can augment hepatic glucose production to meet increased glucose demands is exercise. Hepatic glycogenolysis and gluconeogenesis increase during exercise to equal the increased rate of muscle glucose utilization in order to maintain euglycemia. Glucose output rises 50-100% during short durations of exercise and can increase 2 to 5 fold during moderate to heavy exercise (174). Increases in glycogenolysis and gluconeogenesis contribute to the increase in glucose during moderate intensity exercise. During prolonged exercise gluconeogenesis contribution to total glucose output increases as hepatic glycogen stores are gradually depleted. The increase in gluconeogenesis is facilitated by the marked increase in hepatic gluconeogenic precursor uptake (increases by 50% to 100%) during mild to moderate exercise, mostly due to the augmented availability and uptake of lactate (accounting for 30% to 40% of total glucose output) (174).

Insulin and glucagon play an important role in regulating hepatic glucose release during exercise. Insulin concentrations decrease even during light exercise, while glucagon levels rise during exercise, particularly if hypoglycemia ensues. Research in humans and dogs has demonstrated that the exercise-induced changes in insulin and glucagon account for a major proportion of the increase in hepatic glucose output. This takes place through augmentation of glycogenolysis and stimulation of both glucose precursor extraction and intrahepatic conversion to glucose (33, 177, 185). It is the tight coupling between the increase in glucose demand and a parallel increase in glucose production that allows euglycemia to be maintained during a metabolic stress like exercise. This contrasts with inflammatory stress where this tight coupling does not occur and hyper- or hypo- glycemia can develop.

Hepatic Glucose Production and Stress

During stressful situations changes occur that can have profound effects on glucose homeostasis. A prime example of this is during endotoxemia. The stress response associated with this condition consists of hypermetabolism, a hyperdynamic cardiovascular state, and inflammation (19). During stress, whole-body glucose uptake is increased due to increased non-insulin stimulated glucose uptake in tissues involved in the immune response such as the liver, lung, spleen, and wound organs (101, 110). Changes in glucose flux from the liver during this condition can be derived from changes in glycogenolysis, gluconeogenesis, or both. These alterations in carbohydrate metabolism can result in either hypo- or hyperglycemia.

Trauma and infection are generally hypermetabolic states characterized by increased energy expenditure, increased mobilization of endogenous fuels, and a marked elevation in the circulating hormone levels (99). During the early phase of endotoxemia the hyperglycemia seen during infection is due to increases in gluconeogenesis as well as glycogenolysis. Lactate and alanine are the main substrates for stress-related hepatic gluconeogenesis (182). McGuinness found that net hepatic alanine and lactate were increased by 34 and 54%, respectively during infection induced by a fibrinogen clot containing *E. coli* in the chronically catheterized dog model and a similar amount following the acute administration of endotoxin (104, 108). Lactate is converted to glucose in the liver. During sepsis the combined increase in lactate concentration and the net extraction of lactate by the liver (increased 3-fold) supports the increase in gluconeogenesis from lactate (180). This can lead to increased gluconeogenesis, which is normally suppressed by insulin but in the presence of increased inflammation this

regulation is lost, resulting in increased hepatic glucose output despite hyperinsulinemia. Hyperlactatemia is a common complication in patients with sepsis as well as animal models of endotoxemia with increased levels closely correlated with increased mortality (3, 18). In human subjects Gore *et al.* found that an increased rate of pyruvate production during sepsis leads to the accumulation of lactate in these patients (66). Bellomo *et al.* found that in dogs treated with a bolus infusion of *E. coli* endotoxin (1mg/kg) mean arterial blood lactate levels increased from 0.92 ± 0.11 to 1.60 ± 0.15 mmol/L (15). Similar increases in lactate levels due to endotoxin treatment have been seen in other studies (108, 157, 182). Catecholamine release and direct sympathetic stimulation elicit hepatic glycogenolysis, promoting hyperglycemia. Glucagon levels are normal or elevated during this phase while insulin levels are low relative to the hyperglycemia (54). Increased muscle glycogenolysis also promotes lactate formation by increasing the proportion of glucose that is directed to lactate which in turn can be used as a substrate for glucose production (6).

The increase in glucose production that occurs during the early phases of endotoxemia is not maintained and severe hypoglycemia is common in the latter stages (183). During endotoxemia there is increased glucose utilization via macrophage rich tissues such as the liver and spleen which require large amounts of glucose to function (92, 111). This coupled with reduced hepatic glucose output via impaired gluconeogenesis serves to potentiate the hypoglycemia seen in this setting (53, 103). In human studies, it was found that there is increased peripheral and hepatic insulin sensitivity, which was assessed using a hyperinsulinemic-euglycemic clamp 2 h

following the administration of a low dose of LPS (168). This can also lead to the development of hypoglycemia.

Phosphoenolpyruvate carboxykinase (PEPCK) is an important enzyme in gluconeogenesis and has been associated with endotoxin induced hypoglycemia. Deutschman *et al.* found that the induction of sepsis in rats was associated with a 66% reduction in levels of PEPCK mRNA and an attenuated response of PEPCK expression to stimulation by glucagon (42). This was also confirmed in studies by Canton *et al.* who found that hepatic mitochondrial PEPCK enzymatic activity is decreased by 38% in rats 6 h after LPS administration and this decrease combined with decreases in glucose-6-phosphatase play a key role in the manifestation of hypoglycemia and hyperlactatemia during endotoxemia (23).

Sepsis has been shown to induce hypertriglyceridemia in a variety of species (51, 79, 186). This increase in triglyceride production can be due to increased VLDL secretion from the liver, a decrease in the removal of VLDL-TAG from the circulation, or a combination of both. It is believed that both processes contribute to the increase. Fatty acids in the liver are re-esterified rather than oxidized resulting in increased VLDL-TAG synthesis. Jacoby *et al.* found that after injection with *E. coli* to induce sepsis followed by a 24 h fast, there was a 2-fold increase in *de novo* fatty acids and triglycerides in the livers of rats compared to fasted controls (95). However the rate of VLDL-TG appearance was decreased by 30% in these rats compared to fasted controls. This resulted in an accumulation of lipids in the liver. Despite the fall in VLDL-TG appearance plasma TG concentration increased due to a decrease in VLDL (\downarrow 66%) clearance rate. Others have found that VLDL production can increase (186). The decrease in VLDL clearance

was attributed to a decrease in lipoprotein lipase (LPL) activity in adipose tissue, soleus, and heart. Indeed, Scholl *et al.* found that sepsis induced hypertriglyceridemia is associated with the decreased ability of LPL-containing tissues to clear circulating triglycerides in rats (147). Muscle and adipose tissue biopsies from septic patients showed decreased LPL activity which is believed to contribute to the resulting hypertriglyceridemia (139). Hypertriglyceridemia is thought to be a protective response because it provides a readily available source of energy as well as has the ability to bind endotoxin and render it inactive.

The liver represents an important organ in the maintenance of glucose homeostasis due to its ability to both consume and produce glucose. There are many hormones that play a significant role in preserving the proper function of the liver during normal as well as stressful situations. The impact of endotoxic shock on the liver has been demonstrated in numerous studies. The changes in hepatic carbohydrate metabolism may serve as a metabolic adjustment to limit hepatic damage initiated during sepsis.

Adipose Tissue's Role in Maintaining Glucose Homeostasis

While it was once believed that adipose tissue only served as a storage site for energy, it is now known to play an active role in energy homeostasis. The predominant type of adipose tissue is white adipose tissue (WAT) which is mainly found in the subcutaneous region and around the viscera. It represents a major storage site for triglycerides which play an integral role in glucose homeostasis.

Hormones, as well as the autonomic nervous system, govern the storage in and mobilization of lipid from the adipose tissue. A rise in circulating insulin levels during the fed state promotes triglyceride storage in the adipose tissue. Insulin has a dual function when it comes to the storage of triglycerides: it inhibits lipolysis, which is the breakdown of lipids into fatty acids. This takes place by a mechanism involving the dephosphorylation and thus inhibition of hormone sensitive lipase (HSL), which is the rate-limiting enzyme in the hydrolysis of triglycerides to glycerol and free fatty acids. *In vivo*, selective inhibition of PDE-3 can completely abolish the antilipolytic effect of insulin in human adipose tissue (68). Simultaneously insulin stimulates triglyceride assembly from acylCoA and glycerol via acylCoA carboxylase (ACC) and fatty acid synthase (FAS). Thus insulin promotes both re-esterification of fatty acids as well as the *de novo* synthesis of fatty acids from glucose.

Insulin is also involved in promoting glucose uptake and utilization by fat cells. Fat tissue does not represent a major site of glucose uptake from the whole-body perspective however altered adipose tissue insulin sensitivity appears to be an early and potentially pivotal phenomenon in the development of insulin resistance and type 2 diabetes. The biological actions of insulin in the adipose tissue are mediated by high-affinity cell-surface receptors with intrinsic tyrosine kinase activity (26). Multiple studies have demonstrated that intracellular GLUT4 resides in two distinct, but related vesicular pools in adipocytes. Immunofluorescence analyses and subcellular fractionation techniques show that a significant fraction of GLUT4 is localized in endosomal vesicles constitutively recycling to the plasma membrane, together with other recycling proteins, including GLUT1 and the transferrin receptor (32, 35). However, GLUT4 located in the

'GLUT4 storage vesicle' compartment, which lacks endosomal markers, may contain more than 50% of the GLUT4 present in adipocytes, and is highly insulin-responsive (135). Thus, in the basal state, GLUT4 slowly recycles between the plasma membrane and the endosomal compartment. Insulin induces a marked increase in GLUT4 exocytosis, mainly from the insulin-responsive vesicle pool, and a small reduction in the endocytotic rate, leading to a net increase of GLUT4 molecules at the cell surface and of glucose uptake rates. Although adipose tissue accounts for only a small fraction of insulin-dependent glucose disposal, experimental animals with fat-selective knock-out of the GLUT4 gene show impaired glucose tolerance, suggesting that the functional integrity of adipose tissue is crucial in regulating intermediate metabolism (2).

Adipose tissue synthesizes and secretes cytokines that can affect the metabolism of adipose tissue as well as other organs (34). Cytokine release can be triggered by inflammatory stimuli and is also regulated by various hormones such as insulin, cortisol and catecholamines (50). Although fat cells are known to have the capacity to produce several cytokines, the greater part of cytokines released from adipose tissue have been argued to originate in cells of the stromal-vascular fraction of the tissue (48). Blood cells, e.g. monocytes, have been shown to migrate into adipose tissue and form resident macrophages, which seems to be enhanced in obesity (36). Such cells could substantially contribute to cytokine release of adipose tissue.

In adipocytes, energy is stored primarily as triglycerides, through increased glucose uptake and activation of lipid synthetic enzymes, including pyruvate dehydrogenase, fatty acid synthase and acetyl-CoA carboxylase. In the fasted state the fall in insulin triggers lipolysis through the activation of the sympathetic nervous system

and a rise in glucagon, epinephrine, and glucocorticoids. This process allows fatty acids to be released, which in turn can be oxidized by the liver and muscle. Lipolysis requires three enzymes: hormone sensitive lipase (HSL), which is regulated by reversible phosphorylation, is a key enzyme which mediates the hydrolysis of triacylglycerol (TAG) to monoacylglycerol (MAG), monoglyceride lipase (MGL) to hydrolyse MAG to glycerol and free fatty acids, and adipose triacylglycerol lipase which works in partnership with HSL to lead to the efficient mobilization of triglyceride stores. HSL also requires Perilipin proteins to enhance lipolysis because these proteins are necessary for its translocation to lipid droplets.

The main activators of the lipolytic cascade are catecholamines (88). Catecholamines are elevated in situations of enhanced energy demand, e.g. physical exercise, trauma and stress, and this occurs in order to ensure the short-term delivery of fuel to tissues. They bind to β -adrenergic receptors at the cell surface which mediate a cascade of reactions via elevated levels of cAMP which stimulates cAMP protein kinase (PKA) and in turn activates HSL. HSL activation provides glycerol and NEFA that can be further metabolized by various energy-demanding tissues.

Insulin resistance can originate in adipose tissue. Several factors secreted from the adipose tissue, including pro-inflammatory cytokines and NEFA, can impair insulin signaling, altering insulin-mediated processes including glucose homeostasis and lipid metabolism. Insulin resistance can lead to an increase in lipolysis, with a subsequent release of glycerol and NEFA into the circulation. The increased availability of NEFA can modulate endogenous glucose production by altering the contributions of glycogenolysis and gluconeogenesis to this process (90, 149). The secretion of pro-

inflammatory cytokines as well as NEFA from adipose tissue can also lead to skeletal muscle insulin resistance through impairments in insulin signaling and substrate competition (129, 179).

Adipose Tissue and Stress

Profound changes in lipid metabolism can occur with sepsis. Fat is the preferred fuel for oxidation in individuals with sepsis (155). Cytokines have been shown to increase lipolysis directly and indirectly and there are increased cytokine levels in response to endotoxin which are associated with marked increases in lipolytic activity (131, 169). Sepsis can impair the actions of insulin on fat metabolism, which can lead to increased plasma NEFA. In human patients with severe sepsis during an hyperinsulinemic-isoglycemic clamp there was a diminished sensitivity of lipolysis to an insulin infusion (24). The increased lipolysis provides increased plasma NEFA. The NEFA can be utilized in hepatocytes to enhance endogenous glucose production, for the formation of triglycerides, or synthesis of ketones and supplies glycerol for gluconeogenesis. Fat mobilization induced by stress can increase glycerol's contribution to glucose production by as much as 30% (181).

Septic patients have increased fat mobilization compared to fat oxidation. NEFAs are often released by adipose tissue in excess of what is needed for oxidation. Their subsequent metabolism represents a substrate cycling called the triglyceride-fatty acid cycle. Plasma NEFA are taken up by the liver and re-esterified into triglycerides, a key determinant of this is the rate of delivery of NEFA. These triglycerides are secreted into

the blood stream where they are eventually broken down into NEFA, taken up by adipose tissue and re-esterified into triglycerides completing the cycle (20). Patients with sepsis have a 4-fold increase in NEFA to triglyceride cycling (65). Nordenstrom *et al.* found in traumatized and/or septic patients, that with TPN there was a significant increase in NEFA turnover rate and yet there was a significant decrease in NEFA oxidation. This implied there is an increased rate in the “futile cycling” of FFA in the presence of glucose in ill patients (117).

However, in severe cases of sepsis there can actually be a decrease in fat oxidation. In the dog, Saakurai *et al* found that acute (4 h) high-dose TNF- α infusions led to a 20 and 42% decrease in the rate of appearance of glycerol and NEFA, respectively as well as a 23% decrease in fat oxidation (144). Indeed, Romanosky *et al.* found that there was a 37% decrease in whole-body NEFA turnover in dogs following endotoxin treatment (140). A possible explanation for this is the significant reduction in adipose tissue perfusion post-endotoxin treatment. Compromised adipose tissue blood flow can lead to reduced transport of NEFA which can account for changes in whole body fat oxidation (84).

Although adipose tissue was once thought to play an insignificant role in glucose homeostasis, it is now known to contribute greatly to the process. Hormones, cytokines, and changes in NEFA released by adipose tissue can affect a host of tissues including the brain, liver and muscle. Sepsis leads to alterations in the metabolism of lipids which can lead to increased or in severe cases, decreased mobilization of fat. These alterations can occur due to changes in hormones and/or cytokines released in response to endotoxemia which can have profound effects on lipid metabolism in this and other tissues.

Distributed Control of Muscle Glucose Uptake (MGU)

Glucose uptake by the skeletal muscle is a tightly coupled process that is distributed over several steps which include the rate of delivery of glucose from the blood to the sarcolemma, transport of glucose across the plasma membrane, and intracellular phosphorylation which represents the committed step of the process (Figure 1.1) (176). Each step is regulated by a number of factors. Blood flow and capillary recruitment are important determinants of glucose delivery to the muscle. Transport of glucose across the plasma membrane takes place via facilitated diffusion by the GLUT family of transporters. Under basal conditions GLUT1 is primarily responsible for glucose uptake by the muscle. However, during insulin-stimulated conditions or exercise, GLUT4 is translocated from intercellular pools to the cell surface and leads to an increase in permeability of the membrane to glucose. Once inside the cell, glucose is phosphorylated to glucose-6-phosphate (G-6-P) by hexokinase (HK). The insulin-regulated form of this enzyme found in skeletal muscle is HKII. The phosphorylation of glucose is determined by several factors including the localization of hexokinase within the cell, its activity, as well as the amount of any substrates (such as glucose-6-phosphate) located within the cell that have the ability to regulate this process.

Seminal studies by Dr. Park's laboratory found that in the basal state glucose transport was the primary limitation to MGU and that this shifts to phosphorylation during insulin-stimulated conditions (112, 113, 132). With increasing glucose levels, delivery of glucose became a factor. Since this time, the belief that the regulation of MGU is distributed has been challenged. The discovery of the requirement of insulin-stimulated glucose transporter translocation from sub-cellular compartments to the

plasma membrane for glucose uptake have led many to believe it is the rate-limiting step in the process (37, 156). However, many of these studies have examined the muscle in isolation and did not take in to account what occurs under physiological conditions (70, 136). Recently, elegant studies performed by the Wasserman laboratory examined mouse models overexpressing key proteins involved in MGU under physiological conditions. These studies have shown that, as Park *et al.* suggested, the regulation of MGU can occur at all three steps (57, 59, 61, 69). However, depending on the condition the primary control may shift from one step to another or be shared among multiple steps. Thus depending on the physiological or pathophysiological setting one or more steps may play a role in determining how much glucose is taken up by the cell. Therefore, each of these steps may become a barrier to determining MGU and its response to insulin.

Glucose Delivery

Glucose must travel from the blood to the interstitium and then be transported to the intracellular space where it is phosphorylated to glucose 6-phosphate. The blood glucose concentration, muscle blood flow, and recruitment of capillaries to muscle determine glucose movement from the blood to the interstitium. Clark *et al.* and others determined that capillary recruitment is increased following insulin infusion and that insulin stimulation of capillary recruitment may proceed changes in total blood flow (31, 171, 172). Increased muscle capillary recruitment increases the surface area for diffusion from the blood and decreases the diffusion distance for glucose to muscle. This in turn influences how much glucose is taken up by the muscle.

Endothelium-derived nitric oxide (NO) mediates insulin-induced stimulation of the perfusion of skeletal muscle which can lead to increased glucose disposal (86, 146). Insulin enters the endothelium via caveolae after binding to its receptor. Activation of the insulin receptor leads to phosphorylation of multiple substrates including AKT and endothelial nitric oxide synthase (eNOS) which generates NO. eNOS is expressed in skeletal muscle where it can play a role in regulating glucose homeostasis. Duplain *et al.* found there was a 40% decrease in insulin-stimulated glucose uptake in eNOS knockout mice compared to control mice and this insulin resistance was related to impaired NO synthesis (44). Indeed, when the nitric-oxide synthase inhibitor L-NMMA was used, there was diminished blood flow and glucose uptake in humans (8).

There have been studies in animal and human models that demonstrate a correlation between delivery and muscle glucose uptake. Work done by Baron *et al.* demonstrated that in humans insulin-stimulated muscle blood flow contributes to insulin-responsiveness and sensitivity (9, 10). Conversely, impairments in insulin-induced capillary recruitment result in decreased skeletal muscle glucose uptake (30, 87, 187). In rats administered with an agent to prevent insulin-stimulated capillary recruitment *in vivo* there was an impairment in muscle glucose uptake (134).

Exercise increases both muscle blood flow and glucose uptake. Exercise is an effective way of increasing muscle glucose uptake independent of increases in insulin. During exercise, there is a marked increase in muscle blood flow that replenishes the interstitial glucose as it perfuses the working muscle. In humans there is a tight correlation between muscle blood flow and glucose uptake by the working limb (76). Exercise-induced increases in glucose delivery effectively maintain interstitial glucose in

the muscle such that an increase in fractional glucose extraction is not required to sustain an increase in MGU.

While there are multiple ways in which delivery of blood flow to the skeletal muscle can be increased, there are also settings in which it is inhibited. During the stress response peripheral vasoconstriction and vasodilation have been observed. Sepsis produces relative hypovolemia from venous and arterial dilatation, which reduces right ventricular filling. Investigators have shown that there is a reduced left ventricular ejection fraction, increased end-diastolic and end-systolic volumes (increased compliance) and normal or decreased stroke volume, reduced systemic vascular resistance, and compensatory tachycardia as the characteristic pattern of sepsis-induced heart dysfunction (41, 124, 125). Tissue hypoperfusion can be present in the presence of normal blood pressure and adequate cardiac output. This is related to the maldistribution of blood flow at the regional and microvascular level (143). The changes in flow can be due to endothelial cell dysfunction, altered local perfusion pressures due to regional redistribution of blood flow and functional shunting (75, 152).

Another way that delivery is inhibited is through the release of pro-inflammatory cytokines. Pro-inflammatory cytokines are believed to inhibit insulin action, leading to insulin resistance. A 3 h TNF- α infusion in rats prevented the insulin-mediated increase in femoral blood flow and capillary recruitment. This also led to a 61% decrease in hind-leg glucose uptake as well as ~50% decrease in muscle glucose uptake as measured by 2-deoxy glucose (187). IL-6 through activation of TNF- α has also been shown to decrease capillary recruitment in human aortic endothelial cells (188).

Glucose Transport

Insulin is released by the pancreatic β -cells and binds to its receptors on the skeletal muscle surface where it activates a cascade of signaling events. Insulin is distributed more slowly to the compartment corresponding to the skeletal muscle than to other compartments (11). Chiu *et al.* demonstrated that an injection of insulin directly into the interstitium of skeletal muscle is followed by a prompt increase in glucose uptake (29). They concluded that it is the transport of insulin, and not the diffusion within the interstitial space that accounts for the slow insulin effect on glucose disposal.

Skeletal muscle contains two glucose transporters. Glucose transporter 1 (GLUT1) is the basal glucose transporter responsible for the low-level basal glucose uptake required to maintain respiration in all cells. Glucose transporter 4 (GLUT4) is translocated to the plasma membrane in response to insulin or independent of insulin in response to exercise (83, 138). In the skeletal muscle glucose is stored as glycogen, released as lactate, or is oxidized. GLUT4 is highly expressed in both the adipose tissue and skeletal muscle. Insulin released by the pancreatic β -cells bind to its cell surface receptors, leading to a cascade of signaling events which begins with the autophosphorylation of the insulin receptor. Several signaling events including the phosphorylation of the insulin receptor substrates (IRS) and AKT lead to the translocation of GLUT4 from intracellular vesicles to the plasma membrane (Figure 1.3) (126).

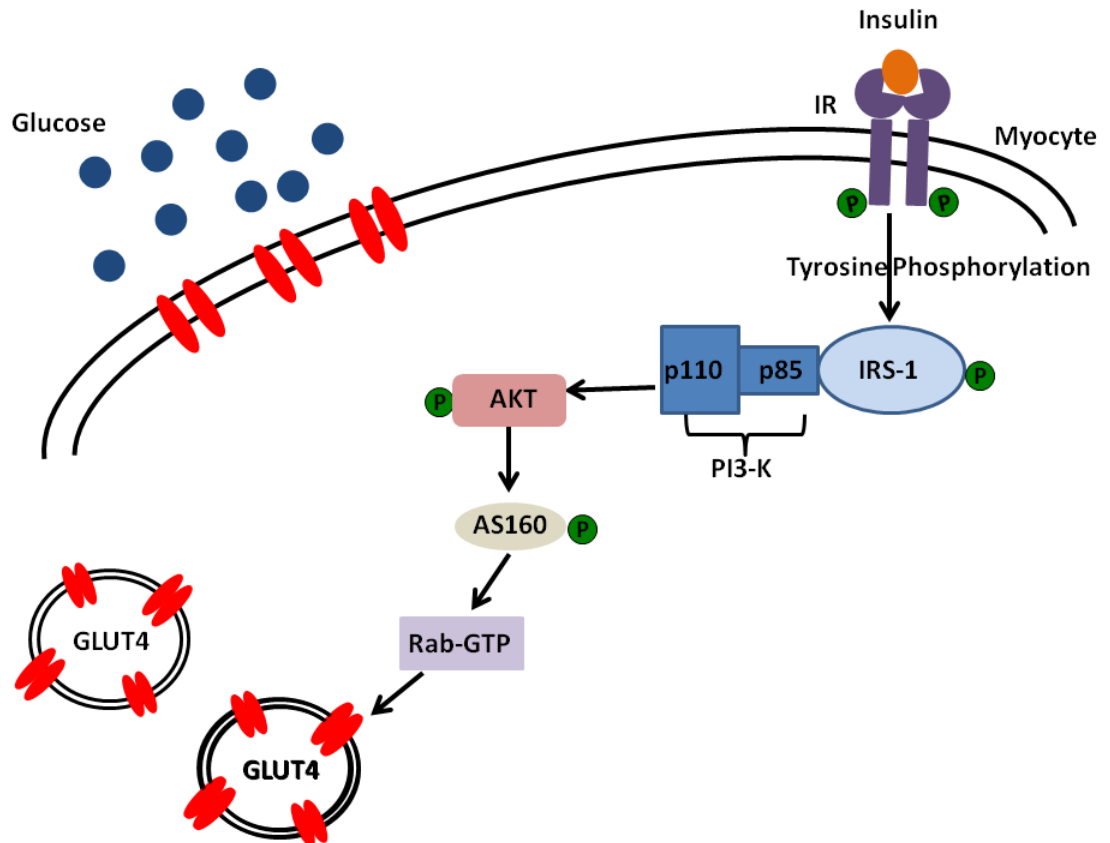


Figure 1.3: Insulin stimulates AKT activation through the phosphorylation of upstream mediators IRS-1 and PI3-K. Activated AKT phosphorylates AS160 on threonine residues. Phosphorylation of AS160 inhibits Rab-GTPase-activating protein (GAP) which promotes the conversion of GDP Rab to the more active GTP Rab. This allows GLUT4 storage vesicles to move to and fuse with the plasma membrane.

Genetically engineered mouse models have offered insight to the importance of GLUT4 in whole-body metabolism. Due to the upregulation of compensatory mechanisms, the GLUT4^{-/-} mouse does not provide much information regarding the importance of GLUT4 in the maintenance of glucose homeostasis (78, 153). However, heterozygous GLUT4^{+/-} mice have been shown to be insulin resistant (141, 154) and overexpression of GLUT4 in the skeletal muscle of these mice normalizes insulin

sensitivity and glucose tolerance (163). Conditional depletion of GLUT4 in the skeletal muscle causes insulin resistance (2, 190). In muscle-specific GLUT4 knockout mice, MGU is impaired but despite insulin resistance the accompanying hyperglycemia partially overcomes the defects in glucose transport capacity (81). On the other hand, mice that overexpress GLUT4 in the skeletal muscle are highly insulin sensitive and glucose tolerant (161, 162).

Cytokines released during inflammation can affect glucose metabolism directly or by augmenting glucoregulatory hormone secretion. Cytokines can also inhibit insulin release (107). In endothelial cells TNF- α reduces tyrosine phosphorylation of the insulin receptor. It also blunts tyrosine phosphorylation of IRS-1 in muscle, hepatocytes, and adipocytes. Furthermore lipopolysaccharide, through the Toll-like receptor 4 (TLR4) pathway activates nuclear factor-kappa B (NF κ B) which triggers the pro-inflammatory cascade further inducing insulin resistance.

Inflammation has also been shown to increase the levels of glucose transporter in a non-insulin stimulated manner. In L6 myotubes treated with endotoxin, Lee *et al.* found that there was increased glucose extraction from the medium accompanied by increased production of glucose transporters *in vitro* (96). Vary *et al.* found that sepsis induced a 67% increase in glucose uptake compared to control rats and led to a 1.7-fold increase in GLUT1 protein expression in rat skeletal muscle (170). Similar results were seen in the muscle of 10-day old rats treated with LPS compared to saline controls. GLUT1 mRNA was also increased 1.5-fold in LPS-treated rats (12). Increased basal glucose transporters can lead to increased glucose uptake without hyperinsulinemia. This stress-induced

glucose uptake promotes glycolytic flux with increased pyruvate and lactate production or aerobic glycolysis (184).

Glucose Phosphorylation

The enzyme hexokinase (HK) catalyzes the committed step in muscle glucose metabolism, the phosphorylation of glucose to form glucose-6-phosphate (G6P), essentially trapping glucose in the muscle. This helps to maintain the downstream concentration gradient which permits facilitated glucose transport into the cell. Once G6P is formed in the muscle there are two possible fates, the glucose can be stored as glycogen or it can be further metabolized in the myocyte.

HK is regulated by many factors. HKII, which is found in skeletal muscle, is a low K_m isozyme meaning it has a high affinity for its substrate glucose however it has a relatively low V_{max} . The activity of the enzyme in skeletal muscle (and adipose tissue) is regulated by insulin and is proportional to the mRNA levels located in the tissue (133). HKII activity can be inhibited through feedback regulation by its product G6P. HKII location in the cell plays an important role as well. It is associated with the mitochondria through binding at the porin providing direct access to ATP which is necessary to catalyze the reaction.

Glucose phosphorylation and transport are tightly coupled with one another. The rapid translocation of GLUT4 to the plasma membrane is stimulated by insulin which in turn stimulates the rate of transcription of the HKII gene. This combination leads to increased glucose utilization. It has been suggested that while glucose phosphorylation is

not a barrier to glucose uptake during the basal state, under conditions where the plasma membrane becomes very permeable to glucose (\uparrow GLUT4, i.e. insulin-stimulation or exercise) phosphorylation becomes a site of resistance (69, 77). Thus HK becomes an important site of regulation (57). The fraction of HKII bound to mitochondria, which constitutes the active state, increases in human skeletal muscle from 50% in the basal state to 75% after 30 min of exposure to physiological insulin (173). Studies have been performed utilizing mice that over- and under-express HKII to determine its role in MGU. Overexpression of HKII increased glucose utilization in the presence of physiological hyperinsulinemia (25, 57, 61). Partial hexokinase knockout mice (HK^{+/-}) have a 25% decrease in insulin action and are impaired during insulin-simulated glucose uptake (60).

A serious problem that occurs during severe sepsis is organ hypoperfusion. This can have effects at the cellular level on mitochondria, which are provided with inadequate oxygen. Lack of oxygen delivery to the cell prompts a stall in the transfer of electrons to the mitochondrial electron transport chain subsequently decreasing acetyl CoA entry into the TCA cycle. Mitochondrial oxidative phosphorylation fails and energy metabolism becomes dependent on anaerobic glycolysis, HKII relies on its association with the mitochondria for the conversion of glucose to G6P. This interaction supplies hexokinase with direct access to ATP generated by the mitochondria which is a necessary substrate for this enzyme's function. When mitochondrial function is impaired, there is an increase in the production of cellular lactate which is indicative of widespread inadequate tissue oxygenation (178). This limits glucose oxidation, increases lactate levels, and can in turn lead to hyperglycemia.

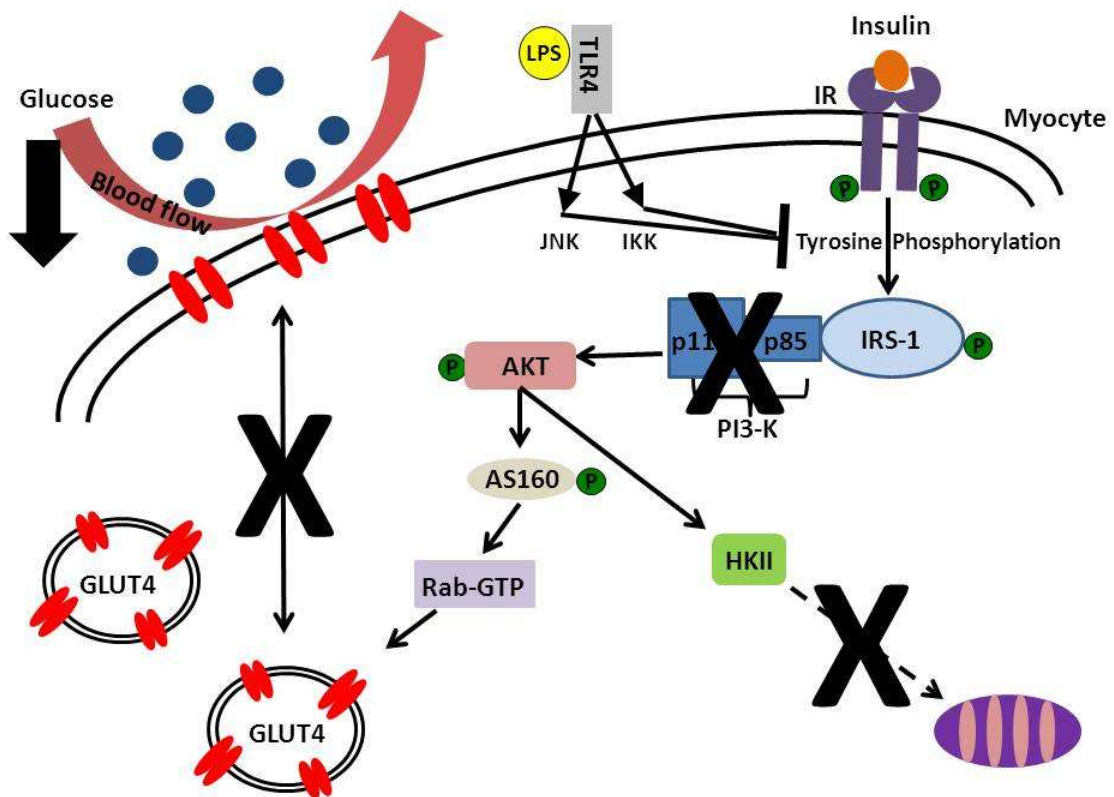


Figure 1.4: Proposed mechanism by which LPS inhibits glucose uptake by the muscle. LPS binds to its receptor on TLR4 and activates the JNK/IKK pathway. This leads to inhibitory phosphorylation of key enzymes in the insulin signaling pathway. This in turns inhibits GLUT4 tranlocation to the plasma membrane as well as HKII binding to the mitochondria. LPS is known to impair tissue blood flow which by decreasing glucose delivery could in turn decrease muscle glucose uptake.

Current Treatments and Controversies

While hyperglycemia during the stress response is thought to be necessary to maintain fuel to the non-insulin-dependent obligatory glucose consuming tissues such as the brain, phagocytes, and reparative cells, there has been evidence that preventing even

moderate hyperglycemia during critical illness improves outcomes (166). van den Berghe *et al.* reported that intensive insulin therapy (maintaining glucose levels between 80 and 110 mg/dl) was effective to control glycemia in the intensive care unit (ICU) (166). It led to a reduction in mortality in the intensive care unit by 8% while conventional insulin treatment (maintaining glucose levels between 180 and 200 mg/dl) only led to a 4% decrease. These results lead to administration of exogenous insulin as the primary treatment for hyperglycemia in the ICU. In additional studies, this same group found that following intensive insulin therapy post-mortem skeletal muscle biopsies contained significantly higher GLUT4 and HKII mRNA expression levels by 70 and 36%, respectively leading to increased peripheral glucose uptake (109). This was corroborated by an increased IRS-1-PI3-kinase association and increased AKT phosphorylation in skeletal muscle (94).

However, a recent large scale randomized trial indicated that such glycemic control is not effective in reducing mortality in critically ill patients. The Normoglycemia in Intensive Care Evaluation — Survival Using Glucose Algorithm Regulation (NICE-SUGAR) study sought to compare intensive insulin therapy to conventional insulin therapy and determine mortality (67). The study found that patients did not benefit from intensive insulin therapy regardless of whether they were in the surgical or medical ICU setting. This tight glycemic control actually increased the risk of hypoglycemia and complications arising from hypoglycemia. Consequently, there was no overall survival benefit in critically ill patients.

Clinical Significance

There is a dysfunction of glucose homeostasis in critically ill patients which results in hyperglycemia, regardless if the patient has previously been diagnosed with diabetes. Correlations have been made between glucose levels and mortality. A major cause of the hyperglycemia is insulin resistance, which is characterized by increased gluconeogenesis and impaired insulin-mediated glucose uptake. Sepsis increases proinflammatory cytokine production which is a major contributor to the underlying insulin resistance. The mechanisms underlying altered glucose metabolism and insulin action in the setting of sepsis need to be understood better to permit rational and targeted applications of protocols for intensive glycemetic control.

The Leuvan SICU study delineated peripheral MGU as the major glucoregulatory target for exogenous insulin in these patients. The decreased morbidity and mortality among acutely ill patients managed in a surgical ICU for more than 3 days and treated with intensive insulin therapy has been suggested to be due to multiple factors including improved glucose transport via GLUT4 as well as increased hexokinase expression. Although the outcomes regarding intensive insulin therapy have been mixed, one common theme in the ICU is marked increases in hypoglycemia and/or glucose variability, both of which are associated with increased morbidity and mortality. By defining how inflammation affects the controllers of MGU, therapies can be incorporated to correct insulin resistance thereby lowering insulin requirements and increasing positive patient outcomes in this setting.

Research Objectives

Glucose delivery, transport, and phosphorylation are closely coupled to one another which can present difficulties in assessing impairments in the distributed control of MGU. The general aim of this body of work was to assess the effect of acute inflammatory stress on skeletal MGU *in vivo*. Specifically we are interested in determining which of the 3 steps controlling MGU serves as the major barrier to the uptake of glucose by the skeletal muscle in this setting. To assess the role of a given step we use mice that overexpress key proteins involved in the process and examine if they modulate MGU. To induce inflammation we utilized lipopolysaccharide (LPS), which is found in the outer membrane of gram-negative bacteria and acts as an endotoxin, to elicit an immune response in C57BL/6J mice. The following specific aims were addressed:

1. To elucidate the physiological dose-dependent effects of LPS on the delivery of glucose and on insulin-stimulate MGU *in vivo* in C57BL/6J mice.
2. To determine if overexpression of the protein primarily responsible for insulin-stimulated glucose transport in skeletal muscle, glucose transporter 4 (GLUT4), will lead to a decrease in the impairment in insulin-stimulated MGU caused by acute inflammatory stress in conscious C57BL/6J mice *in vivo*.
3. To delineate whether increased glucose phosphorylation capacity through overexpression of hexokinase II (HKII) in skeletal muscle will improve insulin-stimulated MGU induced by acute inflammatory stress in conscious C57BL/6J mice *in vivo*.

CHAPTER II

MATERIALS AND METHODS

Animal Care and Husbandry

The Vanderbilt University Institutional Animal Care and Use Committee approved all procedures performed and the NIH guidelines for the care and use of laboratory animals were followed. All of the experiments were performed on male mice with the C57BL/6J background at three months of age. At three weeks of age mice were weaned and separated by gender. A tail biopsy was obtained to isolate DNA by the DNeasy Tissue Kit (Qiagen, Valencia, CA.) Identification of transgenic mice was performed by polymerase chain reaction (PCR). The PCR primers used to determine the genotype were as follows:

GLUT4^{Tg}: 5'-GGTTACAAATAAAGCAATAGCATCAC-3'

5'-GAGTATTTAGGGCCAGATGAGAAC-3'

HKII^{Tg}: 5'-GATATCGACATTGTGGCTCTGGTG-3'

5'-GTTCAGTGAACCCATGTCAATCTC-3'

Mice were maintained at 23°C in micro-isolator cages on a 12-h light/dark cycle with free access to food and water. Mice were fed a standard rodent chow.

Mouse Models

Genetic Manipulations

Mouse models with increased capacity for glucose transport and phosphorylation were utilized. Transgenic mice on a C57BL/6J background for the hGLUT4-11.5 construct (GLUT4^{Tg}) were originally created by Dr. Bess Adkins-Marshall and obtained from Dr. David Wasserman (119). The GLUT4^{Tg} increases the GLUT4 protein content 2- to 4-fold in the skeletal muscle of C57/BL/6J mice. Mice that overexpress HKII specifically in skeletal muscle (HK^{Tg}) were created by Dr. David E. Moller and obtained from Dr. David Wasserman (25). The mice were originally on a FVB/NJ background. HKII overexpression in the skeletal muscle was created using a transgene containing the human HKII cDNA driven by the rat muscle creatine kinase promoter. These mice were backcrossed on a C57BL/6J background for at least 5 generations in the Wasserman laboratory. The HK activity in the transgenic mice is increased 3-, 5-, and 7-fold in the soleus, gastrocnemius, and superficial vastus lateralis (SVL) muscles, respectively (25).

Surgical Procedures

The surgical procedures utilized to implant chronic catheters have been described previously (5, 115). Catheters are prepared prior to surgery. The arterial catheters are made from polyethylene tubing (PE-10) that is connected to silicone tubing (0.3 mm I.D., and 0.64 mm O.D.) 25 mm long while jugular vein catheters are made from silicone tubing (0.3 mm I.D., and 0.64 mm O.D.). These catheters are connected to stainless steel tubes (0.3 mm I.D., 0.41 mm O.D., 15 mm) bent into an L shape. On the free end of the L

shaped stainless steel tube a 20 mm piece of Micro-Renathane tubing (0.36 mm I.D., and 0.84 mm O.D.) is attached. The L shaped stainless steel tubes attached to an arterial and a jugular vein catheter are bundled together with silicone tubing (0.76 mm I.D. and 1.65 mm O.D.) and anchored with Silastic medical adhesive (Silicone Type A). The catheters and the Micro-Renathane-stainless steel tubing are heat sterilized.

Mice were anesthetized with isoflurane. Following anesthesia, the skin on the interscapula and the right and left hand side of the neck was shaved and sterilized with 10% povidone-iodine. Surgery was initiated with the loss of foot withdrawal and corneal blinking reflex. A longitudinal incision (~5 mm) was made over the spot where the anterior jugular, acromiodeltoid, and cephalic veins join together. The connective tissue surrounding the junction was removed and two thin threads of silk (6-0 Silk, Davis+Gech) were passed under the jugular vein below the junction, separated by ~ 3 mm. The cephalic thread is placed below the joint and tied as well as a clamp on the artery to prevent bleeding. An incision is made below the ligature and the catheter is inserted 10 mm into the lumen. A blunt needle (16 gauge) is inserted through the incision on the interscapula and pushed subcutaneously until the end comes out through the incision in the neck. The catheters were pulled through the needle and the incisions were sutured. The catheters are connected to stainless steel tubes and the tubing was implanted under the skin on the interscapula. The implanted catheter was flushed with saline containing 200 IU heparin/ml and 1 mg ampicillin/ml. The mice were injected subcutaneously with 150 mg/kg ampicillin. Animals were individually housed after surgery and body weight was measured daily between the surgery and experiment.

In Vivo Metabolic Experiments

Hyperinsulinemic-Euglycemic Clamp and Saline Control Experiments

All metabolic experiments were performed as follows. Mice were not used in experiments unless their body weight was within 10% of their body weight prior to catheter implantation. Following a ~5-day postoperative recovery period a hyperinsulinemic-euglycemic clamp and saline control experiments were performed. For metabolic studies conscious, unrestrained mice were placed in an ~1-L plastic container lined with bedding at 7:30 am and fasted for 5 h ($t = -300$ min). The mice were immediately connected to a Dual Channel Stainless Steel Swivel (Instech Laboratories, Plymouth Meeting, PA) to allow simultaneous jugular vein infusion and sampling of arterial blood. Mice were not handled and were allowed to move freely to eliminate stress. At $t = -240$ min measurements of mean arterial blood pressure (MAP) were taken from the carotid artery utilizing a Micro-Med, Inc. Blood Pressure Analyzer (Louisville, KY). An arterial blood sample (~50 μ l) was drawn for measurement of blood glucose and plasma cytokine levels. Mice then received a bolus of vehicle or *E. coli* endotoxin (LPS; 0111:B4) (Lot#129K4025, Sigma-Aldrich, St. Louis, MO) at a dose of 1 μ g/gBW (low-dose) or 10 μ g/gBW (high-dose) into the jugular vein catheter. Five μ Ci bolus of [3 H]-D-glucose was given into the jugular vein at $t = -120$ min followed by a constant infusion at a rate of 0.05 μ Ci/min. After a 2 h equilibrium period at $t = 0$ min an additional MAP was taken followed by a baseline arterial blood sample (~150 μ l) for measurement of blood glucose, [3 H]-D-glucose, hematocrit, plasma insulin, and plasma cytokine levels. Red blood cells from a donor mouse on a C57Bl/6J background were washed with 0.9%

heparinized saline and reconstituted in an equal volume of 0.9% heparinized saline (hematocrit ~50%) and infused at a rate of 4 μ l/min for the duration of the study to minimize falls in the hematocrit. Insulin or saline was infused at 4.0 mU/kg/min, 2.5 mU/kg/min, or 2.0 mU/kg/min depending on the treatment. Euglycemia was maintained by measurement of arterial blood samples (~1 μ l) every ten minutes and infusion of 50% dextrose as necessary. At t= 70, 80, 90 and 100 min, blood samples (~50 μ l) were taken to determine [3-³H]-D-glucose. At t= 100 min, a 13 μ Ci bolus of 2-deoxy [¹⁴C] glucose ([2-¹⁴C]DG) was administered into the jugular vein catheter. At t = 102, 105, 110, 115, and 125 min arterial blood (~50 μ L) was sampled to determine blood glucose, plasma [3-³H]-D-glucose and [2-¹⁴C]DG. At t= 125 min, a final arterial blood sample (~150 μ l) was withdrawn to assess circulating hormones and plasma [2-¹⁴C]DG. The mice were then anesthetized with an infusion of pentobarbital (70 mg/kg body weight) and the soleus, gastrocnemius, superficial vastus lateralis (SVL), gonadal adipose tissue (AT), liver, heart, and brain were excised, immediately frozen in liquid nitrogen, and stored at -70°C.

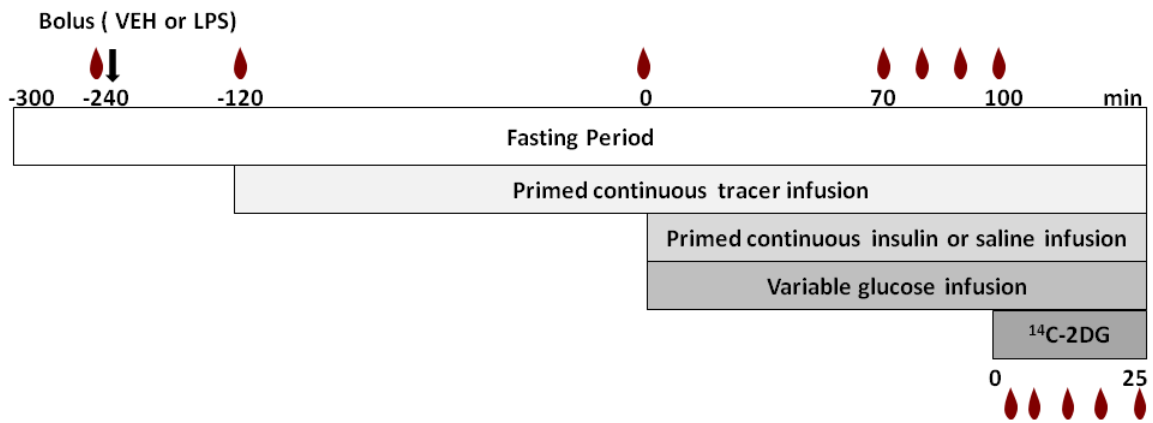



Figure 2.1: Protocol for the *in vivo* metabolic experiments. Experimental protocol for the hyperinsulinemic-euglycemic clamp and saline control experiments. Mice were fasted for 5 h (t= -300 min) prior to the beginning of the experiment. A 13 μ Ci bolus of ¹⁴C-2DG was injected after 100 min of the insulin or saline infusion.  indicates arterial blood sampling.

Indirect Calorimetry

Oxygen consumption (VO_2) and carbon dioxide production (VCO_2) were measured by an Oxymax indirect calorimeter (Columbus Instruments, Columbus, OH). Air flow was set at 0.60 l/min and mice were housed individually for 1 day before entering the calorimeter. After a 1 h adaptation to the metabolic chamber, VO_2 was measured in individual mice for 1 min at 15-min intervals for a total of 48 h under a consistent environmental temperature (22°C). Following 48 h of baseline measurements, food was removed and intraperitoneal injections of vehicle (n= 5), low- (n= 6) or high-dose (n= 9) LPS were administered. VO_2 was calculated for 8 h following the IP

injections. VO_2 is expressed as the volume of O_2 consumed per kilogram body weight per hour.

Echocardiography

Transthoracic echocardiography was performed using a system (Sonos 5500, Agilent, Andover, MA) with a 15-MHz high frequency linear transducer at a frame rate of 100 frames/sec. All images were acquired at a depth setting of 20 mm. Images were acquired at two time points: $t = 0$ min, which represents the time immediately prior to an injection of VEH or LPS and at $t = 360$ min. The mouse was picked up at the nape of its neck and an ultrasound-coupling gel was applied to the precordium, with the ultrasound probe. Two-dimensional targeted M-mode echocardiographic images were obtained at the level of the papillary muscles from the parasternal short-axis views and recorded at a speed of 150cm/s (maximal temporal resolution) for measurements of heart rate. All other measurements were made on screen using the digitally recorded signals. These measurements were used to calculate stroke volume and cardiac output (142, 158):

$$\text{End Diastolic Volume } (\mu\text{L}) = (7/(2.4+\text{LVIDd})) * (\text{LVIDd}^3)$$

$$\text{End Systolic Volume } (\mu\text{L}) = (7/(2.4+\text{LVIDs})) * (\text{LVIDs}^3)$$

$$\text{Stroke Volume } (\mu\text{L}) = \text{End Diastolic Volume} - \text{End Systolic Volume}$$

$$\text{Cardiac Output } (\text{mL} \cdot \text{g}^{-1} \cdot \text{min}^{-1}) = (\text{Stroke Volume} * \text{Heart Rate}) / (\text{Body Weight (g)} * 1000)$$

Where LVIDd and LVIDs are left ventricular internal dimensions during diastole and systole, respectively.

Blood Flow Analysis

Renal blood flow was estimated utilizing the clearance of para-amino hippuric acid (PAH). At t= -120mins, mice received a constant infusion of PAH dissolved in saline into the jugular vein at a rate of 24 $\mu\text{g/g/min}$. Plasma samples were taken at t= -120, 0, 60, and 120 min. The plasma was diluted 1:5 in $\text{Ba}(\text{OH})_2$ and ZnSO_4 , centrifuged at 13,000rpm for 5 min, and the supernatant was diluted 1:6 in ddH₂O. The samples were then diluted 1:6 in the PAH reagent (5g dimethylaminobenzaldehyde, 300mL 95% ethanol, 20mL 2N HCl, and ddH₂O to a final volume of 500mL) and the absorbance of PAH was determined at 465 nm. The PAH clearance (mL/kg/min) was calculated as follows:

$$\text{PAH clearance} = \frac{\text{PAHi}}{[\text{PAH}]} * \frac{1}{(1 - \text{Hct})}$$

Where:

PAHi= PAH infusion rate ($\text{mg}\cdot\text{kg}^{-1}\cdot\text{min}^{-1}$)

[PAH]= arterial plasma PAH concentration (mg/ml)

Hct=hematocrit ratio

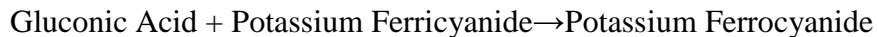
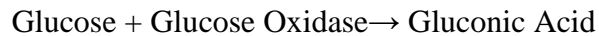
Microsphere Isolation. Microspheres were utilized to measure the effect of inflammation on tissue blood flow. Mice were fasted at t=-300 min and at t=-240 min they received a bolus of either VEH or LPS. At t=120min, mice were injected with 50 μL of microspheres

(Dye-Trak VII, Triton Technology, INC, San Diego, CA) followed by 50 μ L saline into the carotid artery. Mice were anesthetized and tissues were excised.

Processing of Plasma Samples

Blood Glucose Concentration

Blood glucose concentrations were measured every 10 min (beginning at t=-10) during the hyperinsulinemic-euglycemic clamp and the saline control experiments. Approximately 1 μ l of whole blood was obtained and blood glucose concentrations were determined using the BD Logic Blood Glucose Monitor (Franklin Lakes, NJ). The monitor has a glucose oxidase biosensor.



The electrode oxidizes the ferrocyanide, which generates a current directly proportional to the glucose concentration.

Plasma Immunoreactive Insulin

Immunoreactive insulin was measured on plasma samples at t=0, 100, and 125 min. The samples were analyzed via Linco Rat Radioimmunoassay kit (Linco Research, Inc., St. Charles, MO) using a double antibody procedure. This assay utilized ^{125}I -rat insulin and a guinea pig-anti-rat insulin primary antibody that equally cross-reacts with

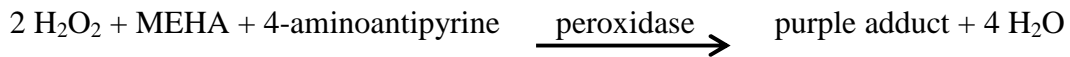
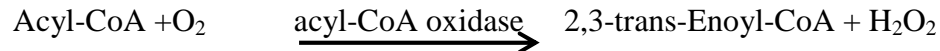
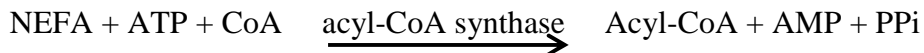
mouse and porcine insulin. A secondary antibody was used to precipitate insulin bound to the primary antibody. Following centrifugation and decanting, pellets were counted in a Packard Gamma counter. The insulin concentration in the sample is inversely proportional to the radioactivity in the pellet. Insulin concentrations were determined using a standard curve generated from known concentrations of insulin and resultant radioactivities.

Plasma Cytokines

Plasma cytokine levels were measured at baseline and 4 h after a bolus of VEH or LPS. Cytokines were analyzed using multiplexing Luminex xMAP technology (Luminex, Austin, TX). Plasma samples were prepared using mouse cytokine/chemokine Lincoplex kit (Linco Research, St. Charles, MO). These are multi-plexed assays using x-map technology via the Luminex100 system. The reactants (i.e. antibodies) in these assays are attached to the surfaces of tiny, fluorescent, microspheres. Each set of microspheres carry a unique biological reagent distinguishable by internal dye ratios. Identification of an analyte is based upon specific fluorescent emission spectra of the bead associated with the analyte. Two laser beams with high speed digital signal processors and computer algorithms distinguish which assay is being carried on each microsphere while quantifying the reaction based on fluorescent reporter signals. This instrumentation allows for the analysis of multiple analytes from a single 25 μ l aliquot of sample. The sensitivity for luminex detection however is less than conventional RIA.

Plasma Non-Esterified Fatty Acids

Non-esterified fatty acids (NEFAs) levels were measured enzymatically on plasma samples obtained at time = 0 and 125 min after a hyperinsulinemic-euglycemic clamp using a commercially available kit (NEFA C kit; Wako Chemicals USA Inc., Richmond, VA). The principle for the assay is as follows:



where MEHA is 3-methyl-N-ethyl-N-(β -hydroxyethyl)-aniline. The absorbance was measured at 550 nm using a 96-well plate on a Spectra Max Plus (Molecular Devices, Sunnyvale, CA).

Plasma Lactate

Plasma lactate levels were measured on samples obtained at 0 and 125 min after a saline infusion or hyperinsulinemic-euglycemic clamp. Two-hundred μL of lactate buffer, which is made up of 24 mL glycerol buffer (glycine, magnesium hexahydrate, and hydrazine hydrate, pH of 9.5) and 11.6 mg NAD was added to a 96-well plate. Ten μL of either the sample (1 part plasma: 3 parts 4% PCA; samples were centrifuged and the

supernatant was used) were added to the lactate buffer. A standard curve was constructed using known concentrations of the analyte prepared in 3% PCA. The samples were mixed and allowed to rest at room temperature for 5 minutes. Baseline fluorescence was measured at an excitation of 340 nm and emission of 450 nm. Next, 10 μL of the enzyme solution (1.8 μL lactate buffer and 122 μL lactate dehydrogenase) was added to the plate, mixed, and allowed to rest for 1 h and 49 minutes. The fluorescence was re-measured at an excitation of 340 nm and emission of 450 nm. The assay involved the following reaction:



Plasma Radioactivity

Plasma 3- ^3H -D-glucose levels were determined by the method of Somogyi-Nelson (151). Ten μl of plasma was added in a 1:1 ratio with saline followed by deproteinization with 100 μl each of barium hydroxide ($\text{Ba}(\text{OH})_2$; 0.075N) and zinc sulfate (ZnSO_4 ; 0.075N). The samples were vortexed to ensure complete mixing and placed at 4°C overnight. They were next centrifuged at 13,000 rpm for 5 min. A 100 μl sample of the supernatant was pipetted into a glass scintillation vial and placed in a heated vacuum oven to evaporate the $^3\text{H}_2\text{O}$. The residue was reconstituted in 1 ml of ddH₂O and 10 ml of liquid scintillation fluid was added to the vial (EcoLite, MP Biomedical, Solon, OH). Concurrently, a 40 μl sample of supernatant was added into a glass scintillation vial and 960 μl of ddH₂O was added followed by 10 ml of liquid scintillation fluid. Standards were created to measure for loss of labeled glucose during deproteinization. Ten μl of the 3- ^3H infusate was diluted with 1990 μl of saturated

Benzoic Acid (1:200). Ten μl of the diluted standard (in triplicate) was treated in the exact matter as the plasma samples (chemical recovery standard, CRS), while 100 μl of the supernatant was added to glass scintillation vials and dried in the heated vacuum (chemical standard evaporated, CSE). One ml of ddH₂O was added to the vials, followed by 10 ml of scintillation fluid. All samples were placed in the Perkin Elmer Liquid Scintillation Counter and the radioactivity was measured. The ratio of radioactivity in the CSE compared to CRS samples were used as a recovery factor to determine the radioactivity in the plasma samples accounting for loss during sample processing.

Processing of Muscle Samples

Muscle Radioactivity

Excised soleus, gastrocnemius, SVL, gonadal adipose tissue (AT), heart, and brain were deproteinized with perchloric acid and then neutralization to a pH of ~ 7.5 . A portion of the sample was counted ([2-¹⁴C]DG and [2-¹⁴C]DG-G-phosphate ([2-¹⁴C]DGP) and a portion was treated with Ba(OH)₂ and ZnSO₄ and the supernatant was counted ([2-¹⁴C]DG). Both [2-¹⁴C]DG and [2-¹⁴C]DG-G-phosphate ([2-¹⁴C]DGP) radioactivity levels were determined using liquid scintillation counting.

Calculations. Glucose flux rates were assessed using non-steady state equations (8) assuming a volume of distribution (130 ml/kg). Tissue-specific clearance (K_g) of [2-¹⁴C]DG and an index of glucose uptake (R_g) was calculated as previously described (9):

$$K_g = [2\text{-}^{14}\text{C}]\text{DGP}_{\text{tissue}}/\text{AUC } [2\text{-}^{14}\text{C}]\text{DG}_{\text{plasma}}$$

$$R_g = K_g \times [\text{glucose}]_{\text{plasma}}$$

where $[2\text{-}^{14}\text{C}]\text{DGP}_{\text{tissue}}$ is the $[2\text{-}^{14}\text{C}]\text{DGP}$ radioactivity (dpm/g) in the tissue, AUC $[2\text{-}^{14}\text{C}]\text{DG}_{\text{plasma}}$ is the area under the plasma $[2\text{-}^{14}\text{C}]\text{DG}$ disappearance curve (dpm/mL/min), and $[\text{glucose}]_{\text{plasma}}$ is the average blood glucose ($\mu\text{g}/\mu\text{l}$) during the experimental period (t=102-125 min). Data are presented as mean \pm SEM and the significance level was set at $p < 0.05$.

Immunoblots

Protein from skeletal muscle, liver, and cardiac tissue was extracted with a buffer containing 50 mM Tris, 1 mM EDTA, 1 mM EGTA, 10% glycerol, and 1% Triton X-100 at pH 7.5. Before using 1 mM DTT, 1 mM PMSF (dissolved in ethanol), 5 $\mu\text{g}/\text{mL}$ protease inhibitor cocktail, 10 $\mu\text{g}/\text{mL}$ trypsin inhibitor, 50 mM NaF, and 5 mM NaPP were added to the buffer. The tissues were homogenized on ice and centrifuged for 20 min in the cold room. The protein extract was collected and stored at -80°C until used. Protein extracts (20 μg) were combined with NuPage LDS sample loading buffer (4X), NuPage reducing agent (10X) (Invitrogen, Carlsbad, CA), and distilled water up to 25 μL . This was placed in a 75°C water bath for 10 min, and size-fractionated by electrophoresis on 10% SDS-polyacrylamide gel (Invitrogen, Carlsbad, CA). Proteins were transferred from the gel to a PVDF transfer membrane by electroblotting. Membranes were incubated at room temperature with 5% nonfat dried milk, in Tris-buffered saline-Tween (TBS-T) (Sigma, St. Louis, MO) for 2 h, washed 3X for 5-10 min in TBS-T, and then incubated overnight at 4°C with mouse anti-pAkt (Ser⁴⁷³) antibody (1:1,000), mouse anti-pAkt

(Thr³⁰⁸) antibody (1:1,000), mouse anti-GSK antibody (1:1,000), mouse anti-Akt antibody (1:500), mouse anti-pIRS-1 (Tyr⁸⁹⁵) antibody (1:1000), mouse anti-pIRS (Ser³⁰⁷) antibody (all antibodies purchased at Cell Signaling Technology, Danvers, MA). After incubation, samples were washed 3X for 5-10 min in TBS-T, incubated with peroxidase-conjugated secondary antibody, and analyzed using enhanced chemiluminescence (GE Healthcare, Piscataway, NJ).

In a separate group of studies the effects of LPS on the acute activation of insulin signaling was examined. Mice were placed on a 5 h fast (t=-300 min) and received either an I.V. bolus of vehicle or high-dose LPS 1 h after the fast began (t=-240 min). Four h later (t=0 min), mice received an I.V. bolus of insulin (10U/kg body weight). At t=10 min, the mice were anesthetized. The gastrocnemius muscle and liver were excised, immediately frozen in liquid nitrogen, and stored at -70°C until future tissue analysis.

Real Time PCR

Total mRNA was extracted from the skeletal muscle and liver using the RNeasy fibrous tissue kit (Qiagen Sciences, Germantown, MD). cDNA was synthesized from 2.5 µg RNA with the SuperScript III first-strand synthesis system first-strand cDNA synthesis kit (Invitrogen, Carlsbad, CA). PCR amplification reactions were performed in triplicate using the ABI detection system (Applied Biosystems, Foster City, CA) and the $\Delta\Delta$ CT method was used to quantify mRNA levels. Gene expression was normalized to 18S rRNA levels. PCR amplification to detect inducible nitric oxide synthase (iNOS) and the housekeeping 18S rRNA was performed with TaqMan gene expression assays

(proprietary primers and probes designed and synthesized by Applied Biosystems). Data are presented as fold increase relative to measurements in vehicle-treated mice.

Microsphere Isolation

The soleus, gastrocnemius, SVL, kidneys, intestines, liver, heart, and brain were excised. The tissues were digested overnight in 1M KOH at 60°C. Following vortex and centrifugation, the pellet containing the microspheres was re-suspended with TritonX-100 and centrifuged. The pellet was re-suspended in ethanol containing 0.2% (v/v) HCL, centrifuged and re-suspended in ethanol. The resulting product was centrifuged and a small amount of ethanol was left on the pellet and allowed to evaporate at room temperature overnight. Cellosolve acetate (250 μ L) was added to the microsphere:ethanol solution to elute the fluorescent dye from the microspheres. The absorbance was determined at 440 and 672 nm. Tissue blood flow was calculated as the product of the ratio of microspheres in a tissue relative to microspheres in both kidneys and PAH clearance (ml/min) divided by tissue weight (ml·g tissue⁻¹·min⁻¹).

Mitochondrial Extraction

Mitochondria were extracted from the gastrocnemius muscle of mice that underwent a hyperinsulinemic-euglycemic clamp utilizing a mitochondrial extraction kit (IMGENEX, San Diego, CA). Approximately 30-50 mg of muscle was placed in a centrifuge tube on ice. Five μ l/mg tissue of Homogenization Buffer was added to the muscle and the muscle was manually homogenized utilizing a small pestle. The samples

were centrifuged at 3000 rpm for 10 min at 4°C and the supernatant was transferred to a clean centrifuge tube and the pellet was discarded. The supernatant was centrifuged again at 12,000 rpm for 30 min at 4°C and the supernatant, which represented the cytosolic fraction, was transferred to the clean centrifuge tube. The pellet was resuspended in 5 µl/mg of the original tissue weight in ice cold Suspension Buffer and centrifuged at 12,000 rpm for 10 min at 4°C. The supernatant was discarded and the pellet was resuspended again in 5 µl/mg of the original tissue weight in ice cold Suspension Buffer and centrifuged at 12,000 rpm for 10 min at 4°C. The supernatant was discarded and the mitochondrial pellet was lysed in 1 µl/mg of the original tissue weight in Complete Mitochondrial Lysis Buffer by mixing for 30 min at 4°C. The sample was centrifuged at 12,000 rpm for 5 min at 4°C and the supernatant, which represented the mitochondrial fraction, was placed in a clean centrifuge tube. The protein concentration was measured and an Immunoblot was used to compare HKII binding to the cytosol and mitochondria.

Immunofluorescence Microscopy

Tissues isolated from mice that have undergone a hyperinsulinemic- euglycemic clamp were embedded in optimal cutting temperature compound. The frozen tissue cross sections (10 µm) were blocked with 3% BSA in PBS for 60 min at room temperature. Primary antibodies were used at the following dilutions: GLUT4 polyclonal antibody (1:1000) and α -dystroglycan (α -DG) antibody (1:50) as previously described (191). Fluorescently conjugated secondary antibodies (1:100, Jackson ImmunoResearch Laboratories) were added to the sections for 30 min at room temperature. After extensive

washing with PBS, the slides were mounted with Vectashield Mounting Medium (Vector Laboratories). The slides were visualized by confocal fluorescent microscopy (model LSM510; Carl Zeiss MicroImaging, Inc.). Quantification of cell surface immunofluorescence was performed using NIH Image software. radioactivity in the plasma samples accounting for loss during sample processing.

Statistical Analysis

Data are presented as the mean \pm SEM. Paired comparisons were performed with the two-tailed Student's *t* test. Differences between groups were determined by ANOVA. The significance level was set at $p < 0.05$.

CHAPTER III

DISASSOCIATION OF MUSCLE INSULIN SIGNALING AND INSULIN-STIMULATED GLUCOSE UPTAKE FOLLOWING LPS INDUCED INFLAMMATION

Aims

The aim of the studies in this chapter was to elucidate the relationship between cardiovascular dysfunction, insulin signaling, and decreased muscle glucose delivery when mice are challenged with LPS *in vivo*. We hypothesized that in the presence of LPS, impaired muscle glucose uptake is due mainly to impairments in the tissue blood flow as opposed to insulin signaling which lead to a decrease in the delivery of glucose to the muscle.

Mediators of the inflammatory response have been shown to impair muscle insulin signaling and blood flow however little work has been done to examine how these factors interact with one another *in vivo*. Youd *et al.* has shown that *in vivo* a 3 hour infusion of TNF- α into anesthetized rats inhibited insulin-stimulated microvascular recruitment and lead to a decrease in insulin-stimulated hind-leg glucose uptake, however they did not measure insulin signaling (187). TNF- α has been shown to impair the vasodilator effects of insulin in skeletal muscle resistant arteries through impairments of insulin activation of AKT in rats *ex vivo* (47) as well as impaired insulin signaling and insulin-stimulated glucose uptake in cultured cells (40). *In vivo* Fan *et al.* has found that LPS lead to whole body insulin resistance in rats and impaired insulin signaling (49) yet a recent *in vivo* study utilizing a hyperinsulinemic- euglycemic clamp in mice was unable

to detect an impairment in glucose uptake by the skeletal muscle following an i.p. LPS injection (123). Therefore it is unclear how much of the impairments seen with acute inflammatory stress are signaling- and/or cardiovascular-mediated. Interestingly the majority of the work has been done in rats, with limited and apparently different responses in mice.

While any number of factors can contribute to inhibition of insulin-stimulated glucose uptake in the presence of an LPS challenge, there has been little work to examine the relationship between the LPS induced inflammatory response and cardiac dysfunction, insulin signaling, and decreased muscle glucose delivery *in vivo*. Therefore the objective of this chapter was to investigate the vascular as well as metabolic events occurring *in vivo* during acute inflammatory stress that can have an effect on glucose metabolism. Specific Aim I will address the relationship between cardiovascular dysfunction, insulin signaling, and decreased muscle glucose delivery when mice are challenged with LPS *in vivo*.

Experimental Approach

Wild-type C57BL/6J mice approximately 12 weeks of age were treated with either vehicle, low- (1 μ g/g BW), or high-dose (10 μ g/g BW) LPS. A hyperinsulinemic-euglycemic clamp was performed to assess the dose-response effect of acute inflammatory stress on insulin action, specifically muscle glucose uptake.

Results

LPS Increased Plasma Cytokine Levels.

Arterial plasma TNF- α , IL-6, IL-1 β , and IL-10 levels were measured 4 and 6-h post-vehicle or LPS injection (Figure 3.1). At 4 h after LPS injection, the mice that received low-dose LPS had significantly higher TNF- α (3-fold), IL-6 (3-fold), IL-1 β (3-fold), and IL-10 (5-fold) above mice that received vehicle. The mice that received high-dose LPS also had significantly higher levels of TNF- α (7-fold), IL-6 (4-fold), IL-1 β (7-fold), and IL-10 (6-fold) over vehicle-treated animals. Only IL-1 β levels was significantly increased in high-dose LPS compared to mice that received low-dose LPS (2-fold). At 6 h post-LPS injection only TNF- α and IL-6 remained significantly increased in mice having received low dose LPS compared to vehicle-treated mice (3- and 6-fold respectively). In mice that received high-dose LPS significant increases in TNF- α , IL-6, IL-1 β , and IL-10 still remained 6 h post injection compared to vehicle-treated animals (4-, 12-, 8-, and 2-fold, respectively) and in IL-6, IL-1 β and IL-10 compared to low-dose LPS treated animals (2-, 4- and 2-fold, respectively).

LPS Inhibited Insulin-Stimulated Muscle Glucose Uptake.

During the saline infusion, there was no significant difference in fasting arterial glucose concentrations between mice that received vehicle, low-, or high-dose LPS (Figure 3.2). However, insulin levels (ng/mL) were significantly lower 4-h post injection (t=0 min; 0.51 ± 0.10 vs. 0.17 ± 0.01) and 6-h post injection (t=125 min; 0.47 ± 0.05 vs. 0.22 ± 0.04) with high-dose LPS administration, while there was an increase with low-

dose LPS administration at t=0 min (0.51 ± 0.10 vs. 0.88 ± 0.07) and t=125 min (0.47 ± 0.05 vs. 1.16 ± 0.22). Basal endogenous glucose production ($\text{mg}\cdot\text{kg}^{-1}\cdot\text{min}^{-1}$) was decreased in mice that received both low- and high-dose LPS compared to vehicle treated animals (10 ± 1.9 , 7.4 ± 1.2 , and 6.3 ± 0.9 ; vehicle, low-dose, and high-dose LPS, respectively). Basal tissue glucose uptake was also assessed in these mice. Basal tissue glucose uptake was significantly decreased by high-dose LPS in all tissues in which it was assessed except for the soleus. The response in the low-dose group was highly variable which prevented us from detecting a decrease in basal tissue glucose uptake (Figure 3.2).

Insulin action was assessed in mice that received vehicle, low-dose, or high-dose LPS under hyperinsulinemic-euglycemic clamp conditions (Table 3.1). Because LPS decreases insulin clearance the insulin infusion rates were varied between the three groups to match insulin concentrations. While glucose levels were maintained at $\sim 120\text{mg/dl}$ between all groups, there was a significant difference in the glucose infusion rate (GIR; $\text{mg}\cdot\text{kg}^{-1}\cdot\text{min}^{-1}$) necessary to maintain euglycemia between the mice that received vehicle and mice that received low- and high-dose LPS (54.2 ± 0.5 vs. 38.6 ± 1.1 vs. 35.4 ± 0.6 ; Figure 3.3). Endogenous glucose production was below zero in all groups indicating complete suppression of liver glucose production by insulin. Low-dose LPS markedly inhibited Rg in the gastrocnemius and SVL muscles with no significant difference in any other tissues measured compared to vehicle. High-dose LPS inhibited Rg in all tissues measured (Figure 3.4). However, when Rg was compared to the fold-change over basal, low-dose LPS did not lead to a significant decrease in the fold increase in glucose uptake in any of the tissues measured while mice that received high-

dose LPS, still had a significant decrease in the fold increase in glucose uptake in the SVL and gastrocnemius muscles when compared to vehicle (Figure 3.4).

LPS Does Not Decrease Insulin Signaling.

We assessed the effects of high-dose LPS treatment on insulin signaling in the gastrocnemius muscle by measuring insulin-mediated phosphorylation of Akt, a key protein involved in insulin-stimulated MGU. When we compared levels of pAkt (Ser⁴⁷³) between control and LPS-treated mice from tissues obtained at the end of the clamp, we found there was no significant difference between the two groups (Figure 3.5). Similar results were seen for GSK (Figure 3.5). When we assessed liver there was also no difference in the phosphorylation of AKT (Figure 3.5).

To determine if LPS altered the magnitude of the initial increase in insulin signaling acutely, 4 h after LPS or vehicle treatment mice received a bolus of insulin (10U/kg body weight) and were sacrificed 10 min later. There was no significant difference in the acute phosphorylation of IRS-1 or Akt signaling between the vehicle- and LPS-treated mice (Figure 3.6). Similar results were seen in the liver (Figure 3.6).

LPS Increased iNOS Expression in Muscle.

We examined the effect of LPS administration on the expression of inducible nitric oxide synthase (iNOS) in skeletal muscle from vehicle- and LPS-treated mice. LPS significantly increased the expression of iNOS mRNA to a similar extent in the muscle of both low- and high-dose LPS treated mice compared to vehicle controls (Figure 3.7).

Similarly, low- and high-dose LPS resulted in a significant increase in the expression of iNOS in the liver (Figure 3.7).

High-Dose LPS Treatment Decreased Muscle Blood Flow.

Mean arterial blood pressure (mmHg) was unchanged in vehicle treated mice. High-dose, but not low-dose, LPS lead to a significant reduction in mean arterial blood pressure (115.8 ± 5.3 vs. 96.6 ± 5.3 [vehicle]; 119.2 ± 3.9 vs. 86.5 ± 3.9 [low-dose LPS], 123.7 ± 3.2 vs. 77.4 ± 3.2 [high-dose LPS], -240 min vs. 0 min, respectively). We next determined if high-dose LPS treatment caused a similar reduction in blood flow. High-dose LPS treatment led to a ~65% decrease in renal blood flow compared to vehicle treated mice. This also resulted in ~65% decrease in muscle blood flow (Table 3.2). There was no significant difference in blood flow between the right and left kidney (data not shown).

High-Dose LPS Impaired Cardiac Function.

The effect of LPS-treatment on cardiovascular parameters and whole body oxygen consumption (VO_2) was examined. There were no significant differences in stroke volume, heart rate, and cardiac output in vehicle and low-dose LPS treated mice 6 h after LPS treatment. While VO_2 was decreased in the low-dose LPS treated mice compared to vehicle it was not significant. However, the administration of high-dose LPS led to a ~30% decrease in heart rate and stroke volume and a ~50% decrease in cardiac output and VO_2 (Table 2.3).

Discussion

The aim of the present study was to use a conscious mouse model to test the hypothesis that there is a significant vascular component to impaired insulin action *in vivo* resulting from an LPS challenge. Skeletal muscle represents an important site for insulin-stimulated glucose disposal. It is well known that insulin-stimulated muscle glucose uptake is impaired in the presence of inflammatory mediators. While it has been suggested from *in vitro* studies that the underlying factors leading to this impairment is defective insulin signaling, the mechanism *in vivo* remains to be clearly elucidated (14, 128). Our findings indicate that the inflammatory stress induced by LPS in the mouse impairs MGU *in vivo* without affecting insulin signaling. The impairment in MGU was associated with decreases in muscle blood flow, suggesting that alterations in muscle glucose delivery play a critical role in the insulin resistance that accompanies acute inflammatory stress (114).

Hyperinsulinemic-euglycemic clamps in chronically catheterized conscious mice were used to determine insulin-stimulated glucose uptake. In initial studies vehicle and high-dose LPS treated mice were both infused with $4 \text{ mU}\cdot\text{kg}^{-1}\cdot\text{min}^{-1}$ of insulin during the clamp. There was no difference in glucose requirements between the groups. However, arterial insulin was two-fold higher in mice that received LPS (5.0 vs. 2.5 ng/ml; LPS vs. vehicle) implying that LPS impaired insulin clearance. In subsequent studies the insulin infusion rate was reduced to $2.5 \text{ mU}\cdot\text{kg}^{-1}\cdot\text{min}^{-1}$ in an attempt to match circulating insulin levels in LPS treated mice to those having received vehicle. Although insulin levels remained somewhat higher, glucose requirements were reduced by 35% and there was a significant decrease in glucose uptake in multiple muscles. When the dose of LPS was

decreased to 1 mg/kg, impairments in insulin-stimulated MGU were not as robust. These results are consistent with findings in a variety of species (91, 98, 130). Our results suggest that decreased insulin clearance by LPS may serve to normalize insulin-stimulated glucose uptake. In a recent study, Park *et al.* found that during a hyperinsulinemic-euglycemic clamp LPS did not affect insulin action *in vivo* (123). In the presence of LPS, there was either an increase or no difference in the glucose infusion rate versus animals that received saline. Similar results were seen when they examined whole-body glucose disposal. They found that while LPS lead to a decrease in hepatic glucose production, muscle glucose uptake was unaltered. Interestingly insulin concentrations were not reported (123, 128). Pilon *et al.* did observe a decrease in whole body glucose uptake during the hyperinsulinemic-euglycemic clamp 6 h after administering a dose of LPS. In contrast to our study, insulin-stimulated glucose uptake by the soleus (other tissues were not evaluated) was markedly decreased (128). However they utilized a higher dose of LPS than our high dose group (20mg/kg). Like Park *et al.*, they also did not report insulin concentrations during the clamp (123). We found that LPS impaired insulin clearance. Therefore the insulin infusion rate during the clamp was decreased to maintain similar arterial insulin concentrations between groups. Thus, it is likely that in that study, an impairment in insulin clearance and the consequent increase in arterial insulin concentrations following LPS treatment offset any underlying impairment in insulin-stimulated tissue glucose uptake.

Defects in insulin signaling in the muscle during an LPS challenge do not contribute to impaired glucose uptake. Consistent with our previous work, LPS treatment increases the plasma levels of inflammatory cytokines (164). de Alvaro *et al.* found that

in cultured rat skeletal muscle cells TNF- α lead to a decrease in insulin signaling through the IR/IRS-1/AKT pathway (39). Impairments in insulin signaling are mediated in part by the increase of cytokines and subsequent NF κ B pathway activation that occurs in response to LPS (22, 55). We observed an increased expression of iNOS in muscle and liver, which is consistent with recent reports (128). Despite the robust activation of the inflammatory response, Akt phosphorylation in gastrocnemius muscle at the end of the clamp was unaltered by LPS. Pilon *et al.* observed a decrease in insulin stimulated IRS-1 associated PI 3-kinase activity in soleus (other muscles were not examined) obtained from control and LPS treated mice (6 h after LPS administration) stimulated *ex vivo* with insulin (128). *Ex vivo* the vascular-dependent effects of insulin are absent. While *in vitro* models can unmask insulin signaling defects it prevents detection of any vascular dependent alterations in insulin action. An additional consideration is that the impairment in insulin signaling may be dependent upon the time of exposure to the inflammatory environment, the dose of LPS administered, and the specific muscle group examined. Pilon examined insulin action utilizing a 2-fold higher dose of LPS than our high-dose group (128). To assess whether the peak phosphorylation events were missed during the 120 min clamp study, Akt phosphorylation was examined 10 minutes following a bolus of insulin. This experiment confirmed the findings from the insulin clamp studies; LPS administration *in vivo* did not blunt insulin signaling in the muscle. Since Akt phosphorylation can be influenced by multiple events, we next looked upstream in the insulin signaling pathway at IRS-1 phosphorylation. We found that LPS administration did not blunt tyrosine phosphorylation nor did it increase serine phosphorylation of IRS-1 compared to vehicle treatment. These data suggest that there is dissociation between

insulin-stimulated muscle glucose uptake and phosphorylation of key proteins in the insulin signaling pathway. This strongly suggests that other factors limit muscle glucose uptake *in vivo*.

Consistent with the insulin signaling data we found that despite the absolute decrease in MGU the fold increase above basal MGU was unaltered in several tissues. Insulin-stimulated MGU increased ~10 fold above vehicle infused mice irrespective of whether they are given LPS. This suggests that the tissues were very responsive to insulin but that other factors such as a decrease in metabolic demand or vascular delivery of glucose limited the absolute magnitude of glucose uptake. Cardiac output following low-dose LPS was not significantly altered. However, we found that high-dose LPS significantly decreased cardiac output by ~50% and mean arterial blood pressure by ~50%. In conjunction with these results, we found that VO_2 was significantly decreased with high-dose LPS (~50%) while low-dose LPS (~20%) did not significantly decrease metabolic demand (i.e. VO_2). A correlation between metabolic demand and insulin stimulated glucose uptake is well established as increasing metabolic demand by exercise can compensate for underlying insulin resistance (43, 102, 138). This may in fact explain why in humans it has been reported that during endotoxemia insulin can initially improve insulin action (168). The low dose of LPS used in human studies induced modest cardiovascular alterations (tachycardia and mild hypotension). In contrast to the mouse, in both the human and pig the dose of LPS used caused hyperthermia, presumably increasing the metabolic rate and limiting cardiovascular disturbances. Therefore depending on the species, the duration of exposure to and the dose of LPS used among other factors such as the metabolic rate and associated cardiovascular events, may offset

any negative effects of LPS on tissue glucose uptake. Thus, the combined decrease in tissue blood flow and VO_2 following LPS may explain the accompanying impairment in MGU seen in our mouse model. Our data suggest that the accompanying cardiovascular events should be considered when interpreting the impact of LPS *in vivo*.

Previous studies have shown that increased blood flow leads to increased glucose uptake provided the muscle membrane is sufficiently permeable to glucose, such as it is during insulin stimulation (9, 148). The impairment in MGU following LPS administration could be due to the combined effects of reduced tissue blood flow and/or extraction of glucose. Using PAH and microspheres to measure tissue blood flow we found that after high-dose LPS muscle blood flow was significantly impaired compared to vehicle-treated animals. This would decrease muscle glucose delivery and, in the absence of a compensatory increase in fractional glucose extraction, MGU. Blood flow and glucose uptake decreased proportionally in both the SVL and gastrocnemius muscle (~69%), which suggests that fractional glucose extraction was unaltered. In contrast, blood flow to the heart and soleus decreased to a greater extent (~70% and 65%, respectively) than the fall in glucose uptake (~50% and 25%, respectively). This suggests that these tissues had a compensatory increase in fractional extraction of glucose and were able to minimize the decrease in tissue glucose uptake. As fat is the preferred substrate in these tissues they may switch to glucose utilization as the preferred substrate in low flow states. Indeed, studies by Petersen *et al.* demonstrated that the extracellular barrier to glucose uptake was lower in Type I muscle fibers (127). Thus tissues with greater oxidative capacity and capillary densities (heart and soleus) have a greater ability to extract glucose in a setting of insulin resistance and low flow states.

An inflammatory state can lead to decreased microcirculatory flow velocity and the density of perfused capillaries in rat models both of which are important factors in determining MGU (46, 89). Our data suggests that high-dose LPS decreases blood flow to the muscle which subsequently impairs MGU. This is consistent with data that there is a redistribution of blood flow during inflammatory stress (93). Unlike glucose, decreased muscle insulin delivery would not necessarily result in decreased insulin signaling because insulin is not consumed by the muscle. Therefore the concentration of insulin presented to muscle cells would be unaltered in a setting of decreased tissue blood flow. The lack of difference in IRS and Akt signaling between vehicle- and LPS-treated mice indicates a disassociation of insulin-stimulated glucose uptake and insulin signaling in muscle. Similar results in insulin signaling were observed by Orellana *et al.* in the neonatal pig (120). The impairment in tissue blood flow following LPS administration is consistent with studies suggesting that skeletal muscle perfusion could act as an independent determinant of insulin stimulated glucose uptake (7-9). Pilon *et al.* observed that mice lacking iNOS are protected from LPS-induced insulin resistance due to diminished nitrosylation of IRS-1 in the soleus muscle (128). However an equally plausible explanation is that these mice are protected from the hypotension and decrease in tissue perfusion that accompanies the excess nitric oxide generation from LPS.

In summary, we have provided evidence that an LPS challenge significantly impairs MGU in mice but does not affect the stimulation of insulin signaling *in vivo*. Our conclusions strongly suggest that the cardiovascular impairments resulting from exposure to LPS impair muscle glucose uptake in the presence of insulin stimulation. Thus

impairments in effective tissue perfusion can contribute to the decreased glucose uptake observed during endotoxemia.

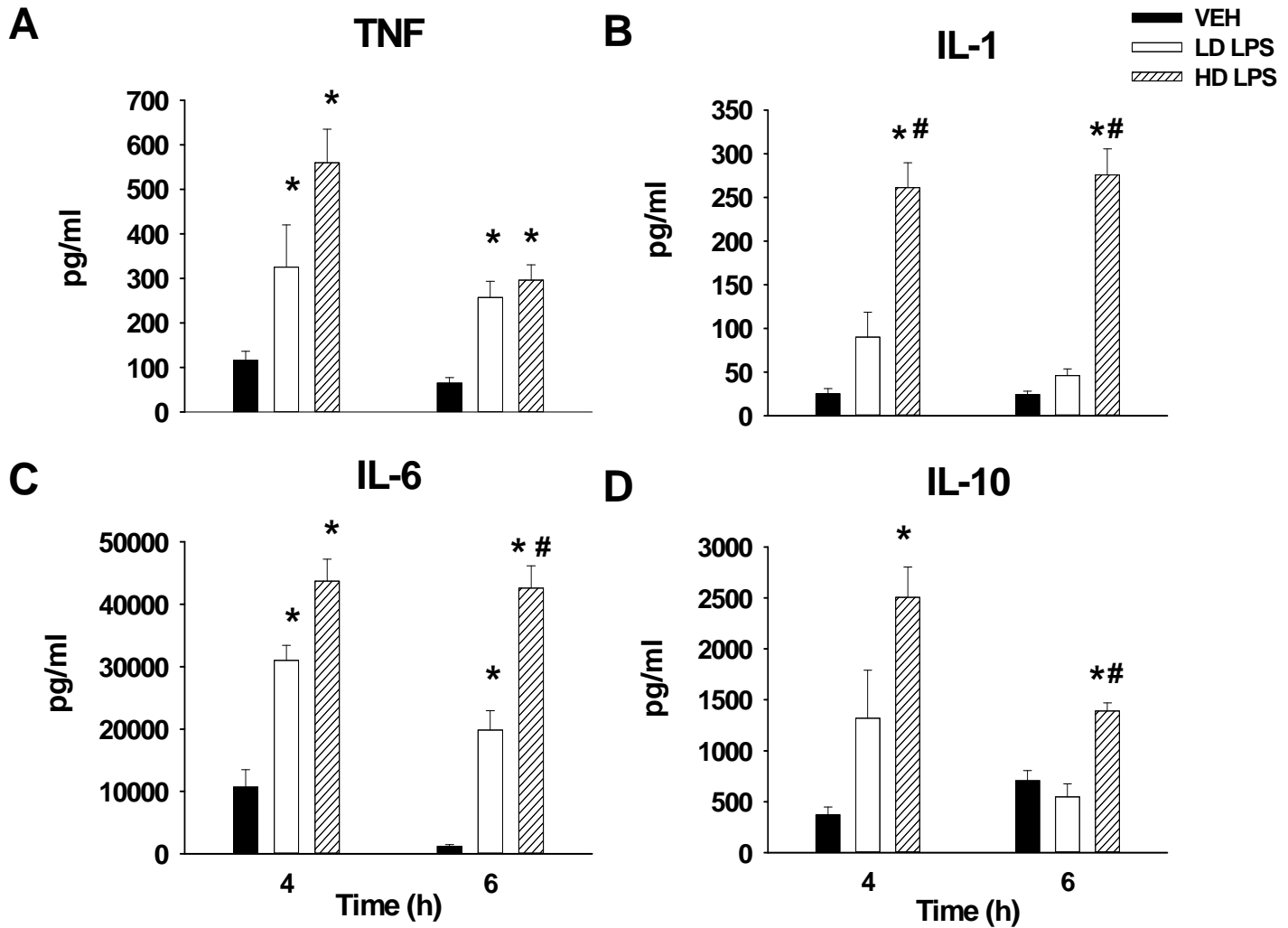


Figure 3.1. Plasma cytokine levels following VEH or LPS treatment. (A) Plasma concentration of tumor necrosis factor- α (TNF- α), (B) interleukin-1 β (IL-1 β), (C) interleukin-6 (IL-6), and (D) interleukin-10 (IL-10) 4- and 6-h following VEH, low- (1 μ g/g BW) or high- (10 μ g/g BW) dose LPS treatment in chronically catheterized conscious C57BL/6J mice. Data are expressed as mean \pm SEM. * $p < 0.05$ vs. VEH, # $p < 0.05$ vs. low-dose LPS.

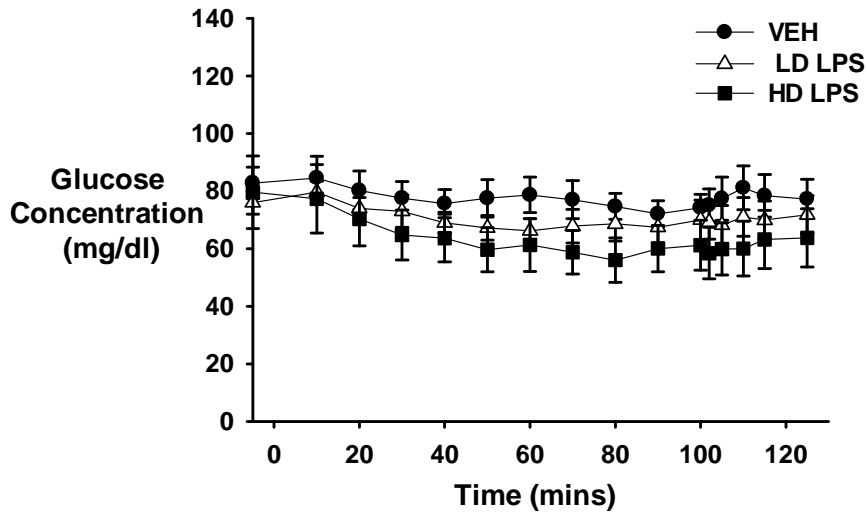
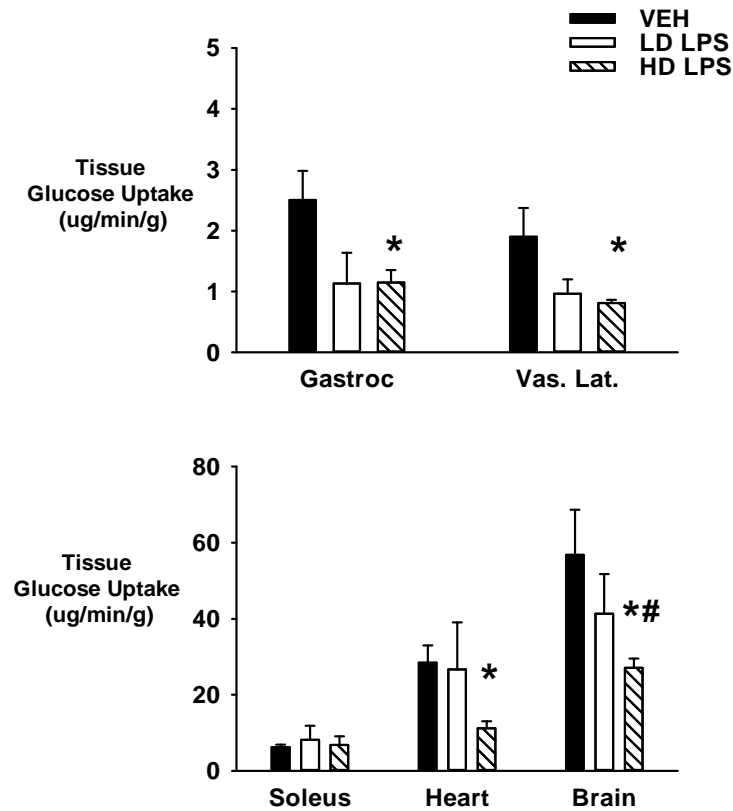
A**B**

Figure 3.2: Basal glucose concentrations and tissue glucose uptake following VEH or LPS treatment. (A) Basal arterial glucose and (B) basal tissue glucose uptake in chronically catheterized 5-h fasted C57BL/6J mice that received VEH, low- (1 μ g/gBW), or high- (10 μ g/g BW) dose LPS. Data are expressed as mean \pm SEM. * p<0.05 vs. VEH, # p<0.05 vs. low-dose LPS.

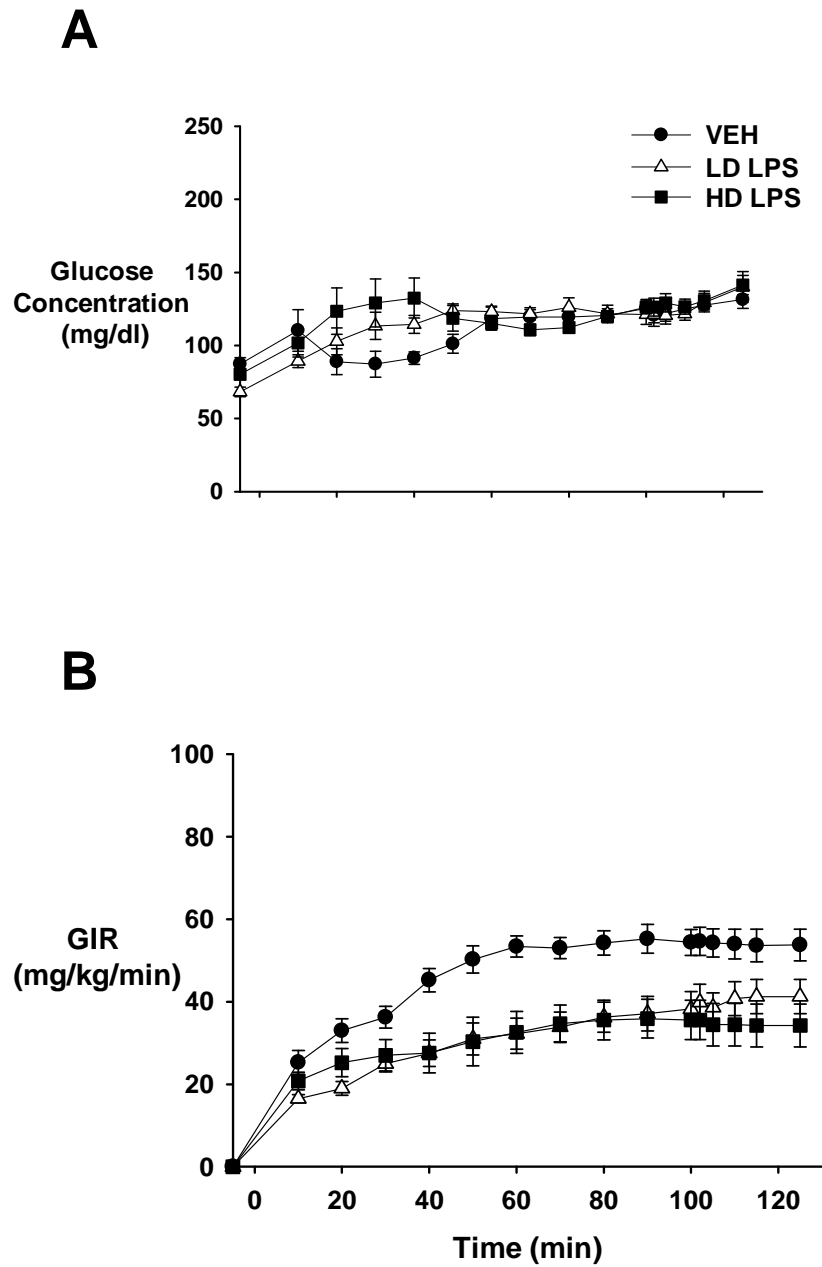


Figure 3.3: Glucose concentrations and glucose infusion rate (GIR) following VEH or LPS treatment. (A) Arterial glucose concentrations and (B) glucose infusion rate (GIR) during a hyperinsulinemic-euglycemic clamp in chronically catheterized 5-h fasted C57BL/6J mice that received VEH, low- ($1\mu\text{g/g}$ BW) LPS, or high- ($10\mu\text{g/g}$ BW) dose LPS.

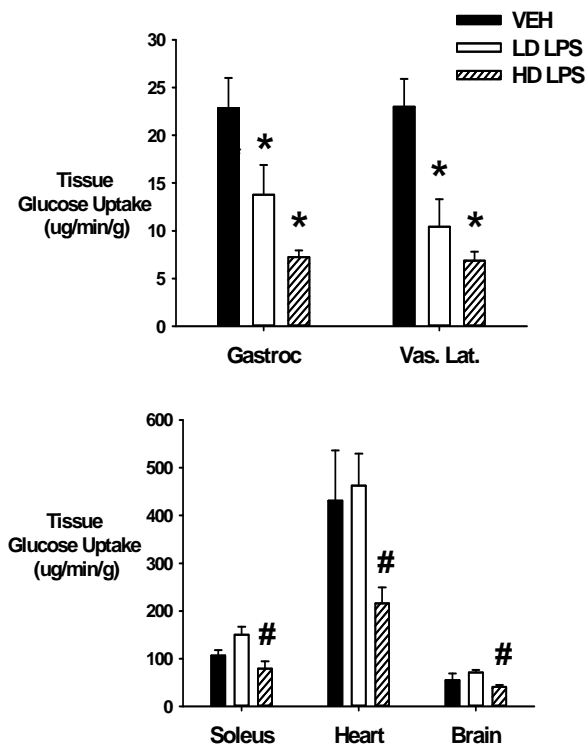
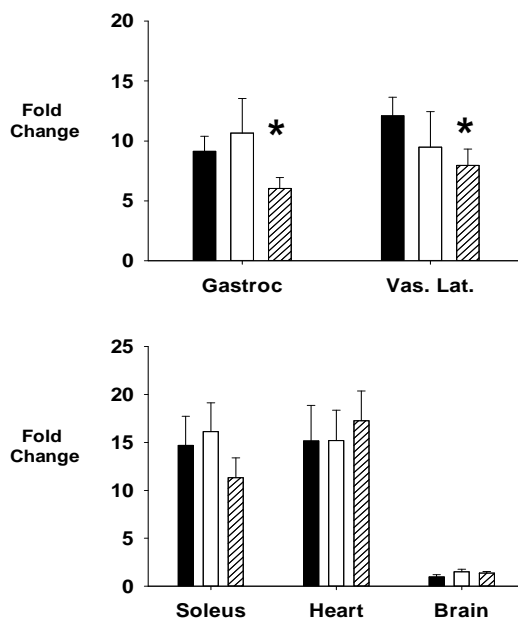
A**B**

Figure 3.4: Insulin-stimulated tissue glucose uptake following VEH or LPS treatment. (A) Tissue (soleus, gastrocnemius, superficial vastus lateralis (SVL), heart, and brain) glucose uptake and (B) fold-change from basal of insulin-stimulated glucose uptake during a hyperinsulinemic-euglycemic clamp in chronically catheterized 5-h fasted C57BL/6J mice that received VEH, low- ($1\mu\text{g/g}$ BW), or high- ($10\mu\text{g/g}$ BW) dose LPS. Data are expressed as mean \pm SEM. * $p < 0.05$ vs. VEH, # $p < 0.05$ vs. low-dose LPS.

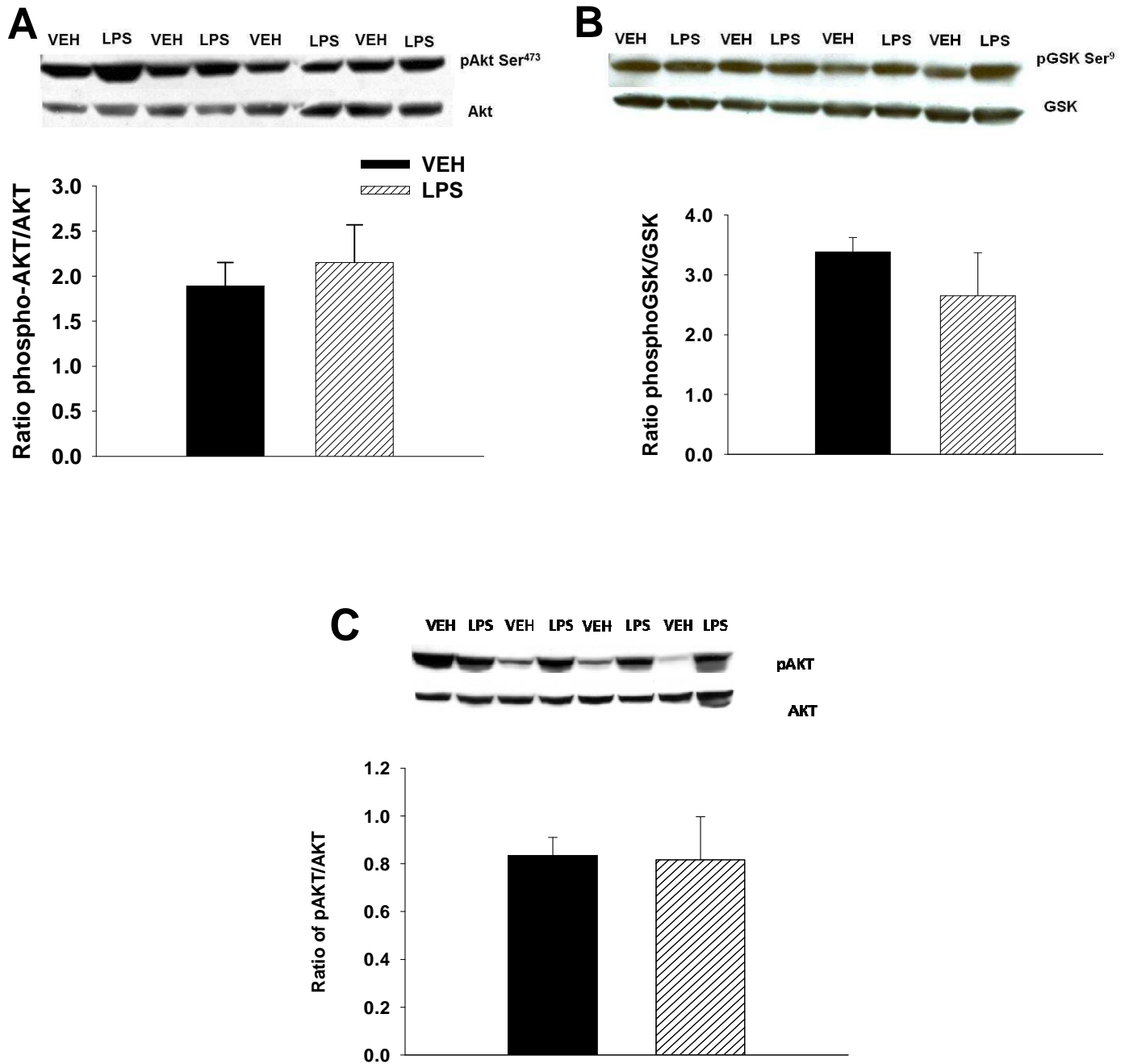


Figure 3.5: Effect of VEH or LPS treatment on insulin signaling in skeletal muscle and liver. (A) Akt phosphorylation (Ser⁴⁷³), (B) GSK phosphorylation in the gastrocnemius muscle, and (C) Akt phosphorylation (Ser⁴⁷³) in the liver of C57BL/6J mice that received VEH or high-dose LPS (10 μ g/g BW) after a hyperinsulinemic-euglycemic clamp (n= 6/group). Data are expressed as mean \pm SEM. *p<0.05.

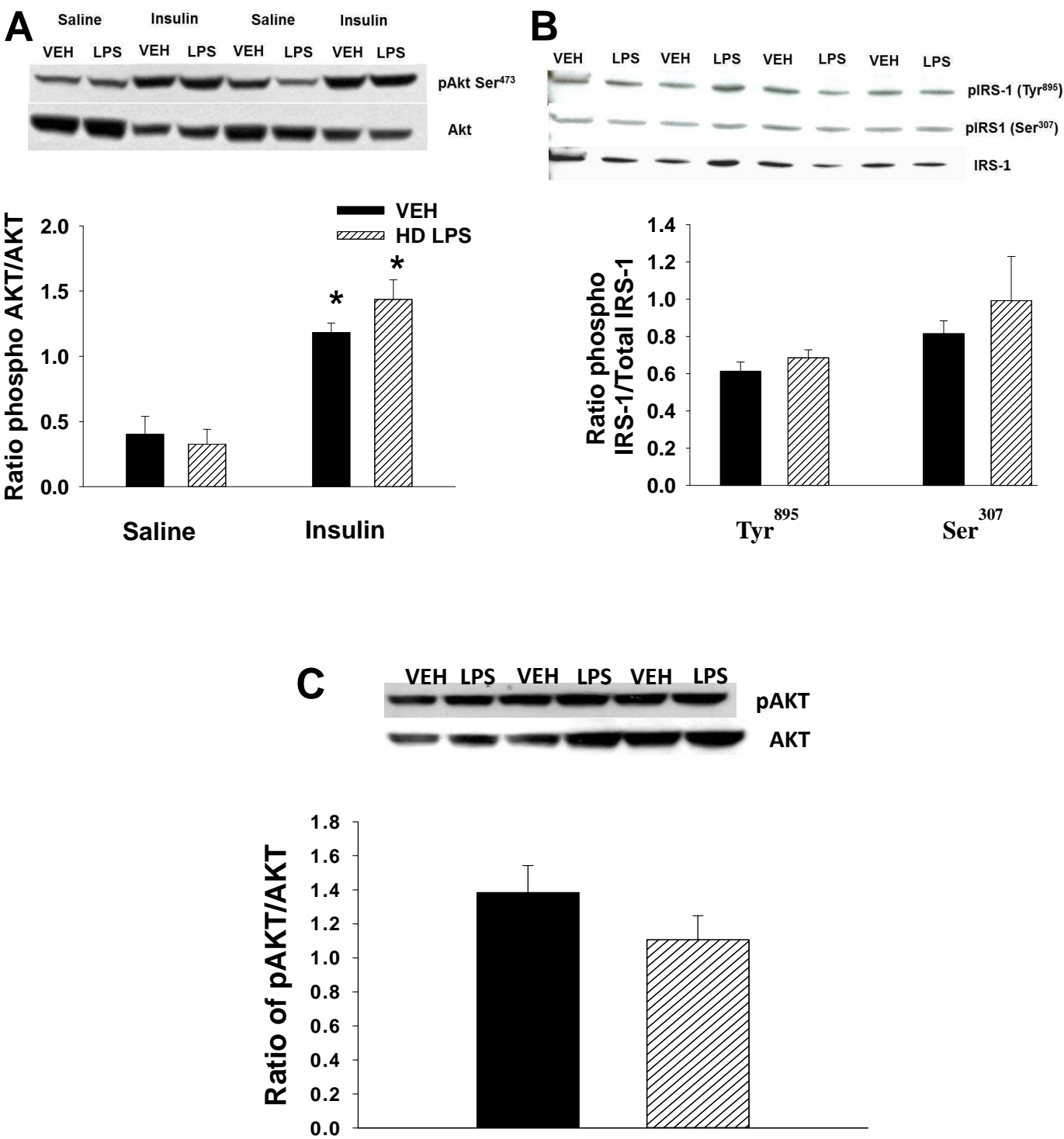


Figure 3.6: Effect of VEH or LPS treatment on acute insulin signaling in skeletal muscle and liver. (A) Akt phosphorylation (Ser⁴⁷³), (B) phosphorylation of IRS-1 (Tyr⁸⁹⁵ and Ser³⁰⁷) in the gastrocnemius muscle, and (C) Akt phosphorylation (Ser⁴⁷³) in the liver of C57BL/6J mice after an acute bolus of saline or insulin. Data are expressed as mean \pm SEM. *p<0.05.

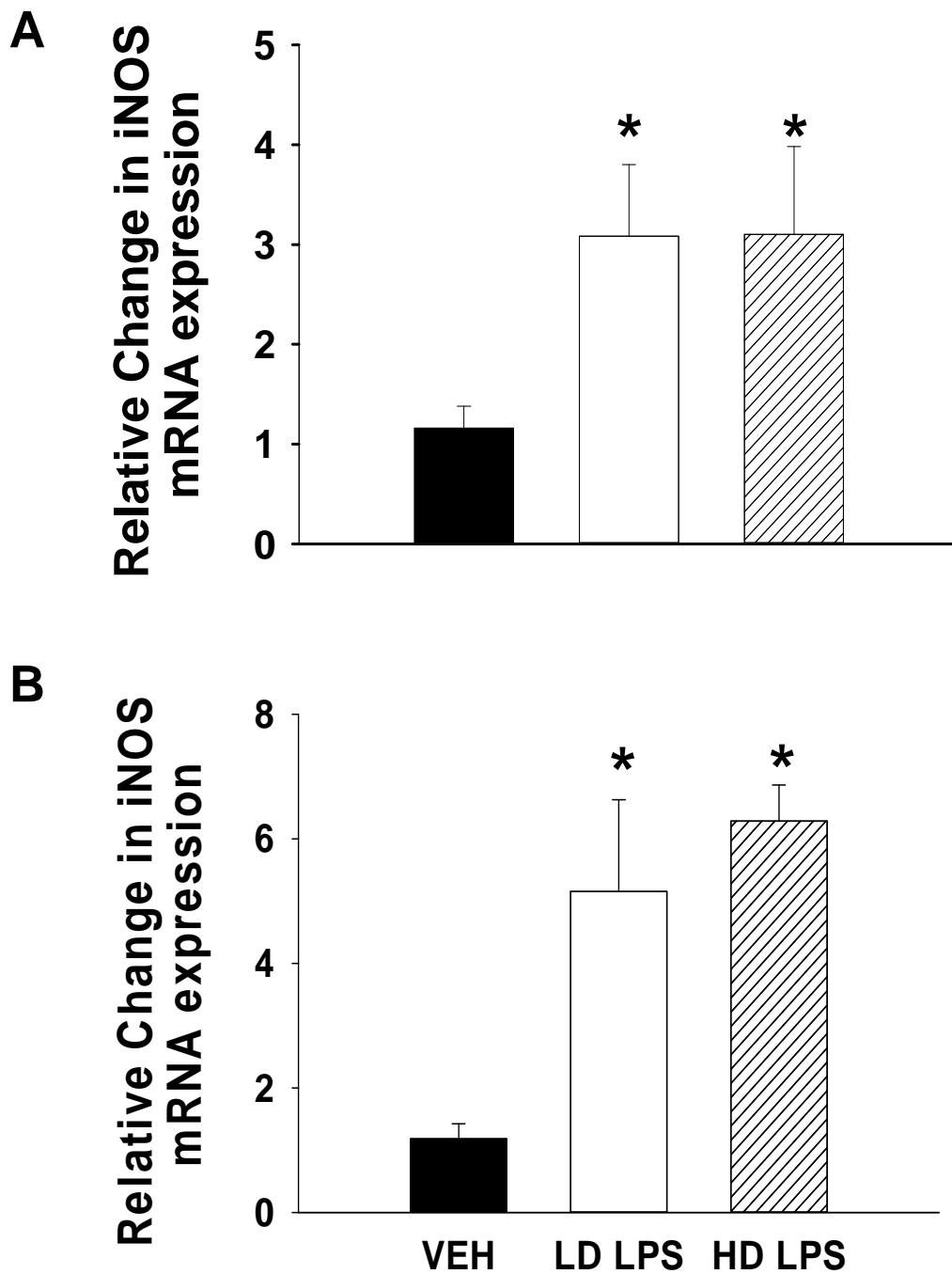


Figure 3.7: Effect of VEH or LPS treatment on the expression of iNOS in skeletal muscle and liver. Expression of inducible nitric oxide synthase (iNOS) mRNA in the gastrocnemius muscle (A) and liver (B) of C57BL/6J mice that received VEH, low- (1 μ g/g BW), or high- (10 μ g/g BW) dose LPS after a hyperinsulinemic-euglycemic clamp. Data are expressed as mean \pm SEM. * p <0.05.

Treatment	Insulin (ng/ml)	
	Basal (4 h)	Clamp (6 h)
Vehicle	0.33±0.09	2.54±0.19
Low-Dose LPS	0.88±0.07	3.04±0.30
High-Dose LPS	0.32±0.04	3.73±0.25

Table 3.1: Arterial plasma insulin levels after a hyperinsulinemic-euglycemic clamp following VEH or LPS treatment. Arterial plasma insulin levels in response to VEH (n=8), low- (1µg/g BW; n=8), or high- (10µg/g BW; n=8) dose LPS in chronically catheterized conscious mice during the basal (4 h after treatment) and clamp period (6 h after treatment). Data are expressed as mean ±SEM.

Tissue	Treatment	
	VEH	LPS
Renal blood flow (ml·kg BW⁻¹ ·min⁻¹)		
Kidneys	363±94	126±8*
Tissue blood flow (ml·g tissue⁻¹ ·min⁻¹)		
Soleus	6805±3440	2219±659*
Gastrocnemius	583±134	194±29*
SVL	976±183	359±88*
Heart	1389±362	416±53*

Table 3.2: Renal and tissue blood flow following VEH or LPS treatment. Renal and muscle (soleus, gastrocnemius, superficial vastus lateralis (SVL), and heart) blood flow were compared in mice that received either VEH or high-(10µg/gBW) dose LPS. Data are expressed as mean ±SEM. * p<0.05.

Treatment	Baseline (0 h)	6 h
Stroke Volume (uL)		
Vehicle	36±3	48±7
Low Dose LPS	63±9	51±6
High Dose LPS	48±2	32±2†
Heart Rate (bpm)		
Vehicle	720±14	648±21†
Low Dose LPS	667±4	667±28
High Dose LPS	678±19	450±49†*#
Cardiac Output (ml·g BW⁻¹·min⁻¹)		
Vehicle	0.67±0.07	0.82±0.16
Low Dose LPS	1.21±0.19	0.99±0.12
High Dose LPS	0.91±0.17	0.42±0.12†*#
VO₂ (ml/kg/h)		
Vehicle	3187±161	3044±249
Low Dose LPS	3346±116	2636±293†
High Dose LPS	3212±61	1653±218†*#

Table 3.3: Cardiovascular parameters following VEH or LPS treatment. Comparison of stroke volume, heart rate, cardiac output, and oxygen consumption (VO₂) in mice at baseline (t=0) and 6 h after receiving VEH, low- (1µg/g BW), or high- (10µg/g BW) dose LPS. Data are expressed as mean ±SEM. † p<0.05 vs. baseline; * p<0.05 vs. VEH at 6 h; # p<0.05 vs. low-dose LPS at 6 h.

CHAPTER IV

ENHANCED GLUCOSE TRANSPORT CAPACITY AMELIORATES INFLAMMATION INDUCED IMPAIRMENTS IN INSULIN STIMULATED MUSCLE GLUCOSE UPTAKE

Aims

The aim of this chapter was to determine if overexpression of the glucose transporter GLUT4 in skeletal muscle will lead to a decrease in the impairment in insulin-stimulated MGU when mice are challenged with LPS. We hypothesized that in the setting of acute inflammatory stress induced by LPS, increased glucose transport capacity would not lead to an increase in skeletal muscle glucose uptake.

Skeletal muscle is an important site for the regulation of glucose disposal. It represents the bulk of insulin-sensitive tissue in the body. The process by which glucose is taken up by skeletal muscle is complex and distributed over three-steps: delivery of glucose from the blood to the interstitium, facilitated transport into the intracellular space by glucose transporters, and irreversible phosphorylation of glucose to glucose-6-phosphate (G6P) by hexokinase (175). In the insulin-stimulated state, glucose transport is determined by the amount of the insulin-stimulated glucose transporter, GLUT4, located at the plasma membrane as well as the intrinsic activity of these transporters. Glucose transport can be regulated in multiple ways. Each step is important; however, depending on the setting, the control may shift allowing one step to play a more dominant role in the process (57).

Several studies have attempted to overcome these barriers by manipulating the amounts of the proteins that regulate these processes. While overexpression of GLUT4 has been shown to increase muscle glucose uptake in the basal state under conditions where there was an increase in GLUT4 translocation to the plasma membrane (e.g. increase in insulin), this offered no added benefit (59, 61). In fact, phosphorylation becomes the major barrier to glucose uptake in this setting (58).

Manipulations of key proteins involved in metabolic pathways can provide insight into how these pathways are regulated. Specifically, utilization of transgenic mouse models with overexpression of GLUT4 in skeletal muscle will allow the characterization of barriers to MGU in the presence of acute inflammatory stress. The objective of this chapter was to determine the extent to which glucose transport in skeletal muscle is a barrier to glucose uptake in the presence of acute inflammatory stress in conscious C57BL6/J mice *in vivo*. Bédard *et al.* demonstrated that when cultured L6 skeletal muscle cells were incubated for 24 h with cytokines (TNF- α and interferon- γ) and LPS there was a significant increase in nitric oxide production. While basal glucose uptake was increased in these cells, insulin-stimulated glucose uptake was markedly decreased. This also led to increased GLUT1 transporter protein levels while GLUT4 expression and protein content were decreased (14). A 4 h infusion of TNF- α in healthy human subjects led to an inhibition of whole-body glucose uptake and induced skeletal muscle insulin resistance *in vivo* (130). Specific Aim II will address whether increased glucose transport capacity through overexpression of GLUT4 can improve glucose uptake by the skeletal muscle in the setting of acute inflammatory stress. While increased GLUT4 expression in skeletal muscle has been shown to increase basal glucose uptake, it becomes a minor

barrier in the insulin-stimulated state (61, 137). We therefore hypothesized that overexpression of GLUT4 will not overcome impairments in MGU induced by LPS.

Experimental Approach

Chronically catheterized conscious wild-type and GLUT4^{Tg} C57/B16/j littermates approximately 12 weeks of age were treated with either vehicle (VEH) or high-dose (10 μ g/g BW) LPS. A hyperinsulinemic-euglycemic clamp was performed to assess whether increased muscle glucose transport capacity can overcome the impairment in glucose uptake due to acute inflammatory stress induced by LPS.

Results

GLUT4-overexpression Inhibits LPS-induced Decreases in Basal Muscle Glucose Uptake.

It has previously been shown that the GLUT4 transgene increases GLUT4 protein content 2- to 4-fold in skeletal muscle of C57BL/6J mice (119). In the presence of a saline infusion, GLUT4^{Tg} mice had lower insulin levels (ng/mL) 4- and 6-h post injection after VEH treatment compared to their WT littermates (Table 4.1). While LPS led to a significant decrease in insulin levels in WT mice, the insulin levels with LPS treatment were similar to VEH in GLUT4^{Tg} mice (Table 4.1). Similarly, fasting glucose levels were higher in WT mice that received VEH compared to WT mice that received LPS and GLUT4^{Tg} mice that received VEH or LPS (Figure 4.1). Basal endogenous glucose production (mg \cdot kg⁻¹ \cdot min⁻¹) was increased in GLUT4^{Tg} compared to WT mice treated with

VEH but decreased to similar levels in the presence of LPS (10.2 ± 0.3 vs. 16.3 ± 0.6 , VEH and 5.7 ± 0.2 vs. 5.3 ± 0.8 LPS; WT vs. GLUT4^{Tg}, respectively). Interestingly, while basal tissue glucose uptake fell significantly with LPS treatment in WT mice, there was no decrease in the GLUT4^{Tg} mice in the presence of LPS and soleus muscle glucose uptake was significantly higher with this treatment (Figure 4.2).

GLUT4--overexpression Inhibits LPS-induced Decreases in Insulin-Stimulated Muscle Glucose Uptake.

A hyperinsulinemic-euglycemic clamp was used to assess differences in insulin action between WT and GLUT4^{Tg} mice. Insulin levels during the clamp were matched between VEH and LPS treated groups (Table 4.2) and glucose concentrations were maintained at ~ 120 mg/dl (Figure 4.3). Endogenous glucose production was suppressed to below zero in all groups. Both GLUT4^{Tg} and WT mice had a similar glucose infusion rate (GIR; $\text{mg} \cdot \text{kg}^{-1} \cdot \text{min}^{-1}$) with VEH treatment (59.5 ± 0.2 vs. 54.2 ± 0.5 , respectively), however GLUT4^{Tg} mice had a slightly higher GIR than WT mice with LPS treatment (45.6 ± 0.2 vs. 35.4 ± 0.6 ; Figure 4.3). While LPS lead to a significant decrease in glucose uptake in the gastrocnemius, SVL, and heart of WT mice compared to VEH treatment, there was no difference in glucose uptake in any tissue due to LPS treatment in GLUT4^{Tg} mice (Figure 4.4).

GLUT4-overexpression Leads to Increased Non-Esterified Free Fatty Acids (NEFA).

The effect of overexpression of the GLUT4 transgene on plasma FFAs under hyperinsulinemic-euglycemic clamp conditions was measured. With VEH treatment, during the basal period GLUT4^{Tg} and WT mice had similar plasma NEFA levels. However, after 125 min plasma NEFAs were significantly increased in the GLUT4^{Tg} compared to the WT mice. With LPS treatment, plasma NEFA levels were increased ~2-fold during the basal period and at the end of the clamp in GLUT4^{Tg} compared to WT mice (Table 4.3).

GLUT4-overexpression Leads to Increased Lactate Levels.

The effect of overexpressing the GLUT4 transgene on plasma lactate levels under basal conditions was measured. GLUT4^{Tg} mice had significantly higher lactate levels following VEH treatment compared to WT mice. While LPS treatment did not lead to a change in plasma lactate levels in GLUT4^{Tg} mice compared to VEH, WT lactate was increased to plasma levels similar to GLUT4^{Tg} mice. (Table 4.4).

GLUT4-overexpression Increases Plasma Membrane Associated GLUT4 with VEH, but not LPS Treatment.

GLUT4 association with the plasma membrane in gastrocnemius muscle of mice that underwent a hyperinsulinemic-euglycemic clamp was examined by immunohistochemistry. With vehicle treatment, there was an increase in cell surface

associated GLUT4 in transgenic compared to WT mice. However, when treated with LPS, both WT and transgenic mice had a decrease of cell surface GLUT4 to similar levels (Figure 4.5).

GLUT4-overexpression Improves Cardiac Function.

The effect of LPS-treatment on cardiovascular parameters in GLUT4^{Tg} (VEH, n=6; LPS, n=5) compared to WT (VEH, n=5; LPS, n=6) mice was examined. There was a decrease in stroke volume and cardiac output in both groups treated with LPS compared to their vehicle-treated counterparts. However, while LPS-treatment led to a ~50% decrease in stroke volume and cardiac output in WT animals and the fall was attenuated in GLUT4^{Tg} mice (Table 4.5).

Discussion

The aim of the present study was to determine if mice overexpressing GLUT4 in skeletal muscle could compensate for impaired insulin action resulting from an LPS challenge *in vivo*. Insulin-mediated translocation of glucose transporters to the plasma membrane is an important mechanism for the removal of glucose during hyperglycemia. In the setting of sepsis, there is an impairment in this process which in part leads to elevated glucose levels. Our previous finding suggested that alterations in muscle glucose delivery played a critical role in the insulin resistance resulting during acute inflammatory stress (114). Here we show the increased ability to transport glucose *in vivo*

limits the impairment in MGU and this protection may be secondary to protection against the cardiac dysfunction associated with endotoxemia.

During the basal state overexpression of GLUT4 led to a decrease in fasting glucose levels and a higher level of basal glucose utilization. We were unable to detect an increase in R_g in any tissues studied except for the soleus with VEH treatment. However K_g (muscle glucose clearance) was improved. This is contrary to previous data which found that GLUT overexpression augments basal MGU, suggesting that glucose transport is the primary site of resistance in the basal state (57, 70, 160, 161). It is possible that the lower glucose concentrations in the present study may have limited our ability to detect a decrease in R_g . As has been previously shown, we found that there was an increase in the availability of the liver gluconeogenic precursor lactate in GLUT4^{Tg} mice, which may serve to maintain the increase in endogenous glucose production in GLUT4^{Tg} mice with VEH treatment (137). However, while there was a significant decrease in R_g in WT mice treated with LPS compared to VEH treatment, GLUT4^{Tg} mice maintained levels of glucose uptake similar to the mice that received VEH treatment.

During the hyperinsulinemic-euglycemic clamp WT and GLUT4^{Tg} mice had similar GIR and tissue glucose uptake with VEH treatment. We did not expect overexpression of GLUT4 to increase glucose uptake under these conditions because previous studies have shown that increased GLUT4 content does not offer any benefit under insulin-stimulated conditions in normal mice. With insulin-stimulation the control of MGU is believed to shift to glucose phosphorylation (61). When mice were treated with LPS, GLUT4^{Tg} mice required higher exogenous glucose infusion rates ($\sim 45 \text{ mg}\cdot\text{kg}^{-1}\cdot\text{min}^{-1}$) during the insulin clamp. This was an improvement of $\sim 10 \text{ mg}\cdot\text{kg}^{-1}\cdot\text{min}^{-1}$ over

WT mice. When we examined tissue glucose uptake LPS treatment led to a significant decrease in MGU compared to VEH treatment in WT mice. However, LPS did not limit the ability of the gastrocnemius and SVL muscle to take up glucose in mice overexpressing GLUT4 compared to VEH treated mice. These results on the surface indicate that in conditions of insulin resistance strategies that augment glucose transport capacity can attenuate barriers to insulin-stimulated glucose uptake. Indeed, during conditions characterized by insulin resistance such as high-fat diet and Type II diabetes, insulin-stimulated glucose transport has been shown to be markedly impaired (62, 82, 85). However as will be discussed later, this protection may be secondary to differing cardiovascular responses to LPS.

The transgenic mouse model used for these studies display increased GLUT4 protein not only in muscle but also in adipose tissue (119). Therefore we compared plasma NEFA levels in WT and GLUT4^{Tg} mice. Increased NEFA levels are associated with a decrease in the responsiveness of adipose tissue to insulin and/or to an increase in autonomic tone and to the lower prevailing arterial glucose concentrations in GLUT4^{Tg} mice. We found no significant difference in glucose uptake by adipose tissue in GLUT4^{Tg} compared to WT mice. Since GLUT4^{Tg} mice exhibited increased plasma NEFA levels with VEH and LPS treatment compared to WT mice it could reflect an increase in lipolysis and a decrease in re-esterification (100, 192). The lower insulin concentration in GLUT4^{Tg} mice may in part explain the higher NEFA levels. However as they also remained elevated when insulin concentrations were increased during the clamp alteration in autonomic tone likely also contributed.

Taken together, the basal and clamp data suggest that overexpression of GLUT4 results in a benefit during acute inflammatory stress. Overexpression of GLUT4 has been shown to alleviate insulin resistance. Ikemoto *et al.* found that a 2-fold increase in GLUT4 at the tissue level improved glycemic control as measured by an oral glucose tolerance test when mice were fed a high-fat diet (74). This increase in glucose uptake was attributed to an increase in glucose transporters at the plasma membrane resulting in increased glucose uptake by skeletal muscle. GLUT4 protein content in the plasma membrane has been shown to be markedly increased compared to WT mice (21). db/db mice overexpressing GLUT4 had improved glucose tolerance that was associated with increased levels of membrane-associated GLUT4 protein (64). Indeed, using immunohistochemistry we found that there was an increase in GLUT4 cell surface expression in gastrocnemius muscle compared to WT mice with VEH treatment. However, when mice were treated with LPS the amount of cell surface GLUT4 was equivalently decreased in both WT and GLUT4^{Tg} mice. These results were interesting due to the fact that our previous data showed insulin signaling through the PI3-K pathway was not impaired with LPS treatment. This pathway is believed to be the major stimulator of GLUT4 translocation to the plasma membrane under insulin-stimulated conditions. This is consistent with a recent report that TNF- α impairs GLUT4 translocation independent of the PI3 kinase pathway (116).

Previous data by our lab showed that there was a significant cardiovascular impairment resulting from LPS treatment (114). Since the improvement in MGU resulting from overexpression of GLUT4 did not appear to be a consequence of increased transporters at the plasma membrane, we next examined if the transgene, which is also

overexpressed in the heart, offered a cardiovascular benefit. The overexpression of GLUT4 attenuates the impairments in stroke volume and cardiac output following LPS. WT mice treated with LPS had a ~50% reduction in stroke volume and cardiac output. While GLUT4^{Tg} mice treated with LPS had a decrease in stroke volume and cardiac output compared to GLUT4^{Tg} mice treated with VEH, it was increased compared to WT mice treated with LPS. In fact, GLUT4^{Tg} mice had a similar stroke volume and cardiac output to WT mice treated with VEH. Under normal conditions cardiac muscle utilizes the oxidation of fatty acids to cover its energy demands, however the failing heart shifts its substrate preference to glucose utilization even in the presence of insulin resistance (165).

Hruz *et al.* utilized a mouse model of dilated cardiomyopathy to demonstrate that the protease inhibitor ritonavir acutely worsened glucose homeostasis in these animals (73). Ritonavir, which directly inhibits GLUT4, significantly decreased cardiac glucose uptake and led to diastolic dysfunction. In addition, lack of GLUT4 aggravates stress induced cardiac dysfunction (159). This suggests that in the setting of cardiac stress, cardiac function is sensitive to GLUT4 activity. Indeed, in disease states such as diabetes there is a downregulation of GLUT4 expression in the heart which is proposed to contribute to myocardial dysfunction (150). In GLUT4-null mice Katz *et al.* observed that while there was a compensatory increase in the GLUT1 transporter, there was a decrease in insulin sensitivity as well as marked hypertrophy (~2-fold) and heart failure (78). With cardiac specific inactivation of GLUT4 there was also a significant increase in cardiac weight as well as the development of cardiac hypertrophy (1). While Abel *et al.* did not observe contractile dysfunction in this model, isolated perfused GLUT4^{-/-} hearts

had increased susceptibility to ischemia and developed irreversible diastolic dysfunction in the presence of significant stress. Similarly in GLUT4^{+/-} mice there is cardiac hypertrophy that is consistent with diabetic cardiomyopathy. These mice also exhibited elevated arterial blood pressure when compared to age-matched controls (154). The introduction of muscle-specific GLUT4 into these mice lead to a reversal of the adverse cardiovascular pathology (163). Since a decrease in GLUT4 expression has a negative affect on cardiac function, it would lead one to believe that overexpression of GLUT4 would improve cardiovascular function. Therefore the improvement in MGU with LPS treatment in GLUT4^{Tg} mice could be due to maintenance of cardiac output and tissue glucose delivery.

In conclusion, our data demonstrate that overexpression of GLUT4 in muscle limits the fall in insulin-stimulated glucose uptake in the presence of an acute inflammatory stress. We have shown that while the GLUT4^{Tg} does not lead to increased glucose transporters at the plasma membrane of skeletal muscle in this setting, the cardiovascular benefit it provides can overcome the impairment in MGU. These data further strengthen our conclusions that cardiovascular impairments caused by an LPS challenge serve as the major barrier to muscle glucose uptake in this setting.

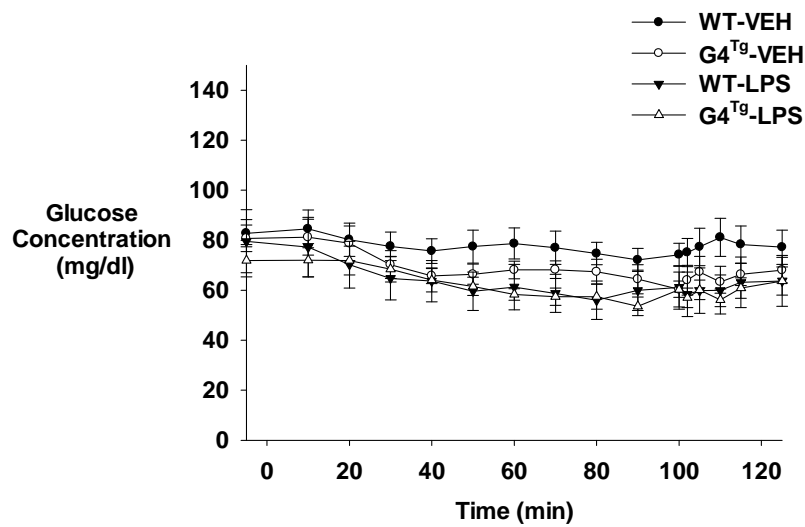
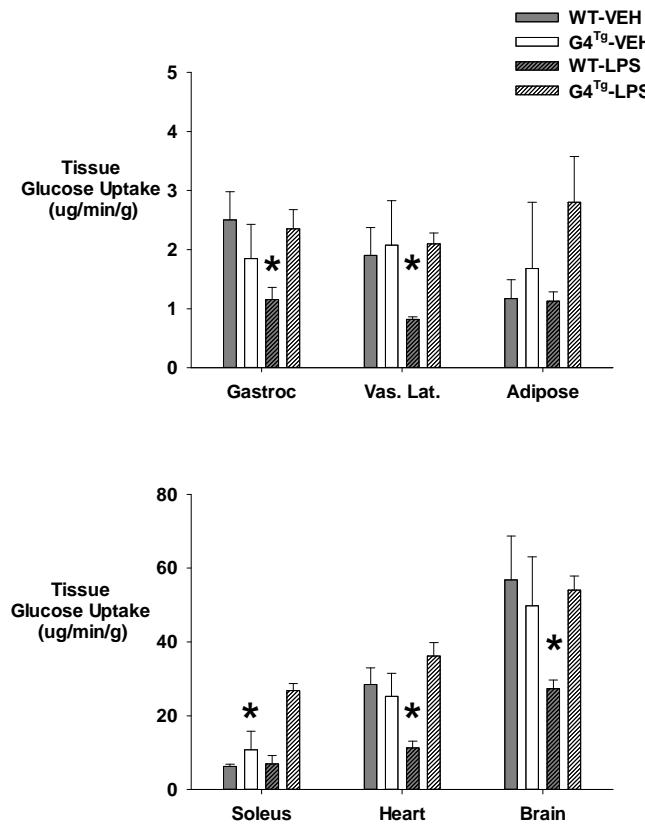
A**B**

Figure 4.1: Basal glucose concentrations and tissue glucose uptake following VEH or LPS treatment in WT and GLUT4^{Tg} mice. (A) Basal arterial glucose and (B) Basal tissue glucose uptake in chronically catheterized 5-h fasted C57BL/6J mice that received VEH or high-dose LPS (10 μ g/g BW). Data are expressed as mean \pm SEM. * $p < 0.05$ VEH vs. LPS, # $p < 0.05$ WT vs. GLUT4^{Tg}.

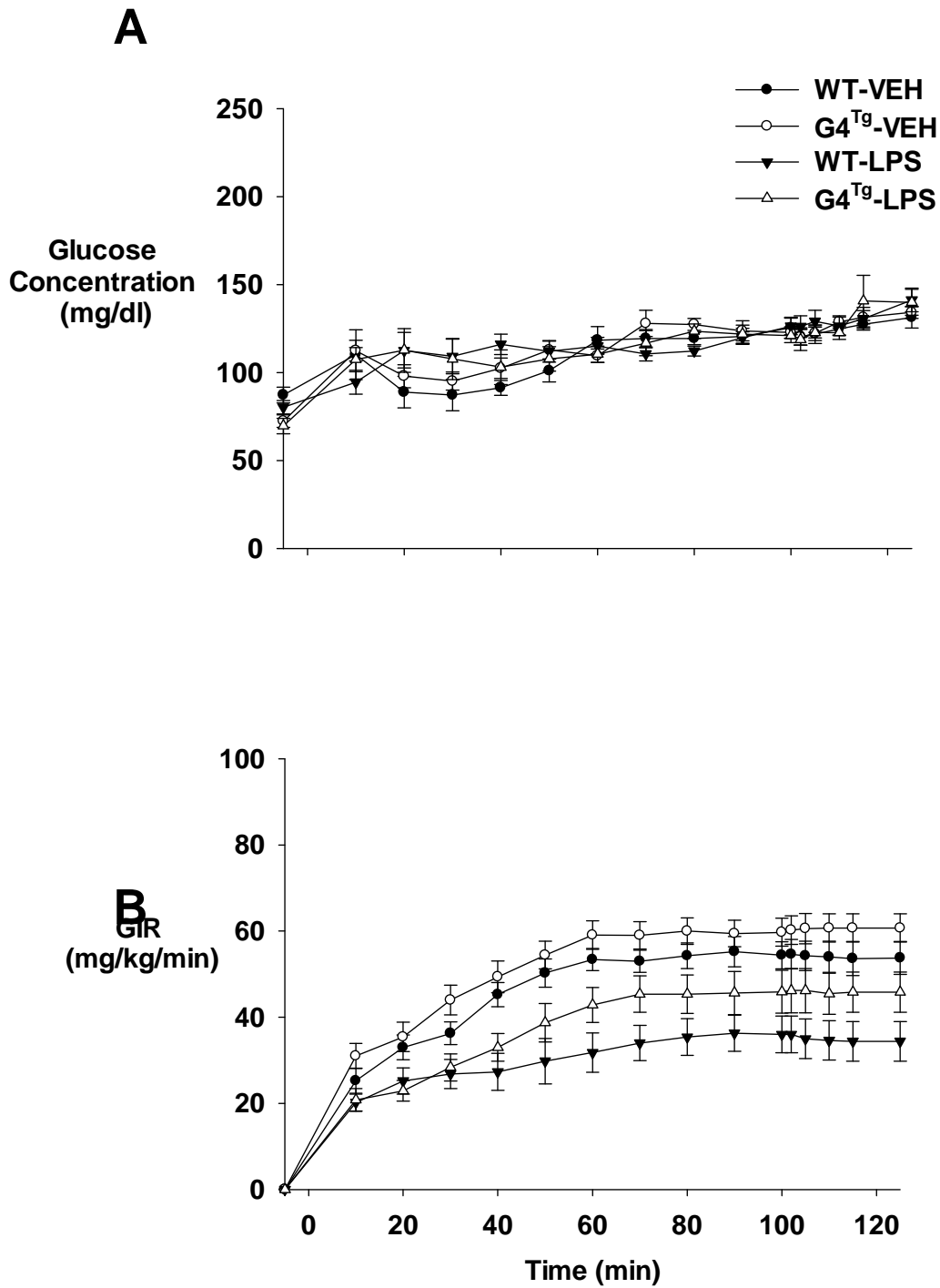


Figure 4.2: Glucose concentrations and glucose infusion rate (GIR) following VEH or LPS treatment in WT and GLUT4^{Tg} mice. (A) Arterial glucose concentrations and (B) Glucose infusion rate (GIR) during a hyperinsulinemic-euglycemic clamp in chronically catheterized 5-h fasted C57BL/6J mice that received VEH or high-dose LPS (10 μ g/g BW).

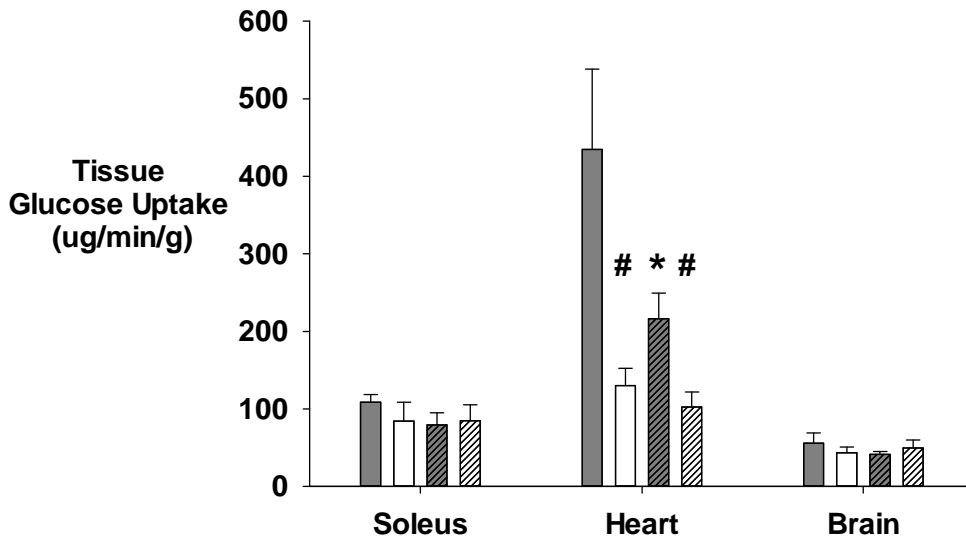
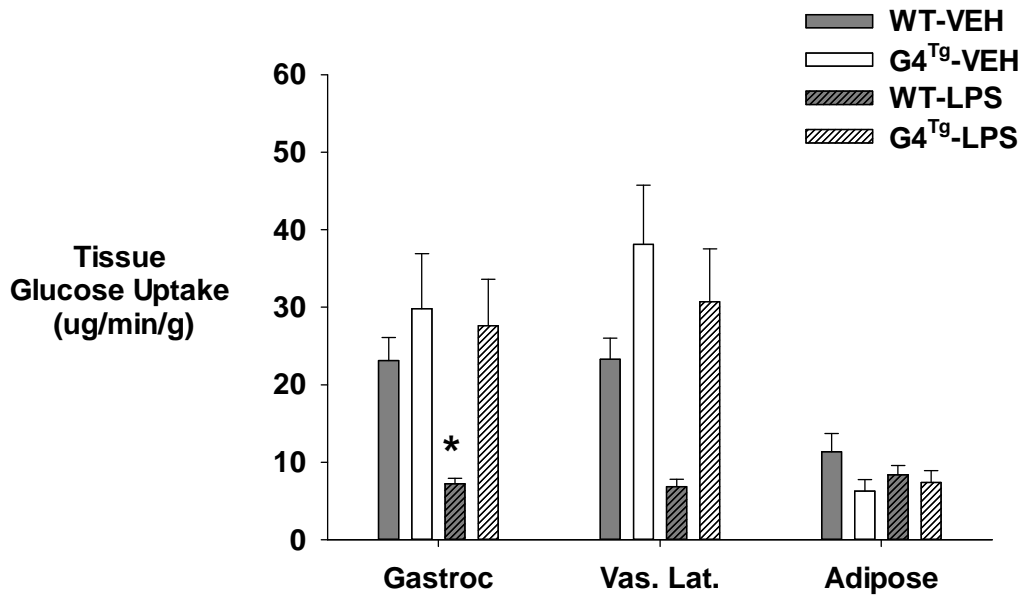


Figure 4.3: Insulin-stimulated tissue glucose uptake following VEH or LPS treatment in WT and GLUT4^{Tg} mice. Tissue (soleus, gastrocnemius, superficial vastus lateralis (SVL), heart, adipose tissue, and brain) glucose uptake during a hyperinsulinemic-euglycemic clamp in chronically catheterized 5-h fasted C57BL/6J mice that received VEH or high-dose LPS. Data are expressed as mean \pm SEM. * $p < 0.05$ VEH vs. LPS, # $p < 0.05$ WT vs. GLUT4^{Tg}.

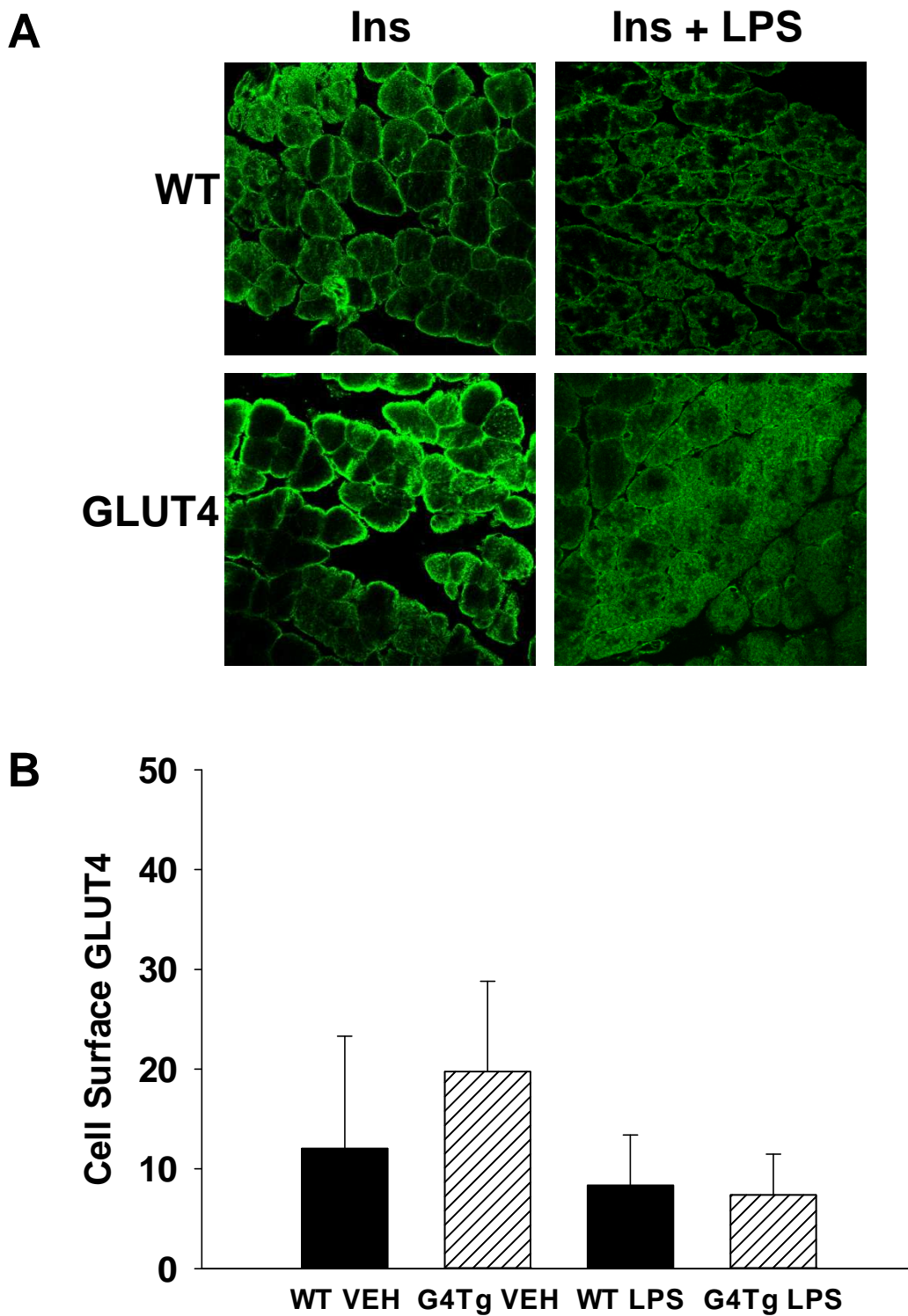


Figure 4.4: Translocation of GLUT4 to the cell surface in the gastrocnemius of WT and GLUT4^{Tg} mice following VEH or LPS treatment. (A) Representative images and (B) quantification of the relative extent of cell surface distribution of GLUT4 was Data are expressed as mean ±SEM.

Genotype	Insulin (ng/ml)	
	Basal (4 h)	Saline (6 h)
VEH		
WT	0.51±0.01	0.56±0.16
GLUT4 ^{Tg}	0.40±0.14	0.27±0.04
LPS		
WT	0.17±0.01	0.22±0.04
GLUT4 ^{Tg}	0.28±0.09	0.26±0.08

Table 4.1: Basal arterial plasma insulin following VEH or LPS treatment in WT and GLUT4^{Tg} mice. Arterial plasma insulin levels (ng/ml) in chronically catheterized conscious mice during the basal period (t= 4 h) and saline infusion (t= 6 h) following VEH or high- (10μg/g BW) dose LPS. Data are expressed as mean ±SEM.

Genotype	Insulin (ng/ml)	
	Basal (4 h)	Clamp (6 h)
VEH		
WT	0.33±0.09	2.54±0.19
GLUT4 ^{Tg}	0.35±0.07	2.99±0.24
LPS		
WT	0.32±0.04	3.73±0.25
GLUT4 ^{Tg}	0.40±0.07	4.61±0.43

Table 4.2: Arterial plasma insulin following VEH or LPS treatment in WT and GLUT4^{Tg} mice. Arterial plasma insulin levels (ng/ml) in response to VEH or high-(10µg/g BW) dose LPS in chronically catheterized conscious mice during the basal period (t=4 h) and hyperinsulinemic-euglycemic clamp (t=6 h). Data are expressed as mean ±SEM.

Genotype	NEFA (mM)	
	Basal (4 h)	Clamp (6 h)
VEH		
WT	2.1±0.1	0.7±0.2*
GLUT4 ^{Tg}	3.0±0.6	1.7±0.1* [#]
LPS		
WT	3.8±0.3	1.4±0.2*
GLUT4 ^{Tg}	6.3±0.8 [#]	2.7±0.5* [#]

Table 4.3: Plasma NEFA levels following VEH or LPS treatment in WT or GLUT4^{Tg} mice. Plasma NEFA levels (ng/ml) in response to VEH or high- (10μg/gBW) dose LPS treatment during the basal period (t=4 h) and hyperinsulinemic-euglycemic clamp (t=6 h). Data are expressed as mean ±SEM. * p<0.05 0 vs. 6 h, # p<0.05 WT vs. GLUT4^{Tg}.

Genotype	Plasma Lactate ($\mu\text{mol/L}$)	
	Basal (4 h)	Clamp (6 h)
VEH		
WT	811 \pm 59	691 \pm 152
GLUT4 ^{Tg}	1962 \pm 670 [#]	1374 \pm 306 [#]
LPS		
WT	972 \pm 83	876 \pm 149
GLUT4 ^{Tg}	1983 \pm 389 [#]	2145 \pm 194 [#]

Table 4.4: Plasma lactate levels following VEH or LPS treatment in WT and GLUT4^{Tg} mice. Plasma lactate levels ($\mu\text{mol/L}$) in response to VEH or high- (10 $\mu\text{g/g}$ BW) dose LPS treatment during the basal period (t=4 h) and following a saline infusion (t=6 h). Data are expressed as mean \pm SEM. * p<0.05 0 vs. 6 h, # p<0.05 WT vs. GLUT4^{Tg}

Genotype	Baseline (0 h)	6 h
Stroke Volume (uL)		
WT VEH	31.1 ± 1.8	32.7 ± 1.9
GLUT4 ^{Tg} VEH	33.6 ± 1.8	36.2 ± 3.3
WT LPS	35.2 ± 2.5	17.4 ± 0.8
GLUT4 ^{Tg} LPS	31.5 ± 5.5	26.2 ± 1.6
Heart Rate (bpm)		
WT Vehicle	690 ± 15	660 ± 14
GLUT4 ^{Tg} Vehicle	697 ± 22	587 ± 18
WT LPS	649 ± 10	473 ± 40
GLUT4 ^{Tg} LPS	656 ± 8	570 ± 32
Cardiac Output (ml·g⁻¹·min⁻¹)		
WT Vehicle	0.57 ± 0.03	0.56 ± 0.03
GLUT4 ^{Tg} Vehicle	0.63 ± 0.05	0.57 ± 0.07
WT LPS	0.62 ± 0.05	0.22 ± 0.02
GLUT4 ^{Tg} LPS	0.54 ± 0.04	0.36 ± 0.04

Table 4.5: Cardiovascular parameters following VEH or LPS treatment in WT and GLUT4^{Tg} mice. Comparison of stroke volume, heart rate, and cardiac output in mice at baseline (t=0) and 6 h after receiving vehicle or high- (10µg/g BW) dose LPS.

CHAPTER V

INCREASED GLUCOSE PHOSPHORYLATION CAPACITY IN SKELETAL MUSCLE DOES NOT REDUCE THE INFLAMMATION INDUCED IMPAIRMENTS IN INSULIN-STIMULATED MUSCLE GLUCOSE UPTAKE

Aims

The aim of this chapter was to delineate whether increased glucose phosphorylation capacity through overexpression of HKII in skeletal muscle leads to an improvement in MGU in the presence of an LPS challenge. We hypothesized that increased skeletal muscle phosphorylation capacity would lead to an increase in MGU in the setting of acute inflammatory stress induced by LPS.

The phosphorylation of glucose to G6P represents the committed step in MGU. Once phosphorylated, glucose is trapped in the tissue and is either stored as glycogen or undergoes further oxidation. Glucose phosphorylation capacity is determined by hexokinase activity, its relationship to its substrate ATP, and the concentration of its inhibitor, G6P.

There are many factors that can augment glucose uptake by the muscle. Depending on the setting each step's contribution to MGU may increase/decrease. While glucose transport is a significant barrier to muscle glucose uptake in the basal state, in insulin-stimulated states phosphorylation becomes a significant barrier (61).

Glucose transport and phosphorylation are tightly coupled to one another. Transgenes that alter the expression of proteins involved in both of these processes have provided insight into how each step individually regulates MGU. Therefore, the objective

of this chapter was to determine if overexpression of HKII capacity in skeletal muscle can overcome decreases in the proceeding steps involved in MGU in the setting of acute inflammatory stress in conscious C57Bl/6J mice *in vivo*. Several studies have found that during acute inflammatory stress there is an increase in the basal glucose transporter, GLUT1, which could augment glucose uptake by the myocytes. Therefore, if we are able to maintain the downhill concentration gradient by increasing phosphorylation capacity, we may see an improvement in MGU in this setting. We hypothesized that by overexpressing HKII in skeletal muscle we would improve the impairments in MGU induced by LPS.

Experimental Approach

Wild-type and HKII^{Tg} C57Bl/6J littermates approximately 12 weeks of age were treated with either vehicle or high-dose (10µg/g BW) LPS. A hyperinsulinemic-euglycemic clamp was performed to assess whether increased muscle glucose phosphorylation capacity can overcome the impairment in glucose uptake due to acute inflammatory stress induced by LPS.

Results

HKII-overexpression Does Not Inhibit LPS-induced Decreases in Basal Muscle Glucose Uptake.

It has previously been shown that the HKII transgene leads to a 3-, 5- and 7-fold overexpression of HKII in the soleus, gastrocnemius, and SVL muscles, respectively in

the C57BL/6/j mice (25). In the presence of a saline infusion, there were no significant differences in insulin levels (ng/ml) between HKII^{Tg} and WT mice with VEH treatment. While HKII^{Tg} mice had elevated insulin levels at t= 0 min compared to WT mice, by t= 125 min the levels were similar (Table 5.1). Basal glucose concentrations were similar between HKII^{Tg} and WT mice with VEH treatment and glucose concentrations fell similarly with LPS treatment (Figure 5.2). Basal endogenous glucose production ($\text{mg}\cdot\text{kg}^{-1}\cdot\text{min}^{-1}$) was significantly higher in HKII^{Tg} compared to WT mice that received VEH treatment and remained slightly elevated compared to WT in the presence of LPS (10.2 ± 0.3 vs. 21.7 ± 1.2 , vehicle and 5.7 ± 0.2 vs. 8.0 ± 0.3 , LPS; vehicle, WT and HKII^{Tg}, respectively). Interestingly, while endogenous glucose production was elevated in HKII^{Tg} mice, there was no significant difference in basal tissue glucose uptake with VEH treatment compared to WT mice, and LPS treatment lead to a similar decrease in glucose uptake (Figure 5.2).

Mice Overexpressing HKII Have Impaired Insulin-Stimulated Muscle Glucose Uptake with LPS Treatment.

A hyperinsulinemic-euglycemic clamp was used to assess differences in insulin action between WT and HKII^{Tg} mice. During the clamp, glucose concentrations were maintained at ~120 mg/dl (Figure 5.3) and there were no differences in insulin levels between the groups with either VEH or LPS treatment (Table 5.2). The glucose infusion rates (GIR; $\text{mg}\cdot\text{kg}^{-1}\cdot\text{min}^{-1}$) were similar in HKII^{Tg} and WT mice with VEH treatment and decreased similarly with LPS treatment (54.6 ± 0.5 vs. 54.2 ± 0.5 , VEH; 35.6 ± 0.4 vs. 35.4 ± 0.6 , LPS, respectively) (Figure 5.3). While there were no differences in

glucose uptake between the groups with VEH treatment, LPS treatment translated into a significant decrease in glucose uptake in the gastrocnemius, SVL, and heart in both groups (Figure 5.3).

HKII-overexpression Does Not Lead to Increased Lactate Levels.

The effect of overexpressing the HKII transgene on plasma lactate levels under hyperinsulinemic-euglycemic clamp conditions was measured. While plasma lactate levels increased with LPS treatment in all groups, HKII^{Tg} mice had significantly higher plasma lactate levels compared to WT mice with either VEH or LPS treatment (Table 5.4).

LPS Treatment Does Not Decrease Binding of HKII to the Mitochondria.

The effect of LPS on HKII binding to the mitochondria in gastrocnemius muscle was examined in WT mice. When comparing HKII located in the cytosolic fraction of the gastrocnemius muscle between mice that received VEH or LPS, there was no difference in the HKII levels. When the amount of HKII located at the mitochondria was examined, we similarly found no differences in the amount of HKII at the mitochondria in mice treated with VEH compared to those treated with LPS (Figure 5.4).

Discussion

Utilizing mice that overexpress the enzyme responsible for the phosphorylation of glucose we sought to test the hypothesis that increased HKII content in skeletal muscle can improve impairments in insulin action *in vivo* resulting from a LPS challenge. In settings of increased blood flow and permeability of glucose to the plasma membrane, the barrier to MGU is believed to shift downstream to phosphorylation capacity. Dysregulation which results in impairments of MGU can occur at multiple steps of the glucose uptake pathway and can lead to a shift in the control. Our findings indicate that during inflammatory stress induced by LPS, mice with increased phosphorylation capacity in skeletal muscle are unable to overcome impairments in glucose delivery and transport to increase MGU *in vivo*.

The overexpression of HKII had no effect on basal MGU. When we compared HKII^{Tg} and WT mice there were no significant differences in plasma glucose or insulin levels with VEH treatment and levels decreased in a similar manner between the two groups when mice received LPS. This translated to a similar decrease in MGU in both groups with LPS treatment. These results were not surprising due to the fact that phosphorylation is not thought to be a site of resistance to glucose influx in the basal state and therefore does not alter R_g (25, 57). During the hyperinsulinemic-euglycemic clamp glucose and insulin levels were matched between WT and transgenic mice. When the mice were treated with VEH, there was no difference in GIR or MGU between WT and transgenic mice. These results were surprising because in previous *in vivo* studies overexpression of HKII has been shown to increase GIR and led to an increase in insulin-stimulated glucose uptake in the soleus, gastrocnemius, and SVL muscle (56, 69).

Hexokinase binds to the voltage dependent anion channel (VDAC or mitochondrial porin) and this binding is required for HKII because of the need of ATP for its activity. Therefore, we utilized a Mitochondrial Extraction Kit to determine if there was a greater fraction of HKII located in the cytosol or mitochondria of mice treated with VEH and LPS. Due to the fact that LPS can induce to mitochondrial dysfunction, we expected that there would be an increase in HKII located in the cytosolic fraction of WT LPS treated mice however transgenic mice treated with LPS would have a greater fraction of HKII located at the mitochondria. Our results indicated that there was no difference in HKII located at the mitochondria in WT mice treated with VEH or LPS under insulin-stimulated conditions. Subsequent attempts to separate the cytosolic and mitochondrial fractions were unsuccessful; therefore we were unable to determine if there was an increase in HKII located in the mitochondrial fraction of transgenic mice.

We were interested in determining the flux of ATP in the skeletal muscle of mice treated with VEH and LPS *in vivo*. To accomplish this, we attempted to use NMR in collaboration with Dr. Bruce Damon to measure the rate of decay of ATP compared to known intrinsic levels of ATP. We hypothesized that there would be a shift to the left in the rate of decay for mice treated with LPS compared to VEH treated mice which would be indicative of skeletal muscle mitochondrial dysfunction. Unfortunately, we were unable to design a ^{31}P surface coil (which takes advantage of several markers related to muscle status, including phosphocreatine (PCr), adenosine triphosphate (ATP) and inorganic phosphate (Pi)) that would work properly on the hind leg of the mouse and therefore were unable to measure muscle energy metabolism.

In conclusion, the results from our study were consistent with the literature. The combination of cytokine and LPS has been shown to increase GLUT1 transporter levels but decrease GLUT4 expression in L6 cells (14). This potentially could lower the transport barrier with LPS-treatment and unmask a phosphorylation dysfunction that could be overcome by increasing the amount of HKII in skeletal muscle. However, a previous study by Hansen *et al.* found that overexpression of HKII on a GLUT1 transgenic background did not increase basal- or insulin-stimulated glucose disposal or glucose transport in isolated skeletal muscle (71). Glucose flux through the glycolytic pathway is elevated in this setting which can lead to increased glucose-6-phosphate levels potentially inhibiting hexokinase activity. Increased phosphorylation capacity was also unable to compensate for impairments seen in another insulin-resistant state induced by high-fat feeding (56). Mice overexpressing HKII placed on a high-fat diet were unable to reverse the impairment in GIR and insulin-stimulated MGU. Unfortunately we were unable to fully explore if there were impairments in HK binding to the mitochondrial and if so, could overexpression of HKII overcome this impairment. We were also unable to determine if ATP flux was impaired in this setting. Since ATP is an important cofactor for HKII activity, if levels are significantly decreased having increased HKII may not alleviate impairments resulting from LPS treatment. From the data that we were able to obtain, we concluded that overexpression of HKII did not improve MGU in the presence of LPS. It appears that defects in MGU during LPS treatment result from impairments upstream or downstream of glucose phosphorylation.

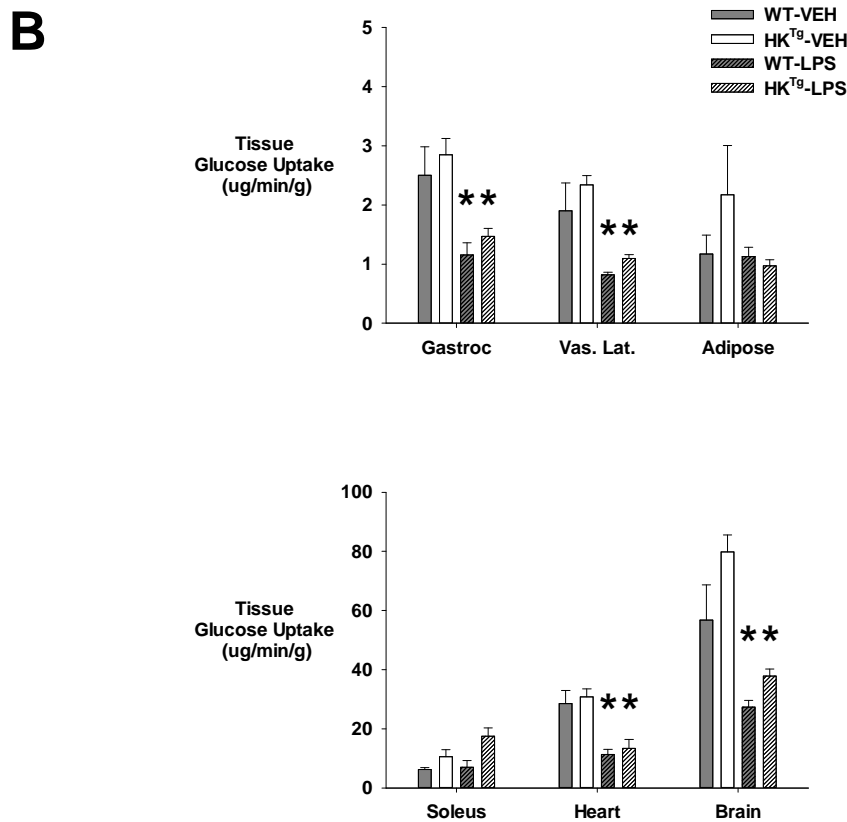
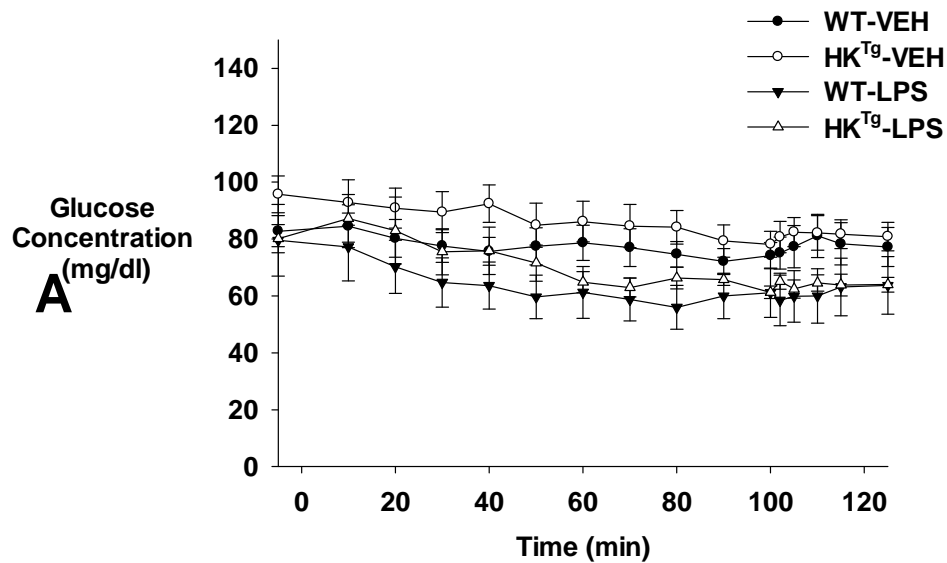


Figure 5.1: Basal glucose concentrations and tissue glucose uptake following VEH or LPS treatment. (A) Basal arterial glucose and (B) Basal tissue glucose uptake in chronically catheterized 5-h fasted C57BL/6J mice that received VEH or high-dose LPS (10 μ g/g BW). Data are expressed as mean \pm SEM. * $p < 0.05$ VEH vs. LPS.

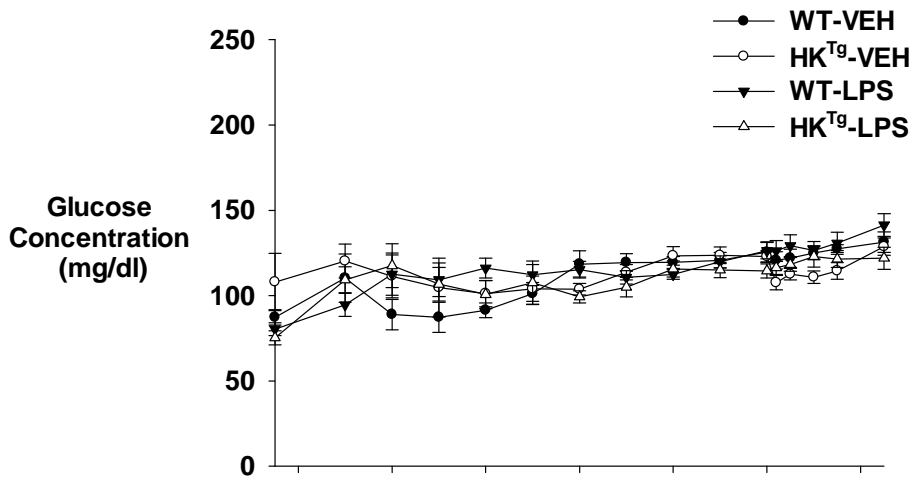
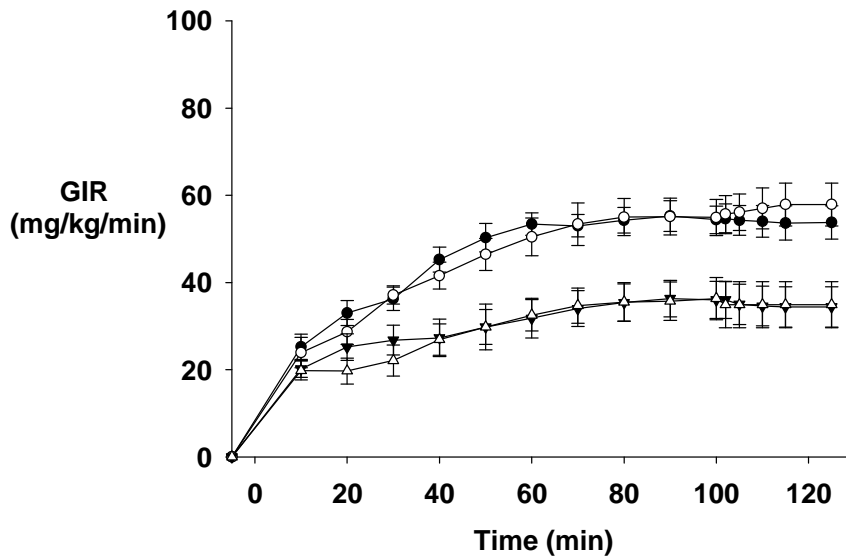
A**B**

Figure 5.2: Glucose concentrations and glucose infusion rate (GIR) following VEH or LPS treatment in WT and HKII^{Tg} mice. (A) Arterial glucose concentrations and (B) Glucose infusion rate (GIR) during a hyperinsulinemic-euglycemic clamp in chronically catheterized 5-h fasted C57BL/6J mice that received VEH or high-dose LPS (10 μ g/g BW).

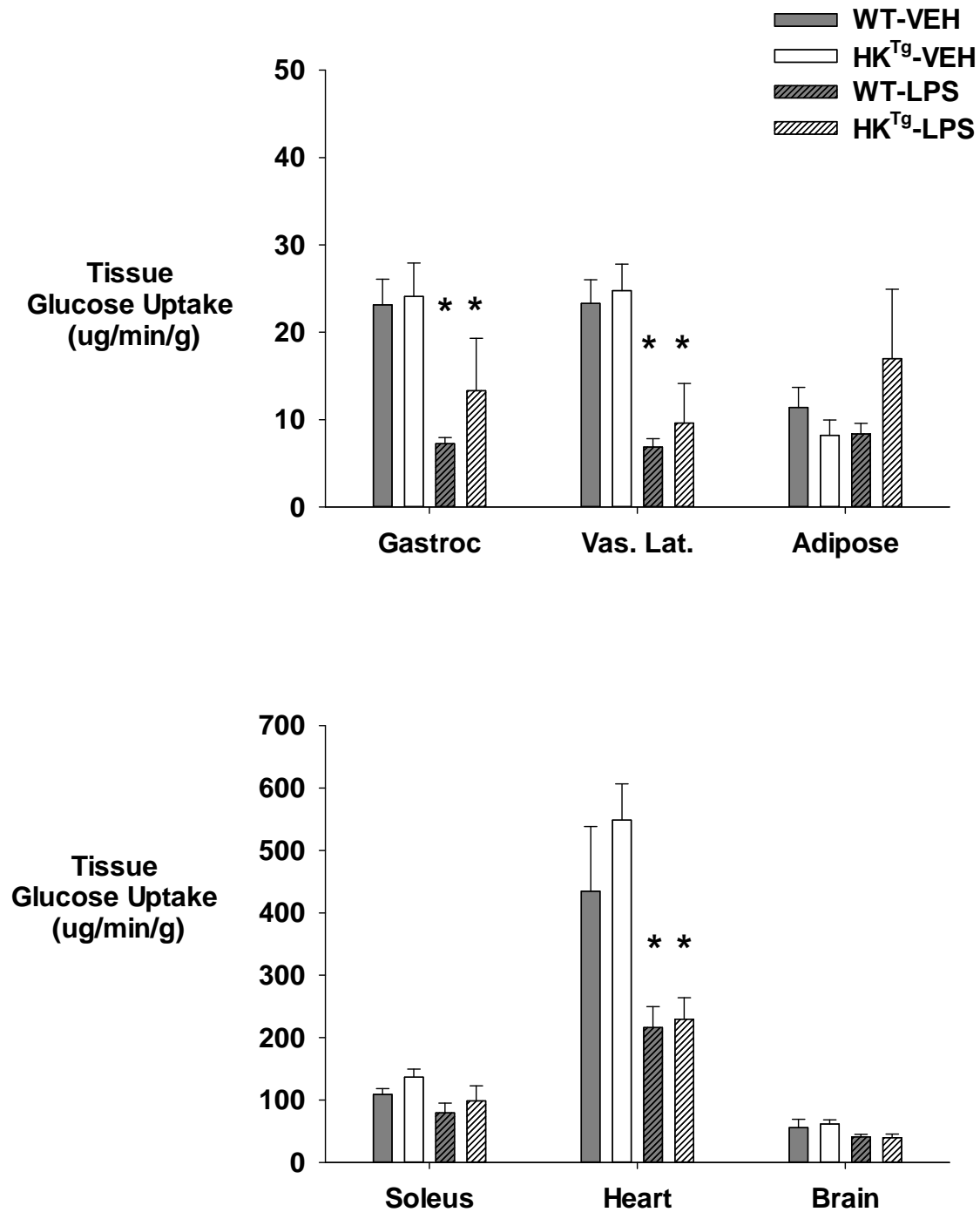


Figure 5.3: Insulin-stimulated tissue glucose uptake following VEH or LPS treatment in WT and HKII^{Tg} mice. Tissue (soleus, gastrocnemius, superficial vastus lateralis (SVL), heart, adipose tissue, and brain) glucose uptake during a hyperinsulinemic-euglycemic clamp in chronically catheterized 5-h fasted C57BL/6J mice that received VEH or high-dose LPS. Data are expressed as mean \pm SEM. * $p < 0.05$ VEH vs. LPS.

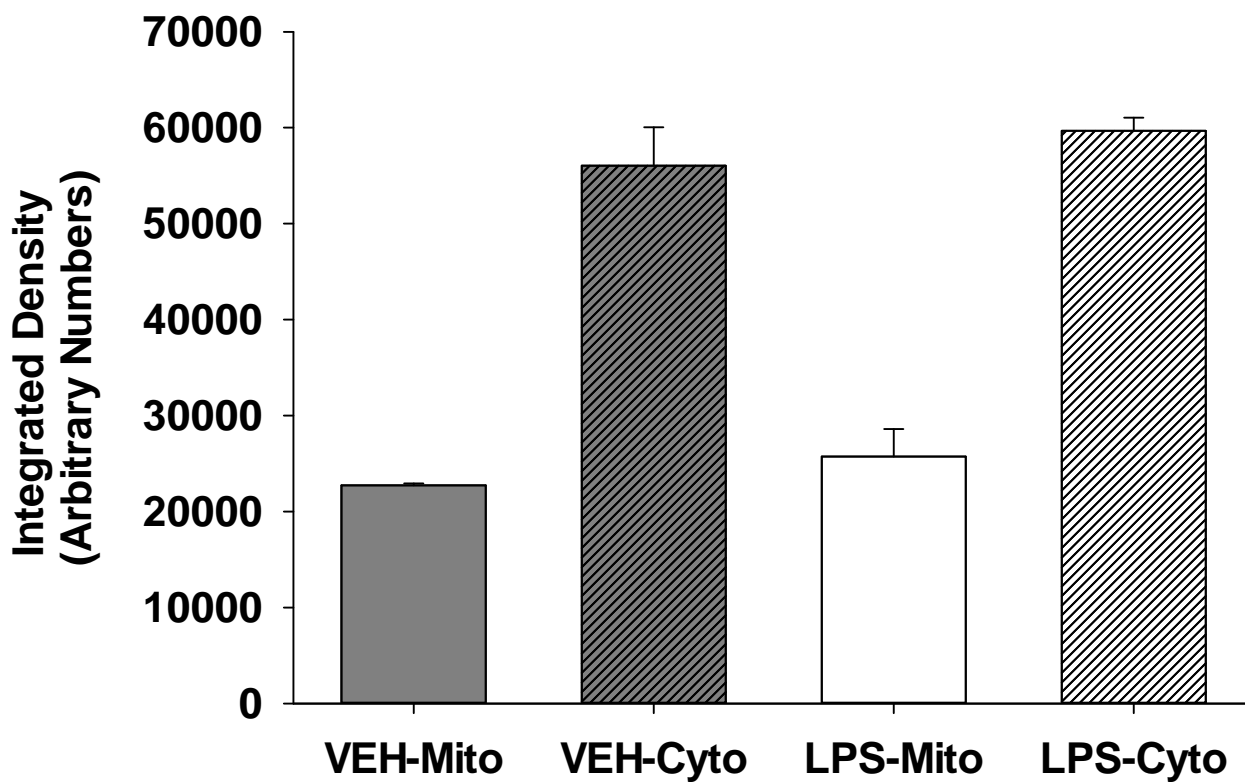


Figure 5.4: Comparison of HKII content in the cytosol and mitochondria of the gastrocnemius muscle following VEH or LPS treatment. HKII content in the cytosol and mitochondria of the gastrocnemius muscle in saline infused WT C57BL/6J mice following either vehicle (n = 3) or LPS (n = 3) treatment.

Genotype	Insulin (ng/ml)	
	4 h	6 h
VEH		
WT	0.51±0.01	0.56±0.16
HKII ^{Tg}	0.51±0.10	0.52±0.16
LPS		
WT	0.17±0.01	0.22±0.04
HKII ^{Tg}	0.32±0.08	0.17±0.02

Table 5.1: Basal arterial plasma insulin following VEH or LPS treatment in WT and HKII^{Tg} mice. Arterial plasma insulin levels (ng/ml) in chronically catheterized conscious mice during the basal period (t=4 h) and a saline infusion (t= 6 h) following VEH or high- (10μg/g BW) dose LPS. Data are expressed as mean ±SEM.

Genotype	Insulin (ng/ml)	
	4 h	6 h
VEH		
WT	0.33±0.09	2.54±0.19
HKII ^{Tg}	0.66±0.18	2.66±0.42
LPS		
WT	0.32±0.04	3.73±0.25
HKII ^{Tg}	0.28±0.04	3.94±0.49

Table 5.2: Arterial plasma insulin following VEH or LPS treatment in WT and HKII^{Tg} mice. Arterial plasma insulin levels (ng/ml) in response to VEH or high-(10µg/gBW) dose LPS in chronically catheterized conscious mice during the basal period (t=4 h) and following a hyperinsulinemic-euglycemic clamp (t= 6 h). Data are expressed as mean ±SEM.

Genotype	Plasma lactate ($\mu\text{mol/L}$)	
	4 h	6 h
VEH		
WT	699 \pm 67	898 \pm 94
HKII ^{Tg}	865 \pm 159	861 \pm 162
LPS		
WT	1126 \pm 188	1479 \pm 95
HKII ^{Tg}	1022 \pm 135	1551 \pm 205

Table 5.3: Plasma lactate levels following VEH or LPS treatment in WT and HKII^{Tg} mice. Plasma lactate levels ($\mu\text{mol/L}$) in response to vehicle or high- ($10\mu\text{g/g}$ BW) dose LPS treatment during the basal period (t=4 h) and following a hyperinsulinemic-euglycemic clamp (t=6 h). Data are expressed as mean \pm SEM.

CHAPTER VI

CONCLUSIONS AND FUTURE DIRECTIONS

Conclusions

Plasma glucose concentrations are normally maintained within a narrow range even though there are fluctuations in the body's supply and demand for nutrients. This tight glucose control is necessary to prevent the deleterious effects of hypo- or hyperglycemia. To maintain stable glucose levels there must be a balance in the rate of delivery of glucose to the systemic circulation balanced by the rate of glucose removal.

During critical illness, patients experience a hypermetabolic state characterized by increased energy expenditure, mobilization of endogenous fuels, and release of cytokines as well as counterregulatory hormones. A common side effect associated with critical illness is hyperglycemia. This hyperglycemia, also known as stress diabetes or diabetes of injury, reflects a combination of factors. These include increased glucose production by the liver sustained by an increase in gluconeogenic substrates as well as insulin resistance by the muscle and adipose tissue. Unless severe, hyperglycemia has generally been thought to be acceptable and was not corrected as it was believed that the duration of exposure was relatively short (as compared to that seen in long standing diabetes). It was also deemed necessary to maintain fuel to the non-insulin dependent glucose utilizing organs such as the brain and immune system. However there is increasing evidence that associates the even relatively brief duration of hyperglycemia in critically ill patients with adverse outcomes.

There has been interest in applications to intensify glycemic control in acutely ill patients. Van den Berghe *et al.* demonstrated that there was a decreased morbidity and mortality among acutely ill patients who were managed in a surgical intensive care unit for more than 3 days and treated with an IV insulin regimen that maintain blood glucose levels within a normal range (166). There was a second study by the same group that showed a decrease in mortality among patients who achieved normoglycemia with the intensive insulin regimen compared with those who maintained a higher blood level glucose (167).

The problem with intensive insulin therapy in the ICU is marked increases in iatrogenic hypoglycemia and/or glucose variability, both of which are associated with increased morbidity or mortality. Those who stayed in the ICU for less than 3 days had increased mortality which was due largely to hypoglycemia. Hypoglycemia occurs in a narrow window with a sudden and unpredictable onset, and requires immediate correction. There have been numerous studies to look at intensive insulin therapy and the outcome is mixed. Van der Crabben *et al.* believed that there is a specific period early in the pathophysiology of sepsis when insulin sensitivity is increased and patients are vulnerable to sudden and severe hypoglycemia, especially with early initiation of intensive protocols (168). Three fourths of critically ill patients who meet the criteria for a diagnosis of sepsis have circulating LPS and elevated serum levels of LPS are associated with septic shock and mortality. They injected healthy volunteers with LPS as a model of sepsis and measured glucose kinetics under euglycemic conditions with a low and moderate level of insulin clamps. LPS was associated with increased insulin sensitivity 2 hours after injection as manifested by enhanced whole body glucose uptake

at both insulin levels and diminished endogenous glucose production at lower insulin levels which occurred despite increases in plasma concentrations of norepinephrine, epinephrine, and cortisol.

From the Van den Berghe study, the favorable outcomes were most attributed to benefits observed among patients who had multiorgan failure with a septic source, patients with some degree of sepsis or septic shock. Conversely, the frequency of severe hypoglycemia is especially high in those with severe sepsis or septic shock, even if the glycemic goal of intensive insulin therapy is adjusted to remain above a strictly normoglycemic range. These opposing outcomes underscore the fact that sepsis is itself a multiphasic and complex condition, associated on the one hand with an acute increase in insulin resistance and hyperglycemia due to the exuberant release of proinflammatory cytokines and the other with an elevated risk of early hypoglycemia. The mechanisms underlying altered glucose metabolism and insulin action in the setting of sepsis need to be understood better to permit rational and targeted applications of protocols for intensive glycemic control.

The work presented in my dissertation has focused on the effect of acute inflammation induced by LPS on MGU. *In vivo* the process of MGU is distributed over 3 tightly coupled steps and depending on the insult, one step may exert greater control over the amount of glucose taken up by this tissue. LPS elicits a strong immune response that leads to increased cytokine production. Cytokines are major contributors to the underlying insulin resistance by promoting hyperglycemia through increased glucose production as well as hepatic and peripheral insulin resistance. Mesotten *et al.* found that in humans that received intensive insulin therapy postmortem biopsies revealed increased

mRNA levels of skeletal muscle GLUT4 and HKII (109). Their conclusion was that this therapy works by normalizing blood glucose levels through increasing peripheral glucose uptake. The major aim of this research was to determine which step of MGU serves as the major barrier to glucose uptake in the presence of acute inflammation induced by LPS and if by increasing proteins involved in transport and phosphorylation we can overcome the impairment in MGU.

We demonstrate that in the conscious mouse *in vivo*, high-dose LPS impaired MGU by inhibiting delivery of glucose to the muscle. We showed there are considerable impairments in several cardiovascular parameters, including stroke volume, heart rate, and cardiac output, in mice receiving a high-dose of LPS compared to those receiving VEH and low-dose LPS. Mice that received high-dose LPS had a significant decrease in glucose uptake by several tissues including the gastrocnemius, SVL, heart, and brain. Impairments in MGU have been attributed to impairments in insulin signaling. We found insulin signaling to be intact in mice treated with high-dose LPS and the differences in insulin-stimulated glucose were less dramatic when we compared VEH, low-dose, and high-dose LPS treated mice. These results, combined with our data showing there is a decrease in blood flow to the muscle with high-dose LPS led to the conclusion that high-dose LPS inhibits MGU by impairing the delivery of glucose to the muscle.

Transport has been regarded as the primary barrier to glucose uptake in the basal state, but under insulin-stimulated conditions, the barrier shifts to glucose phosphorylation. We demonstrated that overexpression of GLUT4 in skeletal muscle can ameliorate impairments in insulin-stimulated MGU caused by LPS. These results were surprising due to the fact that in the previous literature, increased GLUT4 expression

increased glucose uptake in the basal state, but showed no benefit with regards to insulin-stimulated glucose uptake. The immunohistochemistry data showed that while there was an increase in GLUT4 transporters at the plasma membrane in mice overexpressing GLUT4, this overexpression could not overcome the LPS induced decrease in membrane associated GLUT4. These results were surprising due to the fact we hypothesized the benefit seen with these mice would be due to their increased ability to extract glucose because of an increase in transporters at the membrane. This led us to examine whether this perturbation offered any cardiovascular benefit. While the results are preliminary, it appears that increased GLUT4 in the heart limited the LPS induced impairments in cardiovascular function. Our conclusions are that increased GLUT4 provides a cardiovascular benefit that leads to increased MGU in the presence of acute inflammation.

Finally, we demonstrated that overexpression of HKII in skeletal muscle does not lead to an improvement in MGU during acute inflammatory stress. Our original hypothesis was that increased phosphorylation capacity would lead to an increase in MGU due to the fact that the transport barrier would be lowered by the increased expression of GLUT1 in the presence of LPS. While overexpression of HKII has been found to offer no benefit to glucose uptake *in vitro*, during insulin-stimulated states phosphorylation is believed to be the major barrier to MGU. We were interested in determining if the reason why we saw no benefit was due to mitochondrial dysfunction. Since ATP is a necessary cofactor for HKII activity, decreased ATP could hamper any benefit obtained by having increased HKII in the muscle. Our preliminary data showed

there was not a problem with the binding of HKII to the mitochondria in the presence of LPS and we were unable to determine if there was decreased flux of ATP.

Future Directions

Cardiovascular depression is a major hallmark of sepsis and dramatically increases mortality rates (189). This work sheds light on the fact that cardiovascular dysfunction plays a major role in impairing MGU in the presence of acute inflammatory stress. An interesting follow-up to this work would be determining whether minimization of the cardiovascular impairments would increase MGU during acute, LPS-induced inflammatory stress. TLR4 plays a key role in the inflammatory response induced by most forms of sepsis. LPS binds to the TLR4/MD2/CD14 complex leading to the release of inflammatory cytokines and myocardial TLR-4 has been shown to be involved in signaling cytokine production within the heart during endotoxic shock (13). A recent paper by Ehrentraut *et al.* demonstrated that administration of a TLR4 antagonist to mice (eritoran testrasodium, E5564) 15 min prior to a LPS challenge partially prevented the LPS-induced decrease in blood pressure and heart rate, while also preventing an increase in iNOS mRNA levels (45). There was also a decrease in mRNA levels of TNF- α , IL-1 β , IL-6, and iNOS in aortic tissue. It would be interesting to use the TLR4 antagonist in mice treated with LPS (or genetically remove TLR4 from the endothelium) and perform a hyperinsulinemic-euglycemic clamp protocol to determine if the improvement in cardiovascular function seen in this model would lead to an improvement in MGU.

Our studies revealed that iNOS was significantly upregulated in the gastrocnemius muscle extracts with LPS treatment. Currently our lab is examining the

effect of increased nitric oxide delivery on MGU. They have observed significant insulin resistance. There is a possibility that the increased iNOS we observed was not specifically in myocytes but in the endothelium. Therefore another interesting experiment would be to determine if knocking out endothelial iNOS would reverse the LPS induced impairment in MGU.

In our GLUT4^{Tg} mice, we expected that overexpression of GLUT4 would lead to an increase in the transporter at the plasma membrane. This in turn, would increase the ability of the muscle to extract the glucose that was being carried through the bloodstream thereby increasing MGU. However, in the presence of LPS, GLUT4 translocation to the plasma membrane was inhibited, even when the protein was overexpressed. We demonstrated that the beneficial effect of GLUT4 overexpression was not due to increased transporters at the plasma membrane of muscle but due to its ability to increase cardiovascular function. GLUT4 insulin-mediated translocation is regulated through two pathways, a PI3-K dependent pathway which utilizes AKT and the PI3-K independent pathway which requires Cbl associated protein (CAP)-dependent activation of TC10. APS recruits Cbl, along with CAP, to the insulin receptor where it is phosphorylated by insulin. Once phosphorylated, the Cbl-CAP complex is released to lipid rafts where through the activation of C3G and TC10, GLUT4 is translocated to the plasma membrane (145). A recent study by Nohara *et al.* examined the acute actions of TNF- α on 3T3L1 adipocytes (116). They demonstrated that TNF- α can acutely regulate CDK5-dependent phosphorylation of TC10 which induces insulin resistance independent of IRS1-dependent signaling and inhibited GLUT4 translocation. Since our data revealed that there was no decrease in insulin signaling through the AKT pathway yet GLUT4

translocation was inhibited in the presence of LPS, it would be interesting to determine if LPS inhibits GLUT4 translocation through the PI3-K independent pathway.

Due to the fact that phosphorylation exerts the greatest control over MGU under insulin-stimulated conditions our original hypothesis was that increased glucose phosphorylation capacity would lead to an increase in MGU in the presence of LPS. We determined that increased phosphorylation capacity did not lead to an increase in MGU in the presence of LPS. However, once impairments in the vasculature are unmasked there may be impairments downstream of delivery that effect MGU. To that end, it would be interesting to measure the level of mitochondrial dysfunction in our mouse model. While our attempt at using NMR was unsuccessful, we could utilize the OROBOROS O2K Oxygraph to measure O₂ consumption in permeabilized skeletal muscle fibers *ex vivo*.

The findings of this dissertation underscore the need to gain a better understanding of the relationship between acute inflammatory stress, cardiovascular dysfunction and MGU as to provide more targeted therapies for patients in the ICU.

REFERENCES

1. **Abel ED, Kaulbach HC, Tian R, Hopkins JC, Duffy J, Doetschman T, Minnemann T, Boers ME, Hadro E, Oberste-Berghaus C, Quist W, Lowell BB, Ingwall JS, and Kahn BB.** Cardiac hypertrophy with preserved contractile function after selective deletion of GLUT4 from the heart. *J Clin Invest* 104: 1703-1714, 1999.
2. **Abel ED, Peroni O, Kim JK, Kim YB, Boss O, Hadro E, Minnemann T, Shulman GI, and Kahn BB.** Adipose-selective targeting of the GLUT4 gene impairs insulin action in muscle and liver. *Nature* 409: 729-733, 2001.
3. **Abramson D, Scalea TM, Hitchcock R, Trooskin SZ, Henry SM, and Greenspan J.** Lactate clearance and survival following injury. *J Trauma* 35: 584-588; discussion 588-589, 1993.
4. **Adkins-Marshall BA, Myers SR, Hendrick GK, Williams PE, Triebwasser K, Floyd B, and Cherrington AD.** Interaction between insulin and glucose-delivery route in regulation of net hepatic glucose uptake in conscious dogs. *Diabetes* 39: 87-95, 1990.
5. **Ayala JE, Bracy DP, McGuinness OP, and Wasserman DH.** Considerations in the design of hyperinsulinemic-euglycemic clamps in the conscious mouse. *Diabetes* 55: 390-397, 2006.
6. **Bagby GJ, Lang CH, Hargrove DM, Thompson JJ, Wilson LA, and Spitzer JJ.** Glucose kinetics in rats infused with endotoxin-induced monokines or tumor necrosis factor. *Circ Shock* 24: 111-121, 1988.
7. **Baron AD.** Hemodynamic actions of insulin. *Am J Physiol* 267: E187-202, 1994.
8. **Baron AD, Brechtel-Hook G, Johnson A, Cronin J, Leaming R, and Steinberg HO.** Effect of perfusion rate on the time course of insulin-mediated skeletal muscle glucose uptake. *Am J Physiol* 271: E1067-1072, 1996.
9. **Baron AD, Steinberg H, Brechtel G, and Johnson A.** Skeletal muscle blood flow independently modulates insulin-mediated glucose uptake. *Am J Physiol* 266: E248-253, 1994.
10. **Baron AD, Steinberg HO, Chaker H, Leaming R, Johnson A, and Brechtel G.** Insulin-mediated skeletal muscle vasodilation contributes to both insulin sensitivity and responsiveness in lean humans. *J Clin Invest* 96: 786-792, 1995.
11. **Barrett EJ, Eggleston EM, Inyard AC, Wang H, Li G, Chai W, and Liu Z.** The vascular actions of insulin control its delivery to muscle and regulate the rate-limiting step in skeletal muscle insulin action. *Diabetologia* 52: 752-764, 2009.
12. **Battelino T, Goto M, Krzysnik C, and Zeller WP.** Tissue glucose transport and glucose transporters in suckling rats with endotoxic shock. *Shock* 6: 259-262, 1996.
13. **Baumgarten G, Knuefermann P, Nozaki N, Sivasubramanian N, Mann DL, and Vallejo JG.** In vivo expression of proinflammatory mediators in the adult heart after endotoxin administration: the role of toll-like receptor-4. *J Infect Dis* 183: 1617-1624, 2001.
14. **Bedard S, Marcotte B, and Marette A.** Cytokines modulate glucose transport in skeletal muscle by inducing the expression of inducible nitric oxide synthase. *Biochem J* 325 (Pt 2): 487-493, 1997.
15. **Bellomo R, Kellum JA, and Pinsky MR.** Transvisceral lactate fluxes during early endotoxemia. *Chest* 110: 198-204, 1996.
16. **Berglund ED, Lee-Young RS, Lustig DG, Lynes SE, Donahue EP, Camacho RC, Meredith ME, Magnuson MA, Charron MJ, and Wasserman DH.** Hepatic energy state is regulated by glucagon receptor signaling in mice. *J Clin Invest* 119: 2412-2422, 2009.
17. **Bergman RN and Bucolo RJ.** Interaction of insulin and glucose in the control of hepatic glucose balance. *Am J Physiol* 227: 1314-1322, 1974.

18. **Bernardin G, Pradier C, Tiger F, Deloffre P, and Mattei M.** Blood pressure and arterial lactate level are early indicators of short-term survival in human septic shock. *Intensive Care Med* 22: 17-25, 1996.
19. **Bone RC, Sprung CL, and Sibbald WJ.** Definitions for sepsis and organ failure. *Crit Care Med* 20: 724-726, 1992.
20. **Brooks BJ, Arch JR, and Newsholme EA.** Effect of some hormones on the rate of the triacylglycerol/fatty-acid substrate cycle in adipose tissue of the mouse in vivo. *Biosci Rep* 3: 263-267, 1983.
21. **Brozinick JT, Jr., Yaspelkis BB, 3rd, Wilson CM, Grant KE, Gibbs EM, Cushman SW, and Ivy JL.** Glucose transport and GLUT4 protein distribution in skeletal muscle of GLUT4 transgenic mice. *The Biochemical journal* 313 (Pt 1): 133-140, 1996.
22. **Carvalho-Filho MA, Ueno M, Carvalheira JB, Velloso LA, and Saad MJ.** Targeted disruption of iNOS prevents LPS-induced S-nitrosation of IRbeta/IRS-1 and Akt and insulin resistance in muscle of mice. *Am J Physiol Endocrinol Metab* 291: E476-482, 2006.
23. **Caton PW, Nayuni NK, Murch O, and Corder R.** Endotoxin induced hyperlactatemia and hypoglycemia is linked to decreased mitochondrial phosphoenolpyruvate carboxykinase. *Life Sci* 84: 738-744, 2009.
24. **Chambrier C, Laville M, Rhzioual Berrada K, Odeon M, Bouletreau P, and Beylot M.** Insulin sensitivity of glucose and fat metabolism in severe sepsis. *Clin Sci (Lond)* 99: 321-328, 2000.
25. **Chang PY, Jensen J, Printz RL, Granner DK, Ivy JL, and Moller DE.** Overexpression of hexokinase II in transgenic mice. Evidence that increased phosphorylation augments muscle glucose uptake. *J Biol Chem* 271: 14834-14839, 1996.
26. **Cheatham B and Kahn CR.** Insulin action and the insulin signaling network. *Endocr Rev* 16: 117-142, 1995.
27. **Cherrington AD.** Banting Lecture 1997. Control of glucose uptake and release by the liver in vivo. *Diabetes* 48: 1198-1214, 1999.
28. **Cherrington AD, Edgerton D, and Sindelar DK.** The direct and indirect effects of insulin on hepatic glucose production in vivo. *Diabetologia* 41: 987-996, 1998.
29. **Chiu JD, Richey JM, Harrison LN, Zuniga E, Kolka CM, Kirkman E, Ellmerer M, and Bergman RN.** Direct administration of insulin into skeletal muscle reveals that the transport of insulin across the capillary endothelium limits the time course of insulin to activate glucose disposal. *Diabetes* 57: 828-835, 2008.
30. **Clark MG.** Impaired microvascular perfusion: a consequence of vascular dysfunction and a potential cause of insulin resistance in muscle. *Am J Physiol Endocrinol Metab* 295: E732-750, 2008.
31. **Clark MG, Wallis MG, Barrett EJ, Vincent MA, Richards SM, Clerk LH, and Rattigan S.** Blood flow and muscle metabolism: a focus on insulin action. *Am J Physiol Endocrinol Metab* 284: E241-258, 2003.
32. **Clarke JF, Young PW, Yonezawa K, Kasuga M, and Holman GD.** Inhibition of the translocation of GLUT1 and GLUT4 in 3T3-L1 cells by the phosphatidylinositol 3-kinase inhibitor, wortmannin. *The Biochemical journal* 300 (Pt 3): 631-635, 1994.
33. **Coker RH, Krishna MG, Lacy DB, Bracy DP, and Wasserman DH.** Role of hepatic alpha- and beta-adrenergic receptor stimulation on hepatic glucose production during heavy exercise. *Am J Physiol* 273: E831-838, 1997.
34. **Coppack SW.** Pro-inflammatory cytokines and adipose tissue. *Proc Nutr Soc* 60: 349-356, 2001.

35. **Corvera S, Davis RJ, Roach PJ, DePaoli-Roach A, and Czech MP.** Mechanism of receptor kinase action on membrane protein recycling. *Ann N Y Acad Sci* 488: 419-429, 1986.
36. **Curat CA, Miranville A, Sengenès C, Diehl M, Tonus C, Busse R, and Bouloumie A.** From blood monocytes to adipose tissue-resident macrophages: induction of diapedesis by human mature adipocytes. *Diabetes* 53: 1285-1292, 2004.
37. **Cushman SW and Wardzala LJ.** Potential mechanism of insulin action on glucose transport in the isolated rat adipose cell. Apparent translocation of intracellular transport systems to the plasma membrane. *J Biol Chem* 255: 4758-4762, 1980.
38. **Davidson MB.** Autoregulation by glucose of hepatic glucose balance: permissive effect of insulin. *Metabolism* 30: 279-284, 1981.
39. **de Alvaro C, Teruel T, Hernandez R, and Lorenzo M.** Tumor necrosis factor alpha produces insulin resistance in skeletal muscle by activation of inhibitor kappaB kinase in a p38 MAPK-dependent manner. *J Biol Chem* 279: 17070-17078, 2004.
40. **del Aguila LF, Claffey KP, and Kirwan JP.** TNF-alpha impairs insulin signaling and insulin stimulation of glucose uptake in C2C12 muscle cells. *Am J Physiol* 276: E849-855, 1999.
41. **Dellinger RP.** Cardiovascular management of septic shock. *Crit Care Med* 31: 946-955, 2003.
42. **Deutschman CS, De Maio A, and Clemens MG.** Sepsis-induced attenuation of glucagon and 8-Br-cAMP modulation of the phosphoenolpyruvate carboxykinase gene. *Am J Physiol* 269: R584-591, 1995.
43. **Douen AG, Ramlal T, Rastogi S, Bilan PJ, Cartee GD, Vranic M, Holloszy JO, and Klip A.** Exercise induces recruitment of the "insulin-responsive glucose transporter". Evidence for distinct intracellular insulin- and exercise-recruitable transporter pools in skeletal muscle. *J Biol Chem* 265: 13427-13430, 1990.
44. **Duplain H, Burcelin R, Sartori C, Cook S, Egli M, Lepori M, Vollenweider P, Pedrazzini T, Nicod P, Thorens B, and Scherrer U.** Insulin resistance, hyperlipidemia, and hypertension in mice lacking endothelial nitric oxide synthase. *Circulation* 104: 342-345, 2001.
45. **Ehrentraut S, Lohner R, Schwederski M, Ehrentraut H, Boehm O, Noga S, Langhoff P, Baumgarten G, Meyer R, and Knuefermann P.** In vivo toll-like receptor 4 antagonism restores cardiac function during endotoxemia. *Shock* 36: 613-620, 2011.
46. **Ellis CG, Bateman RM, Sharpe MD, Sibbald WJ, and Gill R.** Effect of a maldistribution of microvascular blood flow on capillary O₂ extraction in sepsis. *Am J Physiol Heart Circ Physiol* 282: H156-164, 2002.
47. **Eringa EC, Stehouwer CD, Walburg K, Clark AD, van Nieuw Amerongen GP, Westerhof N, and Sipkema P.** Physiological concentrations of insulin induce endothelin-dependent vasoconstriction of skeletal muscle resistance arteries in the presence of tumor necrosis factor-alpha dependence on c-Jun N-terminal kinase. *Arterioscler Thromb Vasc Biol* 26: 274-280, 2006.
48. **Fain JN, Madan AK, Hiler ML, Cheema P, and Bahouth SW.** Comparison of the release of adipokines by adipose tissue, adipose tissue matrix, and adipocytes from visceral and subcutaneous abdominal adipose tissues of obese humans. *Endocrinology* 145: 2273-2282, 2004.
49. **Fan J, Li YH, Wojnar MM, and Lang CH.** Endotoxin-induced alterations in insulin-stimulated phosphorylation of insulin receptor, IRS-1, and MAP kinase in skeletal muscle. *Shock* 6: 164-170, 1996.
50. **Fasshauer M and Paschke R.** Regulation of adipocytokines and insulin resistance. *Diabetologia* 46: 1594-1603, 2003.
51. **Feingold KR, Memon RA, Moser AH, Shigenaga JK, and Grunfeld C.** Endotoxin and interleukin-1 decrease hepatic lipase mRNA levels. *Atherosclerosis* 142: 379-387, 1999.

52. **Ferrannini E, Galvan AQ, Gastaldelli A, Camastra S, Sironi AM, Toschi E, Baldi S, Frascerra S, Monzani F, Antonelli A, Nannipieri M, Mari A, Seghieri G, and Natali A.** Insulin: new roles for an ancient hormone. *European journal of clinical investigation* 29: 842-852, 1999.
53. **Filkins JP and Cornell RP.** Depression of hepatic gluconeogenesis and the hypoglycemia of endotoxin shock. *Am J Physiol* 227: 778-781, 1974.
54. **Frayn KN.** Hormonal control of metabolism in trauma and sepsis. *Clin Endocrinol (Oxf)* 24: 577-599, 1986.
55. **Frost RA, Nystrom GJ, and Lang CH.** Lipopolysaccharide regulates proinflammatory cytokine expression in mouse myoblasts and skeletal muscle. *Am J Physiol Regul Integr Comp Physiol* 283: R698-709, 2002.
56. **Fueger PT, Bracy DP, Malabanan CM, Pencek RR, Granner DK, and Wasserman DH.** Hexokinase II overexpression improves exercise-stimulated but not insulin-stimulated muscle glucose uptake in high-fat-fed C57BL/6J mice. *Diabetes* 53: 306-314, 2004.
57. **Fueger PT, Bracy DP, Malabanan CM, Pencek RR, and Wasserman DH.** Distributed control of glucose uptake by working muscles of conscious mice: roles of transport and phosphorylation. *Am J Physiol Endocrinol Metab* 286: E77-84, 2004.
58. **Fueger PT, Hess HS, Bracy DP, Pencek RR, Posey KA, Charron MJ, and Wasserman DH.** Regulation of insulin-stimulated muscle glucose uptake in the conscious mouse: role of glucose transport is dependent on glucose phosphorylation capacity. *Endocrinology* 145: 4912-4916, 2004.
59. **Fueger PT, Hess HS, Posey KA, Bracy DP, Pencek RR, Charron MJ, and Wasserman DH.** Control of exercise-stimulated muscle glucose uptake by GLUT4 is dependent on glucose phosphorylation capacity in the conscious mouse. *J Biol Chem* 279: 50956-50961, 2004.
60. **Fueger PT, Lee-Young RS, Shearer J, Bracy DP, Heikkinen S, Laakso M, Rottman JN, and Wasserman DH.** Phosphorylation barriers to skeletal and cardiac muscle glucose uptakes in high-fat fed mice: studies in mice with a 50% reduction of hexokinase II. *Diabetes* 56: 2476-2484, 2007.
61. **Fueger PT, Shearer J, Bracy DP, Posey KA, Pencek RR, McGuinness OP, and Wasserman DH.** Control of muscle glucose uptake: test of the rate-limiting step paradigm in conscious, unrestrained mice. *J Physiol* 562: 925-935, 2005.
62. **Garvey WT, Maianu L, Zhu JH, Brechtel-Hook G, Wallace P, and Baron AD.** Evidence for defects in the trafficking and translocation of GLUT4 glucose transporters in skeletal muscle as a cause of human insulin resistance. *J Clin Invest* 101: 2377-2386, 1998.
63. **Gerich JE.** Control of glycaemia. *Baillieres Clin Endocrinol Metab* 7: 551-586, 1993.
64. **Gibbs EM, Stock JL, McCoid SC, Stukenbrok HA, Pessin JE, Stevenson RW, Milici AJ, and McNeish JD.** Glycemic improvement in diabetic db/db mice by overexpression of the human insulin-regulatable glucose transporter (GLUT4). *J Clin Invest* 95: 1512-1518, 1995.
65. **Goldstein SA and Elwyn DH.** The effects of injury and sepsis on fuel utilization. *Annu Rev Nutr* 9: 445-473, 1989.
66. **Gore DC, Jahoor F, Hibbert JM, and DeMaria EJ.** Lactic acidosis during sepsis is related to increased pyruvate production, not deficits in tissue oxygen availability. *Ann Surg* 224: 97-102, 1996.
67. **Griesdale DE, de Souza RJ, van Dam RM, Heyland DK, Cook DJ, Malhotra A, Dhaliwal R, Henderson WR, Chittock DR, Finfer S, and Talmor D.** Intensive insulin therapy and mortality among critically ill patients: a meta-analysis including NICE-SUGAR study data. *Cmaj* 180: 821-827, 2009.
68. **Hagstrom-Toft E, Bolinder J, Eriksson S, and Arner P.** Role of phosphodiesterase III in the antilipolytic effect of insulin in vivo. *Diabetes* 44: 1170-1175, 1995.

69. **Halseth AE, Bracy DP, and Wasserman DH.** Overexpression of hexokinase II increases insulin and exercise-stimulated muscle glucose uptake in vivo. *Am J Physiol* 276: E70-77, 1999.
70. **Hansen PA, Gulve EA, Marshall BA, Gao J, Pessin JE, Holloszy JO, and Mueckler M.** Skeletal muscle glucose transport and metabolism are enhanced in transgenic mice overexpressing the Glut4 glucose transporter. *J Biol Chem* 270: 1679-1684, 1995.
71. **Hansen PA, Marshall BA, Chen M, Holloszy JO, and Mueckler M.** Transgenic overexpression of hexokinase II in skeletal muscle does not increase glucose disposal in wild-type or Glut1-overexpressing mice. *J Biol Chem* 275: 22381-22386, 2000.
72. **Hermanides J, Bosman RJ, Vriesendorp TM, Dotsch R, Rosendaal FR, Zandstra DF, Hoekstra JB, and DeVries JH.** Hypoglycemia is associated with intensive care unit mortality. *Crit Care Med* 38: 1430-1434, 2010.
73. **Hruz PW, Yan Q, Struthers H, and Jay PY.** HIV protease inhibitors that block GLUT4 precipitate acute, decompensated heart failure in a mouse model of dilated cardiomyopathy. *Faseb J* 22: 2161-2167, 2008.
74. **Ikemoto S, Thompson KS, Takahashi M, Itakura H, Lane MD, and Ezaki O.** High fat diet-induced hyperglycemia: prevention by low level expression of a glucose transporter (GLUT4) minigene in transgenic mice. *Proceedings of the National Academy of Sciences of the United States of America* 92: 3096-3099, 1995.
75. **Ince C and Sinaasappel M.** Microcirculatory oxygenation and shunting in sepsis and shock. *Crit Care Med* 27: 1369-1377, 1999.
76. **Katz A, Broberg S, Sahlin K, and Wahren J.** Leg glucose uptake during maximal dynamic exercise in humans. *Am J Physiol* 251: E65-70, 1986.
77. **Katz A, Sahlin K, and Broberg S.** Regulation of glucose utilization in human skeletal muscle during moderate dynamic exercise. *Am J Physiol* 260: E411-415, 1991.
78. **Katz EB, Stenbit AE, Hatton K, DePinho R, and Charron MJ.** Cardiac and adipose tissue abnormalities but not diabetes in mice deficient in GLUT4. *Nature* 377: 151-155, 1995.
79. **Kaufmann RL, Matson CF, and Beisel WR.** Hypertriglyceridemia produced by endotoxin: role of impaired triglyceride disposal mechanisms. *J Infect Dis* 133: 548-555, 1976.
80. **Kelley D, Mitrakou A, Marsh H, Schwenk F, Benn J, Sonnenberg G, Arcangeli M, Aoki T, Sorensen J, Berger M, and et al.** Skeletal muscle glycolysis, oxidation, and storage of an oral glucose load. *J Clin Invest* 81: 1563-1571, 1988.
81. **Kim JK, Zisman A, Fillmore JJ, Peroni OD, Kotani K, Perret P, Zong H, Dong J, Kahn CR, Kahn BB, and Shulman GI.** Glucose toxicity and the development of diabetes in mice with muscle-specific inactivation of GLUT4. *J Clin Invest* 108: 153-160, 2001.
82. **Kim Y, Tamura T, Iwashita S, Tokuyama K, and Suzuki M.** Effect of high-fat diet on gene expression of GLUT4 and insulin receptor in soleus muscle. *Biochemical and biophysical research communications* 202: 519-526, 1994.
83. **Koistinen HA and Zierath JR.** Regulation of glucose transport in human skeletal muscle. *Ann Med* 34: 410-418, 2002.
84. **Kovach AG, Rosell S, Sandor P, Koltay E, Kovach E, and Tomka N.** Blood flow, oxygen consumption, and free fatty acid release in subcutaneous adipose tissue during hemorrhagic shock in control and phenoxybenzamine-treated dogs. *Circ Res* 26: 733-741, 1970.
85. **Krook A, Bjornholm M, Galuska D, Jiang XJ, Fahlman R, Myers MG, Jr., Wallberg-Henriksson H, and Zierath JR.** Characterization of signal transduction and glucose transport in skeletal muscle from type 2 diabetic patients. *Diabetes* 49: 284-292, 2000.
86. **Laakso M, Edelman SV, Brechtel G, and Baron AD.** Decreased effect of insulin to stimulate skeletal muscle blood flow in obese man. A novel mechanism for insulin resistance. *J Clin Invest* 85: 1844-1852, 1990.

87. **Laakso M, Edelman SV, Brechtel G, and Baron AD.** Impaired insulin-mediated skeletal muscle blood flow in patients with NIDDM. *Diabetes* 41: 1076-1083, 1992.
88. **Lafontan M and Langin D.** Lipolysis and lipid mobilization in human adipose tissue. *Prog Lipid Res* 48: 275-297, 2009.
89. **Lam C, Tymi K, Martin C, and Sibbald W.** Microvascular perfusion is impaired in a rat model of normotensive sepsis. *J Clin Invest* 94: 2077-2083, 1994.
90. **Lam TK, Yoshii H, Haber CA, Bogdanovic E, Lam L, Fantus IG, and Giacca A.** Free fatty acid-induced hepatic insulin resistance: a potential role for protein kinase C-delta. *Am J Physiol Endocrinol Metab* 283: E682-691, 2002.
91. **Lang CH and Dobrescu C.** In vivo insulin resistance during nonlethal hypermetabolic sepsis. *Circ Shock* 28: 165-178, 1989.
92. **Lang CH and Dobrescu C.** Sepsis-induced increases in glucose uptake by macrophage-rich tissues persist during hypoglycemia. *Metabolism* 40: 585-593, 1991.
93. **Lang CH, Dobrescu C, and Meszaros K.** Insulin-mediated glucose uptake by individual tissues during sepsis. *Metabolism* 39: 1096-1107, 1990.
94. **Langouche L, Vander Perre S, Wouters PJ, D'Hoore A, Hansen TK, and Van den Berghe G.** Effect of intensive insulin therapy on insulin sensitivity in the critically ill. *J Clin Endocrinol Metab* 92: 3890-3897, 2007.
95. **Lanza-Jacoby S and Tabares A.** Triglyceride kinetics, tissue lipoprotein lipase, and liver lipogenesis in septic rats. *Am J Physiol* 258: E678-685, 1990.
96. **Lee MD, Zentella A, Vine W, Pekala PH, and Cerami A.** Effect of endotoxin-induced monokines on glucose metabolism in the muscle cell line L6. *Proceedings of the National Academy of Sciences of the United States of America* 84: 2590-2594, 1987.
97. **Liljenquist JE, Mueller GL, Cherrington AD, Keller U, Chiasson JL, Perry JM, Lacy WW, and Rabinowitz D.** Evidence for an important role of glucagon in the regulation of hepatic glucose production in normal man. *J Clin Invest* 59: 369-374, 1977.
98. **Ling PR, Bistrrian BR, Mendez B, and Istfan NW.** Effects of systemic infusions of endotoxin, tumor necrosis factor, and interleukin-1 on glucose metabolism in the rat: relationship to endogenous glucose production and peripheral tissue glucose uptake. *Metabolism* 43: 279-284, 1994.
99. **Losser MR, Damoiseil C, and Payen D.** Bench-to-bedside review: Glucose and stress conditions in the intensive care unit. *Crit Care* 14: 231, 2010.
100. **Lu B, Moser AH, Shigenaga JK, Feingold KR, and Grunfeld C.** Type II nuclear hormone receptors, coactivator, and target gene repression in adipose tissue in the acute-phase response. *J Lipid Res* 47: 2179-2190, 2006.
101. **Maitra SR, Wojnar MM, and Lang CH.** Alterations in tissue glucose uptake during the hyperglycemic and hypoglycemic phases of sepsis. *Shock* 13: 379-385, 2000.
102. **Martin IK, Katz A, and Wahren J.** Splanchnic and muscle metabolism during exercise in NIDDM patients. *Am J Physiol* 269: E583-590, 1995.
103. **McCallum RE and Berry LJ.** Mouse liver fructose-1, 6-diphosphatase and glucose-6-phosphatase activities after endotoxin poisoning. *Infect Immun* 6: 883-885, 1972.
104. **McGuinness OP.** The impact of infection on gluconeogenesis in the conscious dog. *Shock* 2: 336-343, 1994.
105. **McGuinness OP, Fugiwara T, Murrell S, Bracy D, Neal D, O'Connor D, and Cherrington AD.** Impact of chronic stress hormone infusion on hepatic carbohydrate metabolism in the conscious dog. *Am J Physiol* 265: E314-322, 1993.
106. **Mechanick JI, Handelsman Y, and Bloomgarden ZT.** Hypoglycemia in the intensive care unit. *Curr Opin Clin Nutr Metab Care* 10: 193-196, 2007.

107. **Mehta VK, Hao W, Brooks-Worrell BM, and Palmer JP.** Low-dose interleukin 1 and tumor necrosis factor individually stimulate insulin release but in combination cause suppression. *Eur J Endocrinol* 130: 208-214, 1994.
108. **Meinz H, Lacy DB, Ejiolor J, and McGuinness OP.** Alterations in hepatic gluconeogenic amino acid uptake and gluconeogenesis in the endotoxin treated conscious dog. *Shock* 9: 296-303, 1998.
109. **Mesotten D, Swinnen JV, Vanderhoydonc F, Wouters PJ, and Van den Berghe G.** Contribution of circulating lipids to the improved outcome of critical illness by glycemic control with intensive insulin therapy. *J Clin Endocrinol Metab* 89: 219-226, 2004.
110. **Meszaros K, Lang CH, Bagby GJ, and Spitzer JJ.** Contribution of different organs to increased glucose consumption after endotoxin administration. *J Biol Chem* 262: 10965-10970, 1987.
111. **Mizock BA.** Metabolic derangements in sepsis and septic shock. *Crit Care Clin* 16: 319-336, vii, 2000.
112. **Morgan HE, Cadenas E, Regen DM, and Park CR.** Regulation of glucose uptake in muscle. II. Rate-limiting steps and effects of insulin and anoxia in heart muscle from diabetic rats. *J Biol Chem* 236: 262-268, 1961.
113. **Morgan HE, Henderson MJ, Regen DM, and Park CR.** Regulation of glucose uptake in muscle. I. The effects of insulin and anoxia on glucose transport and phosphorylation in the isolated, perfused heart of normal rats. *J Biol Chem* 236: 253-261, 1961.
114. **Mulligan KX, Morris RT, Otero YF, Wasserman DH, and McGuinness OP.** Disassociation of Muscle Insulin Signaling and Insulin-Stimulated Glucose Uptake during Endotoxemia. *PLoS One* 7: e30160, 2012.
115. **Niswender KD, Shiota M, Postic C, Cherrington AD, and Magnuson MA.** Effects of increased glucokinase gene copy number on glucose homeostasis and hepatic glucose metabolism. *J Biol Chem* 272: 22570-22575, 1997.
116. **Nohara A, Okada S, Ohshima K, Pessin JE, and Mori M.** Cyclin-dependent kinase-5 is a key molecule in tumor necrosis factor-alpha-induced insulin resistance. *J Biol Chem* 286: 33457-33465, 2011.
117. **Nordenstrom J, Carpentier YA, Askanazi J, Robin AP, Elwyn DH, Hensle TW, and Kinney JM.** Free fatty acid mobilization and oxidation during total parenteral nutrition in trauma and infection. *Annals of surgery* 198: 725-735, 1983.
118. **O'Brien RM and Granner DK.** Regulation of gene expression by insulin. *Physiol Rev* 76: 1109-1161, 1996.
119. **Olson AL, Liu ML, Moyer-Rowley WS, Buse JB, Bell GI, and Pessin JE.** Hormonal/metabolic regulation of the human GLUT4/muscle-fat facilitative glucose transporter gene in transgenic mice. *J Biol Chem* 268: 9839-9846, 1993.
120. **Orellana RA, Suryawan A, Kimball SR, Wu G, Nguyen HV, Jefferson LS, and Davis TA.** Insulin signaling in skeletal muscle and liver of neonatal pigs during endotoxemia. *Pediatr Res* 64: 505-510, 2008.
121. **Owen OE, Felig P, Morgan AP, Wahren J, and Cahill GF, Jr.** Liver and kidney metabolism during prolonged starvation. *J Clin Invest* 48: 574-583, 1969.
122. **Pagliassotti MJ, Holste LC, Moore MC, Neal DW, and Cherrington AD.** Comparison of the time courses of insulin and the portal signal on hepatic glucose and glycogen metabolism in the conscious dog. *J Clin Invest* 97: 81-91, 1996.
123. **Park HK, Qatanani M, Briggs ER, Ahima RS, and Lazar MA.** Inflammatory induction of human resistin causes insulin resistance in endotoxemic mice. *Diabetes* 60: 775-783, 2011.

124. **Parker MM, Shelhamer JH, Bacharach SL, Green MV, Natanson C, Frederick TM, Damske BA, and Parrillo JE.** Profound but reversible myocardial depression in patients with septic shock. *Ann Intern Med* 100: 483-490, 1984.
125. **Parrillo JE.** Pathogenetic mechanisms of septic shock. *N Engl J Med* 328: 1471-1477, 1993.
126. **Pessin JE and Saltiel AR.** Signaling pathways in insulin action: molecular targets of insulin resistance. *J Clin Invest* 106: 165-169, 2000.
127. **Petersen HA, Fueger PT, Bracy DP, Wasserman DH, and Halseth AE.** Fiber type-specific determinants of Vmax for insulin-stimulated muscle glucose uptake in vivo. *Am J Physiol Endocrinol Metab* 284: E541-548, 2003.
128. **Pilon G, Charbonneau A, White PJ, Dallaire P, Perreault M, Kapur S, and Marette A.** Endotoxin mediated-iNOS induction causes insulin resistance via ONOO induced tyrosine nitration of IRS-1 in skeletal muscle. *PLoS One* 5: e15912, 2010.
129. **Pirola L, Johnston AM, and Van Obberghen E.** Modulation of insulin action. *Diabetologia* 47: 170-184, 2004.
130. **Plomgaard P, Bouzakri K, Krogh-Madsen R, Mittendorfer B, Zierath JR, and Pedersen BK.** Tumor necrosis factor-alpha induces skeletal muscle insulin resistance in healthy human subjects via inhibition of Akt substrate 160 phosphorylation. *Diabetes* 54: 2939-2945, 2005.
131. **Plomgaard P, Fischer CP, Ibfelt T, Pedersen BK, and van Hall G.** Tumor necrosis factor-alpha modulates human in vivo lipolysis. *J Clin Endocrinol Metab* 93: 543-549, 2008.
132. **Post RL, Morgan HE, and Park CR.** Regulation of glucose uptake in muscle. III. The interaction of membrane transport and phosphorylation in the control of glucose uptake. *J Biol Chem* 236: 269-272, 1961.
133. **Printz RL, Koch S, Potter LR, O'Doherty RM, Tiesinga JJ, Moritz S, and Granner DK.** Hexokinase II mRNA and gene structure, regulation by insulin, and evolution. *J Biol Chem* 268: 5209-5219, 1993.
134. **Rattigan S, Clark MG, and Barrett EJ.** Acute vasoconstriction-induced insulin resistance in rat muscle in vivo. *Diabetes* 48: 564-569, 1999.
135. **Rea S and James DE.** Moving GLUT4: the biogenesis and trafficking of GLUT4 storage vesicles. *Diabetes* 46: 1667-1677, 1997.
136. **Ren JM, Marshall BA, Gulve EA, Gao J, Johnson DW, Holloszy JO, and Mueckler M.** Evidence from transgenic mice that glucose transport is rate-limiting for glycogen deposition and glycolysis in skeletal muscle. *J Biol Chem* 268: 16113-16115, 1993.
137. **Ren JM, Marshall BA, Mueckler MM, McCaleb M, Amatruda JM, and Shulman GI.** Overexpression of Glut4 protein in muscle increases basal and insulin-stimulated whole body glucose disposal in conscious mice. *J Clin Invest* 95: 429-432, 1995.
138. **Ren JM, Semenkovich CF, Gulve EA, Gao J, and Holloszy JO.** Exercise induces rapid increases in GLUT4 expression, glucose transport capacity, and insulin-stimulated glycogen storage in muscle. *J Biol Chem* 269: 14396-14401, 1994.
139. **Robin AP, Askanazi J, Greenwood MR, Carpentier YA, Gump FE, and Kinney JM.** Lipoprotein lipase activity in surgical patients: influence of trauma and infection. *Surgery* 90: 401-408, 1981.
140. **Romanosky AJ, Bagby GJ, Bockman EL, and Spitzer JJ.** Free fatty acid utilization by skeletal muscle after endotoxin administration. *Am J Physiol* 239: E391-395, 1980.
141. **Rossetti L, Stenbit AE, Chen W, Hu M, Barzilai N, Katz EB, and Charron MJ.** Peripheral but not hepatic insulin resistance in mice with one disrupted allele of the glucose transporter type 4 (GLUT4) gene. *J Clin Invest* 100: 1831-1839, 1997.

142. **Rottman JN, Ni G, and Brown M.** Echocardiographic evaluation of ventricular function in mice. *Echocardiography* 24: 83-89, 2007.
143. **Sakr Y, Dubois MJ, De Backer D, Creteur J, and Vincent JL.** Persistent microcirculatory alterations are associated with organ failure and death in patients with septic shock. *Crit Care Med* 32: 1825-1831, 2004.
144. **Sakurai Y, Zhang XU, and Wolfe RR.** Short-term effects of tumor necrosis factor on energy and substrate metabolism in dogs. *J Clin Invest* 91: 2437-2445, 1993.
145. **Saltiel AR and Pessin JE.** Insulin signaling pathways in time and space. *Trends Cell Biol* 12: 65-71, 2002.
146. **Scherrer U, Randin D, Vollenweider P, Vollenweider L, and Nicod P.** Nitric oxide release accounts for insulin's vascular effects in humans. *J Clin Invest* 94: 2511-2515, 1994.
147. **Scholl RA, Lang CH, and Bagby GJ.** Hypertriglyceridemia and its relation to tissue lipoprotein lipase activity in endotoxemic, Escherichia coli bacteremic, and polymicrobial septic rats. *J Surg Res* 37: 394-401, 1984.
148. **Schultz TA, Lewis SB, Westbie DK, Wallin JD, and Gerich JE.** Glucose delivery: a modulator of glucose uptake in contracting skeletal muscle. *Am J Physiol* 233: E514-518, 1977.
149. **Shah P, Basu A, and Rizza R.** Fat-induced liver insulin resistance. *Curr Diab Rep* 3: 214-218, 2003.
150. **Slieker LJ, Sundell KL, Heath WF, Osborne HE, Bue J, Manetta J, and Sportsman JR.** Glucose transporter levels in tissues of spontaneously diabetic Zucker fa/fa rat (ZDF/drt) and viable yellow mouse (Avy/a). *Diabetes* 41: 187-193, 1992.
151. **Somogyi M.** Determination of blood sugar. *J Biol Chem* 160: 69-73, 1945.
152. **Spronk PE, Zandstra DF, and Ince C.** Bench-to bedside review: sepsis is a disease of the microcirculation. *Crit Care* 8: 462-468, 2004.
153. **Stenbit AE, Burcelin R, Katz EB, Tsao TS, Gautier N, Charron MJ, and Le Marchand-Brustel Y.** Diverse effects of Glut 4 ablation on glucose uptake and glycogen synthesis in red and white skeletal muscle. *J Clin Invest* 98: 629-634, 1996.
154. **Stenbit AE, Tsao TS, Li J, Burcelin R, Geenen DL, Factor SM, Houseknecht K, Katz EB, and Charron MJ.** GLUT4 heterozygous knockout mice develop muscle insulin resistance and diabetes. *Nat Med* 3: 1096-1101, 1997.
155. **Stoner HB, Little RA, Frayn KN, Elebute AE, Tresadern J, and Gross E.** The effect of sepsis on the oxidation of carbohydrate and fat. *Br J Surg* 70: 32-35, 1983.
156. **Suzuki K and Kono T.** Evidence that insulin causes translocation of glucose transport activity to the plasma membrane from an intracellular storage site. *Proc Natl Acad Sci U S A* 77: 2542-2545, 1980.
157. **Tappy L and Chioloro R.** Substrate utilization in sepsis and multiple organ failure. *Crit Care Med* 35: S531-534, 2007.
158. **Teichholz LE, Kreulen T, Herman MV, and Gorlin R.** Problems in echocardiographic volume determinations: echocardiographic-angiographic correlations in the presence of absence of asynergy. *Am J Cardiol* 37: 7-11, 1976.
159. **Tian R and Abel ED.** Responses of GLUT4-deficient hearts to ischemia underscore the importance of glycolysis. *Circulation* 103: 2961-2966, 2001.
160. **Treadway JL, Hargrove DM, Nardone NA, McPherson RK, Russo JF, Milici AJ, Stukenbrok HA, Gibbs EM, Stevenson RW, and Pessin JE.** Enhanced peripheral glucose utilization in transgenic mice expressing the human GLUT4 gene. *J Biol Chem* 269: 29956-29961, 1994.
161. **Tsao TS, Burcelin R, Katz EB, Huang L, and Charron MJ.** Enhanced insulin action due to targeted GLUT4 overexpression exclusively in muscle. *Diabetes* 45: 28-36, 1996.

162. **Tsao TS, Li J, Chang KS, Stenbit AE, Galuska D, Anderson JE, Zierath JR, McCarter RJ, and Charron MJ.** Metabolic adaptations in skeletal muscle overexpressing GLUT4: effects on muscle and physical activity. *Faseb J* 15: 958-969, 2001.
163. **Tsao TS, Stenbit AE, Factor SM, Chen W, Rossetti L, and Charron MJ.** Prevention of insulin resistance and diabetes in mice heterozygous for GLUT4 ablation by transgenic complementation of GLUT4 in skeletal muscle. *Diabetes* 48: 775-782, 1999.
164. **Tweedell A, Mulligan KX, Martel JE, Chueh FY, Santomango T, and McGuinness OP.** Metabolic response to endotoxin in vivo in the conscious mouse: role of interleukin-6. *Metabolism* 60: 92-98, 2011.
165. **van Bilsen M.** "Energenetics" of heart failure. *Ann N Y Acad Sci* 1015: 238-249, 2004.
166. **van den Berghe G, Wouters P, Weekers F, Verwaest C, Bruyninckx F, Schetz M, Vlasselaers D, Ferdinande P, Lauwers P, and Bouillon R.** Intensive insulin therapy in the critically ill patients. *N Engl J Med* 345: 1359-1367, 2001.
167. **Van den Berghe G, Wouters PJ, Bouillon R, Weekers F, Verwaest C, Schetz M, Vlasselaers D, Ferdinande P, and Lauwers P.** Outcome benefit of intensive insulin therapy in the critically ill: Insulin dose versus glycemic control. *Crit Care Med* 31: 359-366, 2003.
168. **van der Crabben SN, Blumer RM, Stegenga ME, Ackermans MT, Endert E, Tanck MW, Serlie MJ, van der Poll T, and Sauerwein HP.** Early endotoxemia increases peripheral and hepatic insulin sensitivity in healthy humans. *J Clin Endocrinol Metab* 94: 463-468, 2009.
169. **Van der Poll T, Romijn JA, Endert E, Borm JJ, Buller HR, and Sauerwein HP.** Tumor necrosis factor mimics the metabolic response to acute infection in healthy humans. *Am J Physiol* 261: E457-465, 1991.
170. **Vary TC, Drnevich D, Jurasinski C, and Brennan WA, Jr.** Mechanisms regulating skeletal muscle glucose metabolism in sepsis. *Shock* 3: 403-410, 1995.
171. **Vincent MA, Clerk LH, Lindner JR, Klibanov AL, Clark MG, Rattigan S, and Barrett EJ.** Microvascular recruitment is an early insulin effect that regulates skeletal muscle glucose uptake in vivo. *Diabetes* 53: 1418-1423, 2004.
172. **Vincent MA, Dawson D, Clark AD, Lindner JR, Rattigan S, Clark MG, and Barrett EJ.** Skeletal muscle microvascular recruitment by physiological hyperinsulinemia precedes increases in total blood flow. *Diabetes* 51: 42-48, 2002.
173. **Vogt C, Yki-Jarvinen H, Iozzo P, Pipek R, Pendergrass M, Koval J, Ardehali H, Printz R, Granner D, DeFronzo R, and Mandarin L.** Effects of insulin on subcellular localization of hexokinase II in human skeletal muscle in vivo. *J Clin Endocrinol Metab* 83: 230-234, 1998.
174. **Wahren J and Ekberg K.** Splanchnic regulation of glucose production. *Annu Rev Nutr* 27: 329-345, 2007.
175. **Wasserman DH.** Four grams of glucose. *Am J Physiol Endocrinol Metab* 296: E11-21, 2009.
176. **Wasserman DH and Ayala JE.** Interaction of physiological mechanisms in control of muscle glucose uptake. *Clin Exp Pharmacol Physiol* 32: 319-323, 2005.
177. **Wasserman DH, Spalding JA, Lacy DB, Colburn CA, Goldstein RE, and Cherrington AD.** Glucagon is a primary controller of hepatic glycogenolysis and gluconeogenesis during muscular work. *Am J Physiol* 257: E108-117, 1989.
178. **Weil MH and Afifi AA.** Experimental and clinical studies on lactate and pyruvate as indicators of the severity of acute circulatory failure (shock). *Circulation* 41: 989-1001, 1970.
179. **White MF.** Insulin signaling in health and disease. *Science* 302: 1710-1711, 2003.
180. **Wilmore DW, Goodwin CW, Aulick LH, Powanda MC, Mason AD, Jr., and Pruitt BA, Jr.** Effect of injury and infection on visceral metabolism and circulation. *Ann Surg* 192: 491-504, 1980.

181. **Wolfe RR.** Carbohydrate metabolism in the critically ill patient. Implications for nutritional support. *Crit Care Clin* 3: 11-24, 1987.
182. **Wolfe RR and Burke JF.** Effect of glucose infusion on glucose and lactate metabolism in normal and burned guinea pigs. *J Trauma* 18: 800-805, 1978.
183. **Wolfe RR, Elahi D, and Spitzer JJ.** Glucose and lactate kinetics after endotoxin administration in dogs. *Am J Physiol* 232: E180-185, 1977.
184. **Wolfe RR, Jahoor F, Herndon DN, and Miyoshi H.** Isotopic evaluation of the metabolism of pyruvate and related substrates in normal adult volunteers and severely burned children: effect of dichloroacetate and glucose infusion. *Surgery* 110: 54-67, 1991.
185. **Wolfe RR, Nadel ER, Shaw JH, Stephenson LA, and Wolfe MH.** Role of changes in insulin and glucagon in glucose homeostasis in exercise. *J Clin Invest* 77: 900-907, 1986.
186. **Wolfe RR, Shaw JH, and Durkot MJ.** Effect of sepsis on VLDL kinetics: responses in basal state and during glucose infusion. *Am J Physiol* 248: E732-740, 1985.
187. **Youd JM, Rattigan S, and Clark MG.** Acute impairment of insulin-mediated capillary recruitment and glucose uptake in rat skeletal muscle in vivo by TNF-alpha. *Diabetes* 49: 1904-1909, 2000.
188. **Yuen DY, Dwyer RM, Matthews VB, Zhang L, Drew BG, Neill B, Kingwell BA, Clark MG, Rattigan S, and Febbraio MA.** Interleukin-6 attenuates insulin-mediated increases in endothelial cell signaling but augments skeletal muscle insulin action via differential effects on tumor necrosis factor-alpha expression. *Diabetes* 58: 1086-1095, 2009.
189. **Zanotti-Cavazzoni SL and Hollenberg SM.** Cardiac dysfunction in severe sepsis and septic shock. *Curr Opin Crit Care* 15: 392-397, 2009.
190. **Zisman A, Peroni OD, Abel ED, Michael MD, Mauvais-Jarvis F, Lowell BB, Wojtaszewski JF, Hirshman MF, Virkamaki A, Goodyear LJ, Kahn CR, and Kahn BB.** Targeted disruption of the glucose transporter 4 selectively in muscle causes insulin resistance and glucose intolerance. *Nat Med* 6: 924-928, 2000.
191. **Zong H, Wang CC, Vaitheesvaran B, Kurland IJ, Hong W, and Pessin JE.** Enhanced energy expenditure, glucose utilization, and insulin sensitivity in VAMP8 null mice. *Diabetes* 60: 30-38, 2011.
192. **Zu L, He J, Jiang H, Xu C, Pu S, and Xu G.** Bacterial endotoxin stimulates adipose lipolysis via toll-like receptor 4 and extracellular signal-regulated kinase pathway. *J Biol Chem* 284: 5915-5926, 2009.